

Catalytic Oxidation of Ammonia to Nitrogen

Proefschrift

ter verkrijging van de graad van doctor aan de
Technische Universiteit Eindhoven, op gezag van de
Rector Magnificus, prof.dr. R. A. van Santen, voor een
Commissie aangewezen door het College voor
Promoties in het openbaar te verdedigen
op dinsdag 8 januari 2002 om 16.00 uur

door

Lu Gang

geboren te Nanjing-China

Dit proefschrift is goedgekeurd door de promotoren:

prof.dr. R.A. van Santen
en
prof.dr. J.A.R. van Veen

CIP-DATA LIBRARY TECHNISCHE UNIVERSITEIT EINDHOVEN

Gang, Lu

Catalytic oxidation of ammonia to nitrogen / by
Lu Gang.-Eindhoven : Technische Universiteit Eindhoven,
2002. - Proefschrift. – ISBN 90-386-2653-3
NUGI 813

Trefwoorden: heterogene katalyse / zeolieten / katalytische oxidatie ;
ammoniak / koperoxide / zilver

Subject headings: heterogenous catalysis / zeolites / catalytic oxidation ;
ammonia / copper oxide / silver

The work described in this thesis has been carried out at the Schuit Institute of Catalysis, Laboratory of Inorganic Chemistry and Catalysis, Eindhoven University of Technology, The Netherlands. Financial support has been supplied by the Netherlands Technology Foundation (STW) under the auspices of the Netherlands Organization for Scientific Research (NWO).

Printed at *Universiteitsdrukkerij*, Eindhoven University of Technology.

Contents

Chapter 1	General Introduction.....	1
Chapter 2	NH ₃ oxidation to nitrogen and water at low temperatures using supported metal or metal oxide catalysts.....	21
Chapter 3	Selective low temperature NH ₃ oxidation to N ₂ on copper- based catalysts.....	37
Chapter 4	Intermediate species and reaction pathways for oxidation of ammonia on powdered silver catalysts.....	57
Chapter 5	Low temperature selective oxidation of ammonia to nitrogen on silver-based catalysts.....	79
Chapter 6	Bi-functional alumina-supported Cu-Ag catalysts for ammonia oxidation to nitrogen at low temperature.....	101
Summary.....		125
Samenvatting.....		129
Publications.....		133
Acknowledgments.....		135

Chapter 1

General Introduction

Abstract

In this chapter the problems related to the emission of NH_3 , the sources of emission and the possibilities for their removal are discussed. The emphasis is on the removal of ammonia from gas phase. The selective catalytic oxidation (SCO) of ammonia is believed to be a most efficient and promising method for abating ammonia emissions. The state of the art with respect to catalytic solutions to the problem is discussed in detail with emphasis on the catalyst components and performance. Finally the mechanisms of ammonia oxidation on metals and metal oxides are reviewed. The scope of the investigation is also described briefly.

1. The NH₃ pollution problem

The emissions of nitrogen oxides (NO_x) and sulphur oxides (SO_x) give rise to acidification of the environment. NO_x and SO_x are converted in the atmosphere to give nitric and sulphuric acid. However emission of ammonia causes acidification of the environment in an indirect way. Reaction of ammonia with acidic aerosols in the atmosphere, such as aerosols of sulphuric acid or nitric acid, gives aerosols containing ammonium sulphates or ammonium nitrates [1]. Oxidation of ammonia and ammonium-containing aerosols by microorganisms in the soil then gives acidic HNO₃ [2]. Emission of nitrogen oxides and sulphur oxides are the major sources of acidic deposition in most countries. However emission of ammonia from intensive agricultural activities, e.g. cattle breeding, makes a significant contribution to the acidification of the environment in The Netherlands. About 94% of the ammonia emitted originates from agricultural sources in The Netherlands [3]. The damage caused by acidification in The Netherlands is serious: about half of the forests and much of the heather are affected; most of the fens have turned acidic; the nitrate concentration in the groundwater has increased and is still rising [4]; and the nitrogen balance in the ecosystem is seriously disturbed [5]. Ammonia can be health damaging and has an irritating smell. It is known to be a primary pollutant causing severe irritation and is suspected to have long-term effects such as bronchitis. Furthermore, ammonia is an undesired impurity for many industrial processes because it can cause corrosion and plugging of instrumentation.

The major source of ammonia emission has been attributed to the intensive farming areas and notably to livestock manure. This has led to a recent study of the role of ammonia in the formation of a rural version of urban smog [6]. In contrast, NH₃ is used beneficially in industry to reduce NO_x emissions by the so-called selective catalytic reduction process (SCR). It is added to the effluent gas as reductant in order to perform the following reaction: $\text{NH}_3 + \text{NO} + 1/4 \text{O}_2 \rightarrow \text{N}_2 + 3/2 \text{H}_2\text{O}$. However, the reaction is complete only with an excess of NH₃, giving rise to NH₃ “slip”. The unreacted ammonia is present in the off-gas and must therefore be removed in a secondary step [7,8]. Ammonia emissions are also caused by various other sources like: soda production; nitric acid production; metallurgical industry; coal or biomass gasification.

Ammonia is also a potential source of nitrogen oxides (NO_x) when involved in conventional combustion [9]. A typical example is the production of energy by combustion of the gasified biomass. Several projects addressing combined heat and power generation using turbines and heat-recycling system are ongoing [10,11]. The

use of biomass as a primary fuel is particularly interesting since it offers the possibility of no net emission of CO₂. It is also flexible for use in small units for remote locations where no other fuel is available. However biomass contains significant quantities of fuel-bound nitrogen. Gasification results in the formation of NH₃ (600-4000 ppm) in addition to CO (9.8-17.2%), H₂ (9.8-13.2%), CH₄, CO₂, H₂O and N₂. Subsequent combustion of this NH₃ can lead to the formation of an equivalent amount of NO_x, jeopardising all the advantages of the process.

The emission limits for the emission of ammonia to the air are described in the Dutch Emission Directives (Nederlandse emissie Richtlijn, NeR). For the industrial sector, ammonia is classified in the class gaseous inorganic 4 (gA.4). This means that, according to the NeR, the concentration in the outgoing gas flow may not be larger than 200 mg/Nm³. This limit applies to polluted gas flows of at least 5,0 kg/hr. However there might be plans to group ammonia in the class gA.3. This would mean that the concentration must not be larger than 30 mg/Nm³, valid for polluted gas flows of at least 0,300 kg/hr. The NeR-limits for the agricultural sector are much stricter. The ammonia concentration in the outgoing gas flow may not be larger than 5 mg/Nm³. This applies to all polluted gas flows. The ammonia emission for the Netherlands was 188.000 tons in 1996, 188.000 tons in 1997 and 177.000 tons in 1998 [12].

2. Removal of ammonia

Removal of ammonia can be divided in two groups (i) removal of ammonia from liquid phase and (ii) removal of ammonia from gas phase.

2.1 Removal of ammonia from water

Conventional wastewater treatment plants have only limited capacity for nitrogen removal. Plant effluents thus contain large concentrations of nitrogen, with ammonia being the main form. Ammonia concentrations in biologically treated wastewater are generally in the range 12-35 mg/L [13]. Several technically and economically feasible methods are available to reduce this concentration. They are characterized in Table 1.

Table 1 Comparison of ammonia removal process [14,15]

Process	Advantage	Disadvantage	Efficiency (%)	Relative cost
Biological nitrification-denitrification	N ₂ end product All forms of nitrogen removed	Long detention time Sensitive to inhibitors, changing flow and temperature	70-95	1.00
Breakpoint chlorination	Complete removal can be obtained Temperature variation and inhibition proof	Chemicals added Dechlorination is often necessary Continuous control equipment required	90-100	--
Ammonia stripping	Simplicity of operation Ease of control No by-products	Large Scale Inefficient at low temperature	50-95	1.32
Selective ion exchange on clinoptilolite	Wide temperature range and no inhibition	By-product formation(brine)	90-97	1.54

The relative costs of the treatment processes listed in Table 1 are controversial, and some authors claim that ammonia desorption is by far the least expensive ammonia removal process [16]. It should be noticed that the ammonia desorption method is actually change the liquid phase problem into a gas phase problem. Other methods such as catalytic wet oxidation and electrochemical oxidation are still under development [17,18,76].

2.2 Removal of ammonia from gas

Two main sources of waste gas containing ammonia can be identified: gas from industrial processes and gas from agriculture. Examples of industrial processes that produce ammonia are gasification, carbonisation, HDN process and thermal treatment of coal, liquid petroleum, shale oil, biomass and tar sands. The name of the contaminated gas flow is Cokes Oven Gas (referred to as COG-gas). The main source of agricultural pollution in Noord-Brabant is ventilation from sties, stables and manure processing factories. The name of the contaminated gas flow is Sty-gas.

The gas generated from COG-gas usually contains high concentration of ammonia. A conventional method of removing ammonia from COG is conducted by washing the COG with dilute sulfuric acid to recover the ammonia as ammonium sulfate. However the demand of ammonium sulfate for fertilizer has decreased and the market price greatly lowered. As a result, the profit is remarkably inferior and this process is now almost worthless from the industry viewpoint. At present, the ammonium sulfate production process is reduced and changed to other processes such as the Phosam process or Chevron WWT process to produce highly pure liquid ammonia, the Koppers process to separate ammonia followed by direct combustion or the Carl Still process to burn ammonia in the presence of a catalyst. However in the case of the direct combustion process, it is difficult to inhibit the production of NO_x [19-21]. An alternative method to remove NH_3 from COG is the decomposition of NH_3 at high temperature in the presence of a catalyst [22-24]. A few common techniques are schematically presented in Fig.1.

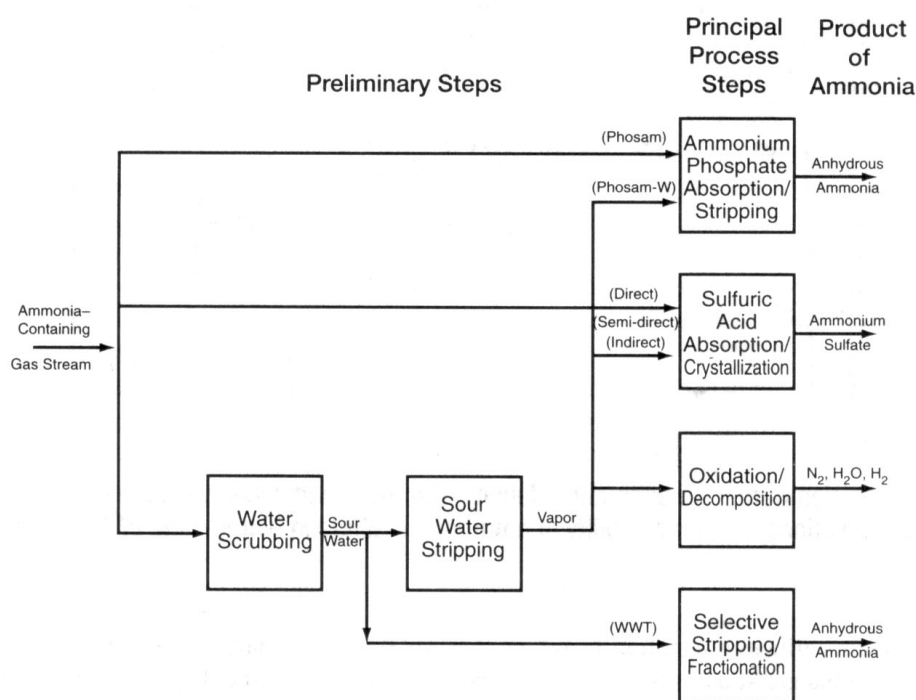


Fig.1 Basis steps in ammonia removal

Biological and acid scrubbing are two current techniques that are available for the removal of NH_3 from Sty-gas, which usually contains low concentrations of ammonia (<1000 ppm). In Noord-Brabant only one manure processing plant is operational (CNC) and another pilot plant is in experimental state (Ferm-O-Feed). Acid scrubbing and biofilters are techniques that are used in manure processing. The scale of the gas flow varies strongly per plant (10,000 – 300,000 m^3/hr). Biofilters are mainly used for

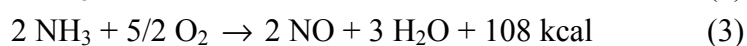
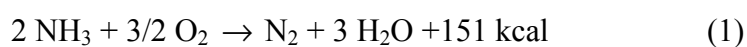
odour removal. The scrubbers are able to remove ammonia to acceptable concentrations. From an economical point of view the acid scrubbing is the most favourable one, because it is much faster. Furthermore the system is more accurately controllable. The biological system produces a larger liquid waste flow. This flow is mixed with manure waste, and the farmer has to pay per m³ to sell the waste.

Apart from COG and Sty-gas, many industrial processes, such as textile treatment, soda production, SCR process and nitric acid production, produce emission streams containing ammonia. These streams usually contain excess O₂, H₂O and very low concentrations of NH₃ (<1000 ppm). The conventional method for NH₃ removal is again by acid scrubbing. It should be pointed out that the acid scrubbing actually change a gas phase problem into a liquid phase problem. At present, the scrubbing liquid containing either NH₄NO₃ or (NH₄)₂SO₄ is sold as a fertilizer. As discussed above, the market for such a fertilizer is reducing due to its low efficiency and the possibility to cause severe soil acidification. In the long run, it is possible to stop use such a kind of fertilizer and the scrubbing liquid then becomes a big problem. Furthermore, acid scrubbing is not suitable to high flow and high temperature flue gases because of the high operation and investment costs [25].

3. Selective catalytic oxidation of ammonia (SCO)

A new technology for the removal of ammonia is using selective catalytic oxidation of ammonia to nitrogen and water. This process which provides an efficient, stable, simple and selective purification of large gas emissions can be applied both in low and high concentrations of ammonia removal. It is also possible to selectively oxidize ammonia to nitrogen in the liquid phase. Another potential application of this process may be in the production of pure nitrogen used as safety gas from air and ammonia. At present nitrogen is mainly produced from air by physical separation, which needs large investments and much energy. Ammonia oxidation by air provides a simplified and flexible process that is especially suitable for small-scale nitrogen production.

The catalytic oxidation of ammonia is one of the most interesting and important heterogeneous catalytic processes. It can proceed in the following three principal ways:



In the presence of platinum or cobalt oxide at high temperature (750-900 °C), mainly NO_x is produced. This constitutes the basis of the industrial manufacture of nitric acid (Ostwald process). At low temperature (< 500 °C), all three nitrogen-containing products (N₂, N₂O and NO) are formed simultaneously in various proportions in the presence of many catalysts. The study of low temperature SCO can be further classified into two categories: high ammonia concentration (1-30%) and low ammonia concentration (< 1000ppm) oxidation. The latter has only recently become of more interest because of the environmental problems.

3.1 High concentrations of ammonia oxidation

Though much attention has been given to high temperature ammonia oxidation, there is still a lot of detailed research in the literature about the low temperature ammonia oxidation over various kinds of metal and metal oxide catalysts. Earlier work on ammonia oxidation was reviewed by Il'chenko [26]. In his review, the activities of metals and metal oxides for ammonia oxidation at low temperature have been systematically compared (Table 2 and Table 3).

Table 2. The oxidation of ammonia in the presence of metals*

catalyst	r, mol cm ⁻² s ⁻¹ (at 300 °C)	E, kcal mole ⁻¹	Temperature of onset of formation, °C	
			N ₂	N ₂ O
Pt	1.70·10 ¹⁷	27	195	215
Pd	2.69·10 ¹⁶	5	100	150
Cu	3.31·10 ¹⁵	12	175	260
Ag	2.52·10 ¹⁵	15	200	210
Ni	1.23·10 ¹⁵	12	210	270
Au	8.32·10 ¹⁴	4	180	300
Fe	6.76·10 ¹⁴	9	230	270
W	5.90·10 ¹⁴	13	225	300
Ti	2.24·10 ¹⁴	5	180	**

*Composition of reaction mixture: P_{NH3}=0.1 atm; P_{O2}=0.9 atm.

**Up to 370 °C, nitrous oxide is not formed

Table 3. The oxidation of ammonia in the presence of metal oxides*

catalyst	Temp. range of catalytic reaction, °C	lg r-11**	E, kcal mole ⁻¹	S _{N2O} at 230 °C, %	Temperature of onset of formation, °C	
					N ₂	N ₂ O
Co ₃ O ₄	130-170	2.35	22	38	130	140
MnO ₂	110-160	2.35	18	43	110	120
CuO	220-260	1.60	23	11	220	230
CaO	200-260	0.54	15	50	<200	200
NiO	80-160	0.40	11	43****	80	105
Bi ₂ O ₃	235-320	0.13	12	0	235	255
Fe ₂ O ₃	220-270	0.07	24	17	220	230
V ₂ O ₅	260-320	-0.16	26	0	260	--
TiO ₂	265-320	-0.36	16	8****	265	290
CdO	205-275	-0.38	9	13	205	230
PbO	240-285	-0.64	16	0	240	260
ZnO	265-380	-0.79	31	0	265	295
SnO ₂	210-260	-0.90	17	16	<210	210
ZrO ₂	245-330	-0.91	18	0	245	>330
MoO ₃	330-370	-1.50	33	0	330	--
WO ₃	200-380	-2.22	22	0	200	>380
Ag ₂ O***	115-155	3.40	18	--	125	147

*Composition of reaction mixture: P_{NH3}=0.1 atm; P_{O2}=0.9 atm.

**r is the rate of overall process(in mol.cm⁻²s⁻¹) at 230 °C.

***The oxide was reduced to the metal during the catalytic reaction.

****S_{N2O} for NiO at 160 °C and for TiO₂ at 290 °C

Table 2 shows that at 300 °C the specific catalytic activity of metals for the overall process decreases in the sequence: Pt>Pd>Cu>Ag>Au>Fe>W>Ti. At low temperature, the ammonia oxidation products in the presence of metals are N₂ and N₂O. The selectivity with respect to nitrous oxide increases with temperature and for transition metals decreases in the sequence: Pt, Pd>Ni>Fe>W>Ti.

Table 3 shows that at 230 °C the specific catalytic activities of the oxides decrease as follows:

Co₃O₄, MnO₂>CuO>CaO>NiO>Bi₂O₃>Fe₂O₃>V₂O₅>TiO₂>CdO>PbO>ZnO>SnO₂
>ZrO₂>MoO₃>WO₃.

In another study [27], a similar sequence was obtained:

Co₃O₄ >MnO₂>Cr₂O₃> Fe₂O₃>CuO>NiO>V₂O₅>MoO₃>U₃O₈>ThO₂>WO₃>SnO₂>
ZrO₂>ZnO>Nb₂O₅>Bi₂O₃>Sb₂O₄>Ta₂O₅.

At low temperature and low degree of conversion, the selectivity of N_2 in general decreases with increasing the catalytic activity except for CuO and falls in the sequence:

ZnO, Bi_2O_3 , PbO, ZrO_2 , MoO_3 , WO_3 > TiO_2 > CuO > CdO > SnO_2 > Fe_2O_3 > Co_3O_4 > MnO_2 , NiO > CaO

The effect of reaction conditions on catalyst performance is the same for both metal and metal oxide catalysts. Increasing temperature and O_2/NH_3 ratio will increase the activity but decrease the selectivity to nitrogen.

Most above mentioned work has been done with single, polycrystalline metals and simple metal oxides, less with supported metals and metal oxides, metal alloys and mixed metal oxides. Several papers published some results of ammonia oxidation over alumina supported Pt catalysts [28-30]. It was discovered that a significant deactivation took place over these catalysts at low temperature (below 200 °C). The crystal size of Pt particle had great influence on catalyst performance. However at high temperature (200-350 °C), no deactivation was observed [30]. For transition metal exchanged zeolites, zeolite Y was the only zeolite reported [31]. By pulsing with a dry NH_3/O_2 mixture, the activity sequence reported was as follows: $CuY > CrY > AgY > CoY > FeY > NiY, MnY$, a little different from the sequence for simple metal oxides. NKK of Japan [32] recently developed a process for decomposing ammonia recovered from coke oven gas through catalytic oxidation. Over $TiO_2-Al_2O_3$ supported Cu-V oxides catalysts, a gas containing about 10% ammonia at 25500 h^{-1} space velocity can be completely cleaned from NH_3 at a temperature of about 500 °C with only a few ppm NO_x emission. It should be noticed that there exist some sulphur containing substances (H_2S , H_2SO_4) in their ammonia containing gas.

3.2 Low concentrations of ammonia oxidation

In recent years a considerable amount of attention has been focused on the catalytic purification of ammonia-containing flue gases with ammonia often present in low concentrations (<1000ppm). Since the surface concentration of nitrogen containing substances plays an important role in the selectivity of the ammonia oxidation, some influence of NH_3 concentration on the activity and selectivity of the catalyst may be expected. De Boer's study [33] shows that both activity and selectivity of ammonia oxidation over supported molybdenum catalyst are greatly influenced by the ammonia concentration (see Table 4).

Table 4. Influence of ammonia partial pressure on the performance of Mo26 catalyst

NH ₃ concentration	rate* T=325 °C	selectivity(%) at T=450 °C		
		N ₂	N ₂ O	NO
1000ppm	8.5	22	18	60
2600ppm	22.6	61	13	26
4200ppm	25.5	80	8	12

*rate in 10^{-8} mole NH₃ s⁻¹ g⁻¹ catalyst

The systems investigated in literature for low ammonia concentration oxidation are V₂O₅, WO₃ and MoO₃ on various supports [33-39] at the temperature of 300--400 °C. The best catalyst was SiO₂ supported molybdenum promoted with PbO over which the ammonia oxidation could be finished completely with 100% nitrogen selectivity at the temperature of around 400 °C.

Sazonova et al.[40] investigated the activity of various catalysts in ammonia oxidation at the temperature of 250--400 °C. They conclude that the most active and selective catalysts are V/TiO₂, Cu/TiO₂ and Cu-ZSM-5. However at low temperature (250 °C), the most active catalysts seem to be Fe-Cr-Zn-O, LaCoO₃ and Cu-ZSM-5 with less selectivity. It is also noticed that Cu/TiO₂ catalysts produced from CuSO₄·5H₂O are similar in activity to those produced from Cu(NO₃)₂·H₂O, but the former oxidise ammonia only to nitrogen.

Haldor Topsøe of Denmark[41] recently patented a process for catalytic low temperature oxidation of ammonia in an off-gas at a temperature of 200--500 °C. The catalysts used were silica supported Cu, Co and Ni oxides doped with small amount of noble metals(100--2000ppm). They claim that the selectivity and activity of the known ammonia catalysts are surprisingly improved when sulphating the catalysts during or prior to contact with ammonia containing gas. Their data show that the selectivity can be improved from 26--53% to 78--99%, indeed very surprising.

Yuejin Li studied the selective NH₃ oxidation to N₂ in a wet stream over ZSM-5 and alumina supported Pd, Rh and Pt catalysts at 200-350 °C [42]. They concluded that the ammonia conversion was not affected at high temperature but decreased at 200-250 °C with the addition of 5% water vapour. Generally, the ion exchanged ZSM-5 catalysts are more active than the alumina catalysts with an identical metal loading and less affected by water vapour. The selectivity to N₂ is relatively high on Rh and Pd catalysts and low on Pt catalysts.

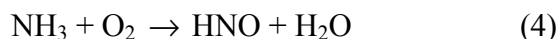
Wollner reported that high degrees of ammonia conversion of 80-100% was obtained over mixed copper-manganese oxides supported on titania catalysts at temperatures greater than about 300 °C [43]. However the selectivity is not reported clearly.

4. Reaction mechanisms of ammonia oxidation

The vast majority of scientific work on ammonia oxidation has been done on platinum catalysts. Therefore, in this section mechanisms of ammonia oxidation on platinum are first discussed. Furthermore, mechanisms of ammonia oxidation on other catalysts such as Cu and Ag, as well as transition metal oxides are also reviewed.

4.1 Mechanisms over platinum catalysts

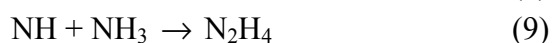
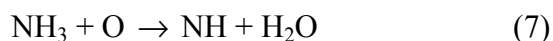
Before 1960 three different general reaction mechanisms on platinum were proposed on the basis of postulation because of the lack of experimental evidence of intermediate species. The nitroxyl (HNO) mechanism was suggested by Andrussov [44]. His hypothesis was based on the formation, during the first stage of the reaction, of the intermediate compound HNO:



Later Bodenstein [45,46] conjectured that the first stage was the formation of hydroxylamine (NH₂OH), which was converted to nitroxyl in a next step:

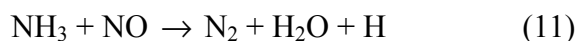
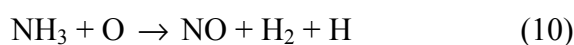


The imide (NH) mechanism was proposed by Raschig [47] and Zawadzki [48], in which the first step yielding imide was postulated. The imide could subsequently react with oxygen or ammonia to form nitroxyl or hydrazine:



According to above mechanisms, the final products NO, N₂O, N₂ and H₂O are formed via a number of stages involving such intermediate compounds as HNO, HNO₂, HNO₃ and N₂H₄ [44-52].

Fogel et al. used polycrystalline Pt wire, with reactant partial pressure of 10⁻⁴ Torr, and worked over the temperature range 25-1200 °C [53]. Using secondary ion mass spectrometry (SIMS), they concluded that the intermediate species HNO, NH₂ON, HNO₂ and N₂O were not formed during the oxidation reaction and therefore proposed a reaction mechanism which had simple steps, with none of the above intermediates involved, based on the two reactions:



N₂ was thus believed to be formed in a bimolecular surface reaction between NO and NH₃, with the transition from N₂ to NO formation occurring at a surface temperature when NO has too short a surface residence time to take part in reaction (11), i.e. when NO starts to desorb from the surface. In a series of molecular beam mass spectrometry experiments on a platinum filament Nutt and Kapur [54,55] suggested a very similar reaction mechanism. The only difference with the Fogel mechanism is that they find that ammonia adsorbs dissociatively on Pt and the so formed NH₂ reacts with O₂ to give NO, which consequently reacts with NH₂ to give N₂. In none of the low pressure (< 100 Pa) studies nitrous oxide was detected, so it does not figure in the stories.

It should be pointed out that the above models for the overall behavior of the ammonia oxidation reaction on Pt appear reasonable. They do, however, address only the overall reaction mechanism and do not go into the details of the elementary reaction steps. New insights in the reaction mechanism of ammonia oxidation were obtained from surface science experiments. Asscher et al. [56] used a laser multiphoton technique, combined with molecular beams under UHV conditions, to probe NO formation during reaction on a Pt{111} crystal. By analyzing the decay in the NO signal after pulsing NH₃, they identified two different NO production kinetics and assigned them to the following mechanisms:

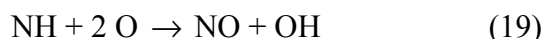


They found reaction (12) to be the faster mechanism, which was enhanced at high O_2/NH_3 ratios and had a higher activation energy than reaction (13), the slower mechanism.

More recently the ammonia oxidation was studied by Mieher and Ho [57] on the Pt{111} surface with TPD, temperature programmed reaction spectroscopy (TPRS), electron energy loss spectroscopy (EELS) and low energy electron diffraction (LEED). Using EELS they identified OH, NH and NH_2 as intermediate species but were unable to comment on NO due to ambiguities of the NO frequency. They concluded that the reaction proceeded via the simple stripping of NH_3 by oxygen atoms followed by the combination of nitrogen atoms with oxygen, to form NO, or with nitrogen atoms, to form N_2 (reaction (14)-(18)):



Another recent surface science study on ammonia oxidation was done by Bradley and King [58] on Pt{100} using surface molecular beams under UHV conditions. The mechanism proposed is similar to the mechanism of Mieher and Ho. However the production of nitrogen and NO was found to occur through other paths. They suggested that NO was directly produced by reacting NH with O. The formation of N_2 resulted from the consecutive dissociation of NO:

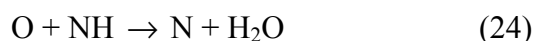
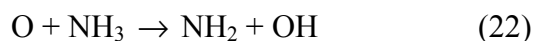


Since only NO and N_2 were produced under the reaction conditions of these studies, the formation of N_2O was not discussed. The recent study of Van den Broek and van Santen [59,60] showed that NH and OH were the main surface species adsorbed on Pt sponge catalysts after ammonia oxidation in atmospheric pressure. The reaction of NH and OH was thought to be the rate-determining step under their reaction conditions. They argued that N_2O was produced by NO reacting with adsorbed N. A density functional study has also been done by Fahmi and van Santen [61] on ammonia oxidation on a Pt_6 cluster. It was found that ammonia only dissociates when oxygen is present on the surface. The reaction mechanism was found to generally

follow the Miehler and Ho mechanism. Furthermore it was established that water could poison the ammonia oxidation reaction, since water is more acidic than ammonia.

4.2 Mechanisms over other catalysts

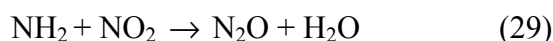
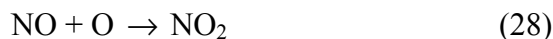
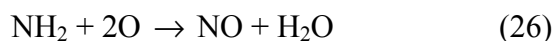
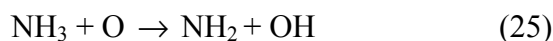
The XPS, EELS and STM techniques were used by the group of M.W. Roberts [62-65] to study ammonia oxidation on copper surfaces. They observed that at very low temperatures (< 300 K) ammonia could be oxidized to adsorbed NH_2 and NH species through oxydehydrogenation steps. At higher temperature (400 K) a fraction of the imide species was further dehydrogenated into atomic nitrogen:



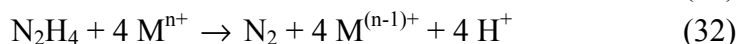
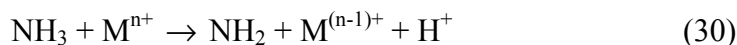
The STM image clearly showed that the atomic nitrogen produced at 400 K could block the ends of the $-\text{Cu}-\text{O}-$ rows, inhibiting further reactions and creating stable mixed N-O structures on the copper surface. Step defects on the surface had strong influence on the reactivity of oxygen adatoms. Reactivity was high at the top and bottom of a [110] step and at the bottom of a [001] step, whereas it was low at the top of a [001] step.

Ammonia adsorption on Ag(110) has been studied previously by TPD, TPRS and by EELS with and without coadsorption of molecular and atomic oxygen [66]. It was concluded that a diffusing nitrogen adatom was the reactive intermediate in NO and N_2 formation. On the basis of a combination of XPS and vibrational electron energy loss (VEEL) spectra a dioxygen- NH_3 complex had been suggested to be a key intermediate in the oxidation of ammonia on Ag(111) surfaces [67,68]. No report has been published to-date on the intermediate species and reaction mechanisms on polycrystalline silver at atmospheric pressure.

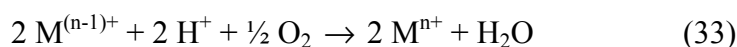
Ammonia oxidation mechanisms on Cr_2O_3 , MoO_3 , Fe_2O_3 and ZnO have been studied by the group of Matyshak [69-72] using spectrokinetic method. Surface complexes $\text{NH}_{3\text{ads}}$, $\text{NH}_{2\text{ads}}$, and NO_{ads} were shown to be intermediate species. They concluded that ammonia oxidation was first preceded by ammonia adsorption in the form of coordinated ammonia and then through an oxy-dehydrogen step producing NH_2 . The NH_2 could be directly oxidized to NO, which will react with NH_2 to give N_2 . The N_2O was believed to be produced by NO_2 reacting with NH_2 :



The adsorption and oxidation of ammonia over sub-monolayer TiO_2 -anatase supported chromium, manganese, iron, cobalt, nickel and copper oxides, has been investigated using FT-IR spectroscopy by Ramis et al. [73-75]. NH_2 , HNO and N_2H_4 intermediate species were observed. They figured out that the following mechanism was active:



Under SCO catalytic reactions the following reoxidation reaction closes a Mars-Van Krevelen-type redox mechanism:



In summary on both metal and metal oxide catalysts two major routes have been proposed in the literature for the selective production of N_2 from the oxidation of ammonia. The first is a direct route based on the oxidation of NH_x species directly to atomic nitrogen and then the recombination of two nitrogen atoms forming N_2 , or the recombination of NH_x species giving rise to an hydrazinium intermediate N_2H_4 and then oxidizing to N_2 . The other is the in situ or “internal” selective catalytic reduction (SCR) and is a two-step mechanism, in which the NH_x species are oxidized to NO_x species in the first step. The NO_x species reacted consequently with NH_x species giving rise to N_2 through a surface SCR reaction.

5. Scope of this thesis

It can be seen from above review that various catalysts of different types have been tested for the low temperature ammonia oxidation reaction: biological catalysts, metal oxide catalysts, ion-exchanged zeolites and metallic catalysts. When the various types of catalysts are compared it appears that the metallic catalysts such as Pt and Ir are the most active but less selective. Significant amounts of N_2O are produced on these catalysts. The metal oxide catalysts such as CuO , V_2O_5 and MoO_3 show very

promising selectivity but the reaction temperature needed is too high to be matched with some industrial applications.

The research described in this thesis was aimed at the development of new, active and selective catalysts for low temperature (<300 °C) selective ammonia oxidation to nitrogen. In Chapter 2 an elementary catalyst screening study was performed in order to find new catalysts for the SCO reaction. The emphasis was on zeolite-based and alumina-supported metal or metal oxide catalysts. Copper-based and silver-based catalysts were found to be the most promising catalysts for low temperature SCO process. Therefore in Chapter 3 various kinds of copper oxides supported on alumina and on zeolite Y have been prepared and studied in detail. TPD, TPR, UV-vis spectroscopy and high-resolution electron microscopy (HREM) were used to characterize these catalysts in an attempt to shed light on the optimal preparation for active and selective low-temperature ammonia oxidation catalysts. The results showed that a CuAl_2O_4 -like phase was more active than a CuO phase for SCO reaction. For copper zeolite catalysts $[\text{Cu-O-Cu}]^{2+}$ -like species or small copper oxygen aggregates were the likely forms of the catalytically active centers at low temperature. The activity of CuY was increased by treating the sample with NaOH. This treatment presumably increases the amount of low temperature active centers. In Chapter 4 ammonia oxidation reaction pathways on high surface area silver powder have been studied by TPD, TPR, FT-Raman and transient as well as steady-state ammonia oxidation experiments. It was found that NO was the main reaction intermediate to give N_2O as well as N_2 . Even at room temperature NO could be formed and, when oxidized to NO_x , it could become adsorbed to the silver surface, which will block the active sites for oxygen activation. The adsorption of oxygen was thus believed to be the rate-controlling step for ammonia oxidation. The adsorbed NO_x , N_2O_x species were actually inhibitors for ammonia oxidation but these adsorbed species lowered the surface oxygen coverage. So the selectivity to nitrogen was improved with the increasing amount of these adsorbed species. In Chapter 5 low temperature gas phase oxidation of ammonia to nitrogen has been studied over alumina-supported, silica-supported and unsupported silver catalysts to distinguish the support effect on silver-based catalysts. TPD, TPR, TEM, XRD and FT-Raman were used to characterize the different silver catalysts. The results showed alumina-supported silver to be the best catalyst due to the interaction of silver with alumina. Pretreatment had a great affect on the catalyst performance. Reduction in hydrogen at 200 °C without any pre-calcination gave the best activity while reduction at higher temperatures showed little difference from calcination pretreatment. At least four types of oxygen species were produced when silver was oxidized at high temperature. These species are adsorbed molecular oxygen, adsorbed atomic oxygen, strongly adsorbed atomic oxygen and

subsurface oxygen respectively. Ammonia oxidation activity at low temperature is related to the catalyst's ability to dissociatively or non-dissociatively adsorption of oxygen. In addition, a good correlation existed between the N_2 selectivity for SCO reaction and the SCR performance of NO with NH_3 for the silver-based catalysts, i.e., the higher SCR yield of nitrogen, the higher the SCO N_2 selectivity. In Chapter 6 a new bi-functional copper-silver catalyst was developed based on the reaction mechanism study, which showed not only high activity but also high selectivity for ammonia oxidation. The silver was very active for ammonia oxidation to NO but less active for SCR reaction to nitrogen. Therefore a large amount of N_2O was produced on catalysts with silver alone. With the introduction of copper into silver-based catalysts the SCR reaction to nitrogen increased greatly and thus the selectivity to nitrogen increased accordingly.

References

- [1] E. Buijsman and W. Asman, *Chemisch Magazine*, 12 (1983) 654.
- [2] A.J. Frantzen, R. Adolphs and W. Schipper, *Lucht en Omgeving*, 10 (1985) 132.
- [3] E.H.T.M. Nijpels and G.J.M. Braks, *Nationaal Milieubeleidsplan* (National environmental management scheme), Tweede kamer, vergaderjaar 1988-1989, 21, 137, No. 1-2: 1-258.
- [4] T. Schneider and A.H.M. Bresser, Dutch priority program on acidification: program and projects-RIVM 00-04: 1-75.
- [5] S.I. Bestebroer and A.J. Elshout, *Electrotechniek*, 67 (1989) 233.
- [6] Manure causing white haze, *Sci. Environ. Bull.*, 8 (1999) 12.
- [7] M. Amblard, R. Burch and B.W.L. Southward, *Appl. Catal. B* 22(3) (1999) L159.
- [8] J.J.P. Biermann, Ph.D. Thesis, University of Twente, Twente, 1990.
- [9] M. Amblard, R. Burch and B.W.L. Southward, *Catal. Today*, 59 (2000) 365.
- [10] UK power goes green and clean, BBC News Website, December 11, 1998.
- [11] Development of improved stable catalysts and trace element capture for hot gas cleaning, DTI/ETSU/Clean Power Generation Group, Project Profile No. 178, 1996.
- [12] Coordinatiecommissie Doelgroepmonitoring, December 1999, Emissies en afval in Nederland, Jaarrapport 1997 en ramingen 1998, No. 1, p16.
- [13] R.W. Wilson, *J. Water Pollut. Control Fed.*, 53(8) (1975) 34.
- [14] Process Design Manual for Nitrogen Control, U.S. Environmental Protection Agency, 1975.
- [15] T.H. Davies and S.Y. Ip, *Water Res.*, 15(5) (1981) 65.
- [16] J.G. Gonzales and R.L. Culp, "New Developments in Ammonia Stripping, Part One", *Pub. Works* (May 1973).

- [17] T.Y. Yan and P. Wayne, U.S. Patent, 5552063, 1996.
- [18] M. Ljiljama and F.B. Leitz, The electro oxidation of ammonia in sewage to nitrogen, Environmental Protection Agency, PB 204526, 1970.
- [19] H. Bosch and F. Janssen, *Catal. Today*, 2 (1988) 369.
- [20] M. Wojciechowska, On the catalytic removal of nitrogen oxides, in *Catalysis and adsorption in fuel processing and environmental protection*, proc. 3rd international conference Kudowa Zdroj Poland (1999).
- [21] A. Fritz and V. Pitchon, *Appl. Catal. B*, 13 (1997) 1.
- [22] C.H. Liang, W.Z. Li, Z.B. Wei, Q. Xin and C. Li, *Ind. Eng. Chem. Res.*, 39 (2000) 3694.
- [23] F. Qiu and S. Lu, *Chin. J. Appl. Chem.*, 5 (1988) 39.
- [24] W. Mojtahedi and J. Abbasian, *Fuel*, 74 (1995) 1698.
- [25] G.I. Golodets, *Heterogeneous Catalytic Reactions Involving Molecular Oxygen in: Studies in Surface Science and Catalysis*, (Ed J.R. Ross), p.312, Elsevier, Amsterdam, 1983.
- [26] N.I. Il'chenko, *Russian Chem. Rev.*, 45(12) (1976) 1119.
- [27] J.E. Germain and R. Perez, *Bull. Soc. Chim. France*, 2 (1972) 2024.
- [28] J.J. Ostermaier, J.R. Katzer and W.H. Manogue, *J. Catal.*, 41 (1976) 277.
- [29] J.J. Ostermaier, J.R. Katzer and W.H. Manogue, *J. Catal.*, 33 (1974) 457.
- [30] J.E. Delaney and W.H. Manogue, *Proc. Int. Congr. Catal.* 5th, 1 (1973) 267.
- [31] O.V. Al'tshuller and M.Ya. Kushnerev, *Problemy Kinetiki I Kataliza*, 15 (1973) 56.
- [32] T. Shikada, M. Asannma and Y. Tachibana, US Patent 5,139,756 (1992).
- [33] M. de Boer, A.J. van Dillen and J.W. Geus, *Catalysis Letters*, 11 (1991) 227.
- [34] F.J.J.G. Janssen and F.M.G. van den Kerkhof, *Selective Catalytic Removal of NO from Stationary Sources*, KEMA Sci. & Techn. Reports, 3(6) (1985).
- [35] J.P. Chen and R.T. Yang, *Appl. Catal.*, 80 (1992) 135.
- [36] G. Tuenter, W.F. van Leeuwen and L.J.M. Snepvangers, *Ind. Eng. Chem. Prod. Res. Dev.*, 25 (1986) 633.
- [37] E.T.C. Vogt, A. Boot, J.W. Geus and F.J.J.G. Janssen, *J. Catal.*, 114 (1988) 313.
- [38] E.T.C. Vogt, Ph.D. Thesis, University of Utrecht(1988).
- [39] J.J.P. Biermann, F.J.J.G. Janssen and J.W. Geus, *J. Mol. Catal.*, 60 (1990) 229.
- [40] N.N. Sazonova, A.V. Simakov and H. Veringa, *React. Kinet. Catal. Lett.*, 57(1) (1996) 71.
- [41] F. Dannevang, US Patent 5,587,134 (1996).
- [42] Y. Li and J.N. Armor, *Appl. Catal. B*, 13 (1997) 131.
- [43] A. Wollner and F. Lange, *Appl. Catal. A*, 94 (1993) 181.
- [44] Andrussov, L., *Z. Ang. Ch.*, 39 (1926) 321.
- [45] Bodenstein, M., *Z. Elektroch.*, 41 (1935) 466.

- [46] Bodenstein, M., *Z. Elektroch.*, 47 (1935) 501.
- [47] Raschig, F., *Z. Ang. Ch.*, 40 (1927) 1183.
- [48] Zawadzki, J., *Disc. Faraday Soc.*, 8 (1950) 140.
- [49] L. Andrussov, *Z. Elektroch.*, 36 (1930) 756.
- [50] M. Bodenstein, *Z. Ang. Ch.*, 40 (1927) 174.
- [51] B. Neumann and H. Rose, *Z. Ang. Ch.*, 33 (1920) 41.
- [52] L. Andrussov, *Z. Ang. Ch.*, 40 (1927) 166.
- [53] Fogel, Ya.M., Nadykto, B.T., Rybalko, V.F., Shvachko, V.I., and Korobchanskaya, I.E., *Kinet. Catal.*, 5 (1964) 431.
- [54] C.W. Nutt and S. Kapur, *Nature*, 220 (1968) 697.
- [55] C.W. Nutt and S. Kapur, *Nature*, 224 (1968) 169.
- [56] Asscher, M., Guthrie, W.L., Lin, T.H., and Somorjai, G.A., *J. Phys. Chem.*, 88 (1984) 3233.
- [57] Mieher, W.D., and Ho, W., *Surf. Sci.*, 322 (1995) 151.
- [58] Bradley, J.M., Hopkinson, A., and King, D.A., *J. Phys. Chem.*, 99 (1995) 17032.
- [59] Van den Broek, A.C.M., Van Grondelle J., and Van Santen, R.A., *J. Catal.*, 185(2) (1999) 297.
- [60] Van den Broek, A.C.M., Ph.D. Thesis, Eindhoven University of Technology, 1998.
- [61] A. Fahmi and R.A. van Santen, *J. Phys. Chem.*, 197 (1996) 203.
- [62] Carley, A.F., Davies, P.R. and Roberts, M.W., *Chem. Commun.*, 35 (1998) 1793.
- [63] Carley, A.F., Davies, P.R., Kulkarni G.U., and Roberts, M.W., *Catal. Lett.*, 58 (1999) 97.
- [64] Afsin, B., Davies, P.R., Pashusky, A., Roberts, M.W., and Vincent, D., *Surface Science.*, 284 (1993) 109.
- [65] X.C. Guo and R.J. Madix, *Faraday Discuss.*, 105 (1996) 139.
- [66] Thornburg, D.M., and Madix, R.J., *Surf. Sci.*, 220 (1989) 268.
- [67] Carley, A.F., Davies, P.R., Roberts, M.W., Thomas, K.K. and Yan, S., *Chem. Commun.*, 35(1998)12.
- [68] Carley, A.F., Davies, P.R. and Roberts, M.W., *Current Opinion in Solid State and Materials Science*, 2(5) (1997) 525.
- [69] V.A. Matyshak, O.N. Sil'chenkova, I.N. Staroverova and V.N. Korchak, *Kinetics and Catalysis*, 36(5) (1995) 677.
- [70] O.N. Sil'chenkova, A.A. Ukharskii and V.A. Matyshak, *Kinetics and Catalysis*, 35(5) (1994) 708.
- [71] V.A. Matyshak, A.A. Burkhardt and K.H. Schnabel, *Kinet. Katal.*, 26(2) (1995) 334.
- [72] V.A. Matyshak, *Kinet. Katal.*, 30(1) (1989) 160.

- [73] J.M.G. Amores, V.S. Escribano, G. Ramis and G. Busca, Appl. Catal. B, 13 (1997) 45.
- [74] G. Ramis, L. Yi and G. Busca, Catalysis Today, 28 (1996) 373.
- [75] M. Trombetta, G. Ramis, G. Busca, B. Montanri and A. Vaccari, Langmuir, 13 (1997) 4628.
- [76] A.C.A. de Vooy, Ph.D. Thesis, Technical University of Eindhoven, Eindhoven, 2001.

Chapter 2

NH₃ oxidation to nitrogen and water at low temperatures using supported metal or metal oxide catalysts

Abstract

The ability of several alumina-supported metal or metal oxide catalysts and transition-metal ion-exchanged zeolite Y catalysts to oxidize ammonia to nitrogen and water at low temperature (between 200° and 350 °C) was tested both at high and at low ammonia concentrations. Copper-containing zeolite Y catalysts were comparable in activity and were more selective than alumina-supported noble metal catalysts. Cu / zeolite-Y catalysts were superior to copper / molybdenum and vanadium / alumina catalysts. Post-synthesis treatment of Cu / zeolite-Y with NaOH increased the activity for ammonia oxidation; dispersion and size of the supported copper-oxide particles were very important parameters. Alumina-supported silver catalysts showed very high activity and selectivity for ammonia oxidation at high ammonia concentration. At low ammonia concentration, silver catalysts were even more active than noble metal catalysts but the selectivity to nitrogen was not satisfying. Co-fed steam dramatically increased the deactivation on all catalysts, especially at lower temperatures. The selectivity to nitrogen was greatly decreased by decreasing the ammonia concentration. At high O₂/NH₃ ratio the activity of all catalysts increased but the selectivity for nitrogen production decreased.

1. Introduction

The removal of ammonia from air or water is environmentally important. Currently, ammonia is removed from industrial flue gases via biological treatment, by absorption, or by thermal combustion. An attractive alternative process is the use of selective catalytic oxidation to nitrogen and water. Such technology may also find application in combination with the selective catalytic reduction (SCR) process in which NO_x is reduced to nitrogen using ammonia. At present unreacted ammonia is present in the off-gas and must therefore be removed in a secondary step [1,2].

Early research involving ammonia oxidation has been reviewed and the activities of several metals and metal-oxides for nitrogen and NO_x formation at low temperature have been systematically compared [3]. Most of these studies involved either single, poly-crystalline metals or simple metal oxides. Supported metals, supported metal-oxide, metal alloys, and mixed- metal oxides have been studied to a lesser extent. Several papers have been published regarding the ammonia oxidation over alumina-supported platinum catalysts [4-6]. It was discovered that significant deactivation occurred on these catalysts at temperatures below 200 °C. To date zeolite Y is to our knowledge the only zeolite studied in some detail for this reaction [7]. Some initial screening studies have also been reported for ZSM-5 [8]. Investigations involving ammonia oxidation on V₂O₅, WO₃ and MoO₃, themselves supported on various metal-oxides, at temperatures between 300° and 400 °C have been reported [9-15]. Of these, the best catalyst reported was a silica- supported, PbO-promoted, molybdenum catalyst on which ammonia could be oxidized with 100 % selectivity to nitrogen at temperatures of about 400 °C [13]. Li and Armor studied the selective NH₃ oxidation to N₂ in wet streams over ion-exchanged ZSM-5 and alumina-supported Pd, Rh and Pt catalysts at 200° to 350 °C [16]. They concluded that the ammonia conversion was not affected by co-feeding steam at high temperature but was decreased at lower temperatures (200° - 250 °C) when 5 vol % water vapor was added. Generally, ion-exchanged ZSM-5 catalysts were more active than alumina-supported catalysts of identical metal loadings and were less affected by the addition of water vapor. The selectivity to N₂ was observed to be relatively high on Rh and Pd catalysts and low on Pt catalysts. Wollner reported that high degrees of ammonia conversion (80 – 100 %) could be obtained over mixed copper- / manganese-oxides supported on titania at temperatures greater than about 300 °C [17]. Unfortunately the selectivity of this process was not clearly reported.

The above studies show that noble metals such as platinum are very active for ammonia oxidation but form large amounts of nitrogen oxides. Although supported

molybdenum and vanadium catalysts show very promising selectivity, the reaction temperature needed is a too high to be matched with some industrial applications. The aim of this study is the development of active new catalytic materials that are capable of selective oxidation of ammonia to nitrogen at low temperatures. For this purpose we have screened the performance of several transition-metals deposited either onto alumina (by incipient wetness impregnation) or into sodium zeolite Y by ion-exchange. The results obtained are reported below.

2. Experimental

2.1. Catalyst preparation

Ion-exchanged CuNaY, CoNaY, AgNaY, ZnNaY, MnNaY and FeNaY catalysts

Ion-exchange was performed using: Cu(NO₃)₂·3H₂O, Co(NO₃)₂·6H₂O, AgNO₃, Zn(NO₃)₂·6H₂O, MnSO₄·H₂O and Fe(NO₃)₃·9H₂O. In most cases the sodium form of zeolite Y (NaY from Akzo, Si/Al=2.4) (10g) was stirred for 24 hours at room temperature in aqueous solutions (400 ml, dissolved metal salt concentration adjusted to match 100% Na ion exchange). In the case of (Fe / Na) ion-exchange, only 2 hours of stirring were required. The slurry was then filtered and the solid was washed three times with deionized, distilled water and oven-dried at 110 °C overnight. Catalysts were made into pellets by compressing the powder using 10 ton pressure (250-425 µm particles). The catalysts were activated at 400 °C for 2 hours in a flow of oxygen / helium (20 / 80: v/v) before catalyst testing.

Alumina-supported Cu, Ag, Mo, V, Pt, Ir, Rh, Pd catalysts

These catalysts were prepared by incipient wetness impregnation. A commercial γ-Al₂O₃ (Akzo/Ketjen 000 1.5E) with a specific surface area of 235 m²/g and a BET pore volume of 0.55 ml/g was used as support. The precursors were: Cu(NO₃)₂·3H₂O, AgNO₃, (NH₄)₆Mo₇O₂₄·4H₂O, NH₄VO₃, H₂PtCl₆, IrCl₃·3H₂O, Rh(NO₃)₃, PdCl₂. Metal loadings (weight percent) were: 5-15%, 10-15%, 15%, 10%, 1.2%, 1.2%, 1.2 %, 1.2 % respectively. All catalysts were calcined in flowing air at 500 °C for 24 hours before testing.

2.2. Catalyst testing

Catalytic activity measurements were carried out in a quartz-tube, fixed-bed reactor (4mm internal diameter). About 0.2 g catalyst was used (250-425 μm particles). Experiments were performed using either an excess of ammonia or an excess of oxygen. Ammonia, oxygen and helium flow rates were controlled using mass-flow meters. Water vapor was introduced by passing the helium flow through a water saturator at elevated temperature ($T = 50\text{ }^{\circ}\text{C}$). The inlet and outlet gas compositions were analyzed by a gas chromatograph equipped with a thermal conductivity detector. A quadruple mass spectrometer was also used to distinguish different products. For kinetic measurement of the catalysts, the conversion of ammonia was kept below 10 %. The amount of catalyst used was 0.1 gram. The reactor was assumed to be differential at low conversion, using calculated estimations of diffusion and heat transfer. The catalyst bed was proved experimentally to be isothermal. No internal diffusion was observed when decreasing the particle size further.

3. Results and Discussion

3.1. Zeolite-based catalysts

Various ion-exchanged Na zeolite-Y catalysts were tested and the resulting ammonia conversion and nitrogen selectivity data are shown in Table 1. Clearly, only CuY is very active and selective for ammonia oxidation. All of the other ion-exchanged catalysts had almost no activity, in fact they are worse than NaY itself. This is quite different from the simple metal-oxide catalysts published in the literature.

Table 1. Activity of various transition-metal ion-exchanged zeolite Y catalysts for ammonia oxidation.

catalyst	Temperature $^{\circ}\text{C}$	NH ₃ conversion %	N ₂ selectivity %
CuY	400	94	98
NaY	400	18	99
CoY	400	4.5	--
AgY	400	0.6	--
ZnY	400	2.3	--
MnY	400	1.7	--
FeY	400	13	96

Reaction conditions: NH₃ = 1.33%; O₂ = 0.91%; H₂O = 2.08%; (vol%)
flow rate = 30.7 Nml/min; cat. Weight = 0.2g

Table 2. The affect of post-synthesis NaOH treatment on the zeolite Y catalysts.

catalyst	temperature °C	NH ₃ conversion %	N ₂ selectivity %
CuY (3.7 wt%)	250	16	97
	300	54	98
CuY (8.4 wt%)	250	25	97
	300	88	97
CuY(3.7%) (after NaOH treatment)	200	19	97
	250	56	97
	300	100	98
CuY(8.4%) (after NaOH treatment)	200	35	95
	250	68	97
	300	100	98
AgY (after NaOH treatment)	250	11	75
	300	81	80
CoY (after NaOH treatment)	250	14	71
	300	42	75

Reaction conditions: NH₃ = 1.14 vol%; O₂ = 8.21%; flow rate = 74.7 Nml/min; cat. weight = 0.2g

Ione et al. [18] and Schoonheydt et al. [19] reported that polynuclear nickel or copper-ion complexes were formed in the framework of zeolite Y when NaY was ion-exchanged with aqueous Ni(NO₃)₂ or Cu(NO₃)₂ solutions at pH 6-7. These polynuclear cations gave a higher activity for CO oxidation than did the mononuclear ions. Suzuki et al. also successfully prepared an excellent CO oxidation catalyst of highly-dispersed, nickel-oxide catalyst by hydrolysing a Ni²⁺-exchanged zeolite Y with either aqueous NaOH or ammonia solutions at different pH values. We were curious to see the effect that such NaOH treatment would have on the ammonia oxidation reaction. Table 2 shows resulting conversion and selectivity data obtained following treatment of zeolite-based catalysts with NaOH solutions (pH = 10) following ion-exchange. This treatment procedure was the same as proposed by Suzuki et al. [20,21].

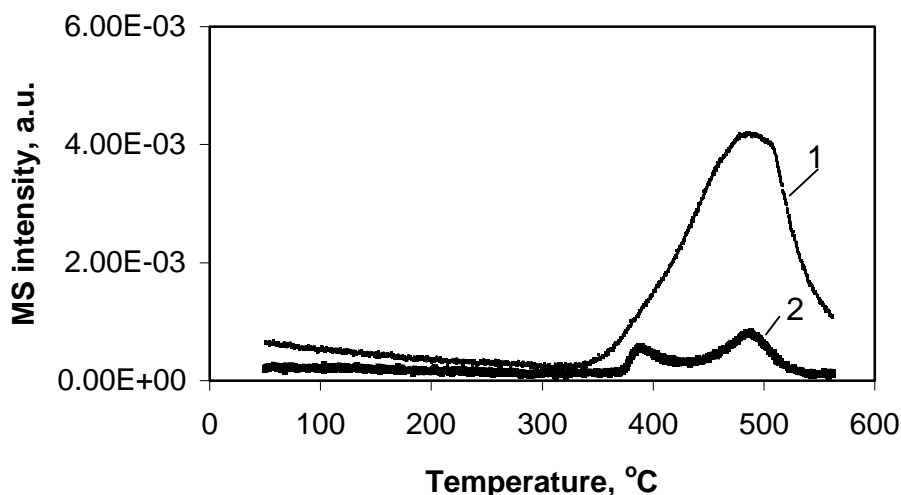


Fig.1 Temperature-programmed O₂ desorption profiles obtained on CuY (8.4 wt%) catalysts with (1) and without (2) treatment using NaOH following ion-exchange. (Desorption in flowing He (50 Nml/min), ramp rate = 10 °C/min, cat. weight = 0.6g)

The activity of all metal zeolite catalysts for ammonia oxidation increased drastically following this NaOH treatment. This significantly higher activity was apparently induced by the formation of small metal-oxide particles in the zeolite. As can be seen in Fig.1 there are two peaks for O₂ TPD profiles on an 8.4 wt % copper ion-exchanged zeolite Y (CuY-8.4) catalyst. Since no O₂ desorption is observed on NaY, these two O₂ desorption peaks must involve the Cu on the zeolite. Following NaOH treatment the amount of O₂ desorbed was greatly increased. Many studies on the complete oxidation of CO and of hydrocarbons have shown that the activity is directly dependent on the amount of adsorbed oxygen [22,23]. This increased oxygen adsorption capacity of the catalyst following NaOH treatment may be the reason for the enhanced performance in ammonia oxidation.

Table 3. Activity of various alumina-supported transition-metal catalysts for ammonia oxidation.

catalyst	Temperature °C	NH ₃ conversion %	N ₂ selectivity %
Cu/Al ₂ O ₃ (5 wt%)	250	0	--
	300	21	97
	350	75	96
Cu/Al ₂ O ₃ (10 wt%)	250	15	97
	300	90	96
	350	100	90
Cu/Al ₂ O ₃ (15 wt%)	250	9	97
	300	46	96
	350	100	94
Ag/Al ₂ O ₃ (10 wt%)	200	11	91
	250	98	86
Ag/Al ₂ O ₃ (15 wt%)	200	19	92
	250	100	88
Mo/Al ₂ O ₃ (15 wt%)	300	8	88
	400	74	89
V/Al ₂ O ₃ (10%)	400	45	95

Reaction conditions: NH₃ = 1.14%; O₂ = 8.21%; (vol%)
flow rate = 74.7 Nml/min; cat. weight = 0.2g

3.2. Alumina-supported metal catalysts

Metal particle size is known to be an important parameter in the activity of catalysts for ammonia oxidation. The size of metal particles on alumina can easily be controlled by varying the metal-loading, the calcination temperature, or the calcination time. Several such experiments were performed on alumina-supported metal catalysts. The results are shown in Table 3. It can be seen that alumina-supported silver catalysts are very active and selective for ammonia oxidation. Increasing silver loading will increase the activity of ammonia oxidation. Alumina-supported copper catalysts are also very active for ammonia oxidation. There exists an optimal metal loading that may indicate that copper dispersion becomes poorer on alumina at metal-loading higher than circa 10 wt%. Indeed, results previously obtained by us using high-resolution transmission electron microscopy (HREM) and ultraviolet spectroscopy revealed the absence of either copper or copper oxide particles of detectable size on alumina at loading of 10 wt % or lower [24]. However, small particles of CuO were detected at 15 wt %. The fact that zeolite-based copper catalysts are superior to alumina-supported copper catalysts may be attributable to the high dispersion of copper in the zeolite. As shown in Table 3, the conventionally used

supported-molybdenum and supported-vanadium catalysts cannot compete with copper catalysts at low temperature.

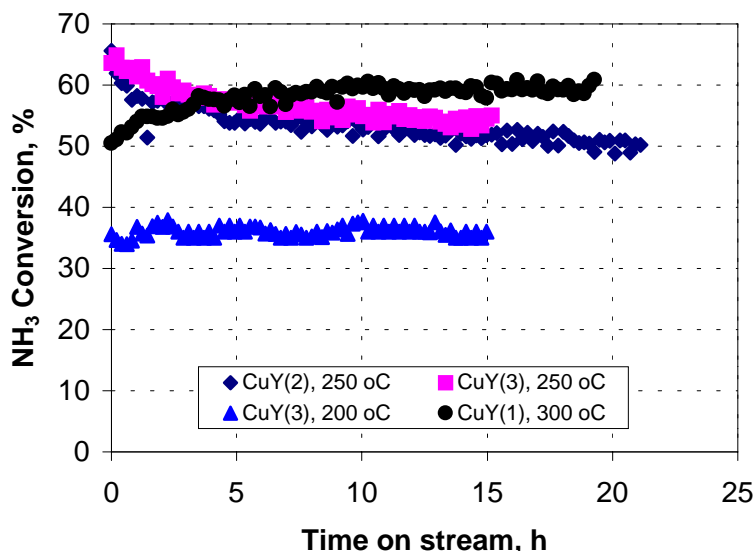


Fig. 2 The stability of Cu-zeolite Y catalysts: NH₃ conversion vs. time on stream at different reaction temperatures.

CuY(1)---ion-exchanged with 8.4 wt% loading;

CuY(2)---after NaOH treatment, 3.7 wt%;

CuY(3)---after NaOH treatment, 8.4 wt%

(Reaction conditions: NH₃ = 1.14 vol%; O₂ = 8.21 vol%; Flow rate = 74.7 Nml/min; cat. weight = 0.2g)

3.3. The stability of catalysts

Fig.2 shows the measured NH₃ conversion versus time on stream at various temperatures for Cu-ion exchanged catalysts under high ammonia concentration conditions. It can be seen in the figure that the catalysts were fairly stable. Catalysts subjected to NaOH treatment showed a slight initial deactivation at 250 °C. But at 200 °C deactivation was absent. The CuY catalyst untreated by NaOH showed a very stable activity, perhaps even a slight increase in activity with time. Large initial deactivation was observed for alumina-supported copper and for the reduced noble metal catalysts (see Fig. 3) during similar ammonia oxidation experiments. At low ammonia concentration conditions no deactivation was observed during one-day catalyst testing on all types of catalysts. As all of the alumina-based catalysts were calcined at high temperature and there were no hydrocarbons in the reaction system, metal sintering and coking were excluded as possible causes of this deactivation. Our experiment also showed that the activity could be recovered completely by calcining the deactivated catalyst at 500 °C again. This indicates that the metal sintering in our

case is very unlikely. The most probable reason for deactivation is either reconstruction of the metal surface or a change in the chemical state of the surface caused by ammonia-induced species since ammonia concentration has a great influence on the catalyst deactivation behavior.

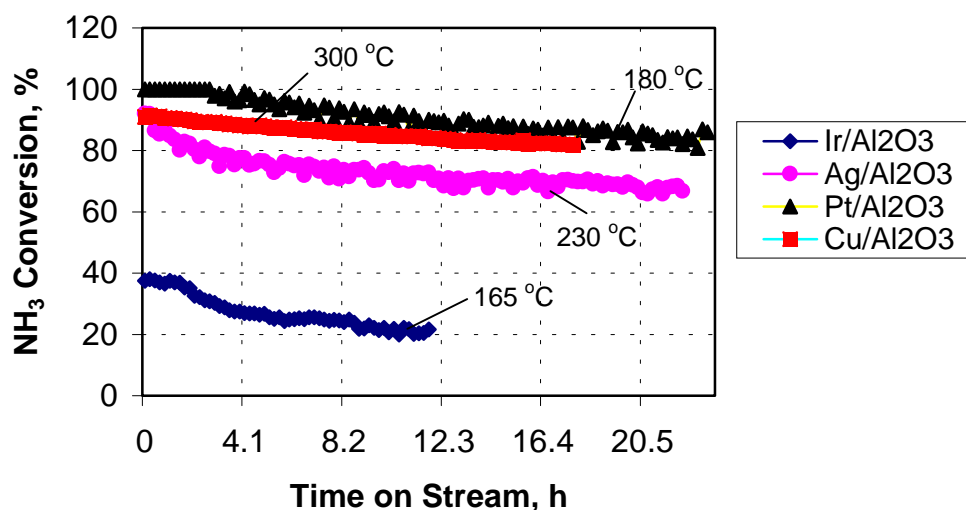


Fig. 3 The stability of various alumina-supported, transition-metal catalysts during ammonia oxidation at different temperatures ($\text{NH}_3 / \text{O}_2 = 0.14 \text{ v / v}$, flow rate=74.7 Nml/min, $[\text{NH}_3] = 11400 \text{ ppm}$ in He, cat. weight = 0.2g)

3.4. Effect of O_2 / NH_3 ratio and water vapour

The O_2 / NH_3 ratio had a large affect on both the activity and the selectivity of all catalysts. Increasing the O_2 / NH_3 ratio increased the activity but decreased the selectivity (see Table 4). It should be noticed that the activity of silver-based catalysts was greatly increased compared with other catalysts when the O_2 / NH_3 ratio was increased. However, the O_2 / NH_3 ratio had less influence on the selectivity of CuY catalyst. Co-fed steam in the feed gas lowered the activity of the catalysts at low temperature but had less effect at high temperature (see Table 5). Since the ammonia oxidation reaction is irreversible, water should have no effect on this reaction from thermodynamic point of view. This effect may be caused by the adsorption of water or by condensation of water on the catalysts resulting in partial blocking of the active sites.

Table 4. The dependence of the activity for ammonia oxidation on O₂/NH₃ feed ratio.

catalyst	temperature (°C)	O ₂ / NH ₃ ratio	NH ₃ conversion (%)	N ₂ selectivity (%)
CuY (8.4 wt%)	300	0.68	21	99.5
	300	2.60	46	99.0
	300	7.20	88	97
Ag/Al ₂ O ₃ (10 wt%)	300	0.68	12	92
	300	2.60	75	86
	300	7.20	100	83
Pt/Al ₂ O ₃ (1.2 wt%)	200	0.68	66	90
	200	2.60	86	89
	200	7.20	100	87

Flow rate = 74.7 Nml/min; cat. wt. = 0.2g; [NH₃] = 11400 ppm

Table 5. The effect of co-fed water vapor on the activity during ammonia oxidation.

Catalyst	Temperature °C	feed	NH ₃ conversion %	N ₂ selectivity %
Cu/Al ₂ O ₃ (10 wt%)	300	dry	90	96
	300	wet	21	97
	350	dry	100	94
	350	wet	100	95
Ag/Al ₂ O ₃ (10 wt%)	230	dry	63	88
	230	wet	38	90
	300	dry	100	83
	300	wet	100	85
CuY(8.4wt%) (NaOH treatment)	250	dry	56	97
	250	wet	15	98
	300	dry	100	98
	300	wet	82	97
	350	wet	100	98

Reaction conditions: NH₃ = 1.14%; O₂ = 8.21%; H₂O = 5.2%
flow rate = 74.7 Nml/min; cat. weight = 0.2g

3.5. Effect of ammonia concentration

In recent years considerable attention has been focused on the catalytic removal of ammonia from flue gases. The ammonia concentration in such exhaust streams is often quite low (<1000ppm). Since the surface concentration of nitrogen-containing

substances plays an important role in the selectivity of the ammonia oxidation, some influence of NH₃ concentration on the activity and on the selectivity of the catalyst may be expected. It has been shown previously, over supported-molybdenum catalysts [15], that both the activity and the selectivity were greatly decreased by decreasing the ammonia concentration.

Table 6. The activity of various catalysts for ammonia oxidation at low ammonia feed concentration (1000 ppm) in helium.

catalyst	Temperature °C	NH ₃ conversion %	N ₂ selectivity %
Ir/Al ₂ O ₃ (1.2 wt%) (reduced)	180	52	88
	190	91	86
	200	100	84
Pt/Al ₂ O ₃ (1.2 wt%) (reduced)	180	66	75
	190	96	74
	200	100	75
Cu/Al ₂ O ₃ (10 wt%)	200	16	93
	230	66	86
	250	95	82
CuY(8.4 wt%) (with NaOH treated)	200	36	92
	230	73	95
	250	100	94
Ag/Al ₂ O ₃ (10 wt%)	130	56	82
	140	95	82
	160	100	81

Reaction conditions: NH₃ = 1000 ppm; O₂ = 10%; O₂/NH₃ = 100
flow rate = 50 Nml/min; cat. weight = 0.1g

Oxidation of ammonia at low concentrations (1000 ppm NH₃ in He) was investigated at low temperatures and the results are shown in Table 6. In all cases, the observed selectivity of the catalysts decreased relative to those observed previously at higher concentrations. However, the selectivity observed on CuY catalysts at low concentrations still exceeded that obtained either on copper-alumina or on noble-metal catalysts under similar conditions. The measured performance of these catalysts at higher NH₃ concentration (11400 ppm NH₃ in He) is shown in Table 7.

Table 7. Activity of various catalysts for ammonia oxidation at high ammonia concentration (11400 ppm NH₃ in helium).

catalyst	Temperature °C	NH ₃ conversion	N ₂ selectivity
		%	%
CuY(8.4%) (NaOH treated)	200	35	95
	230	52	96
	250	63	97
Ag/Al ₂ O ₃ (10 wt%)	200	11	91
	230	67	89
	250	98	86
Pt/Al ₂ O ₃ (1.2 wt%) (reduced)	180	9	83
	190	33	82
	200	100	87
Ir/Al ₂ O ₃ (1.2 wt%) (reduced)	165	32	92
	180	87	94
	200	100	95
Rh/Al ₂ O ₃ (reduced) (1.2 wt%)	350	25	90
	380	78	88
	400	100	86
Pd/Al ₂ O ₃ (reduced) (1.2 wt%)	250	60	97
	280	88	97
	300	100	98

Reaction conditions: NH₃ = 1.14 vol %; O₂ = 8.21 vol %; O₂/NH₃ = 7.2
flow rate = 74.7 Nml/min; cat. weight = 0.2g

Table 8. Kinetic measurements over different catalysts

Catalyst	reaction order in	reaction order in	E _{act} (kJ/mole)
	O ₂	NH ₃	
Ag/Al ₂ O ₃ ^a	0.61	0.21	65
CuY ^b	0.18	0.46	35
Pt/Al ₂ O ₃	0.32	0.10	92
Ir/Al ₂ O ₃ ^c	0.24	0.06	128

^a: order measured at 200 °C, E_{act} determined at 150-200 °C

^b: order measured at 140 °C, E_{act} determined at 140-160 °C

^c: order measured at 200 °C, E_{act} determined at 170-200 °C

3.6. Kinetic studies over different catalysts

The results of the steady state kinetic measurements for different catalysts are given in Table 8. Compared with noble metal catalysts the Ag/Al₂O₃ and CuY catalysts have a much lower activation energy. This means that temperature has more influence on

noble metal catalysts than on Ag/Al₂O₃ and CuY catalysts. It is clear that Ag/Al₂O₃ is very sensitive to oxygen concentration since it has the highest reaction order in oxygen. The CuY catalyst shows the highest reaction order in ammonia and for the same reason the ammonia concentration has a great influence on this catalyst. On the contrary the reaction orders in ammonia for noble metal catalysts are extremely low, which indicates much less influence of ammonia concentration on the activities of these catalysts.

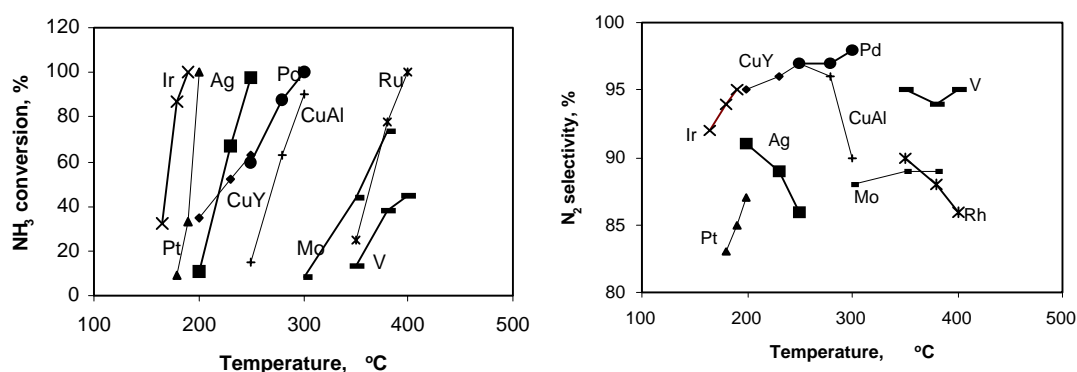


Fig. 4 Comparison of different catalysts for high concentration of ammonia oxidation
(reaction conditions are same as in Table 7)

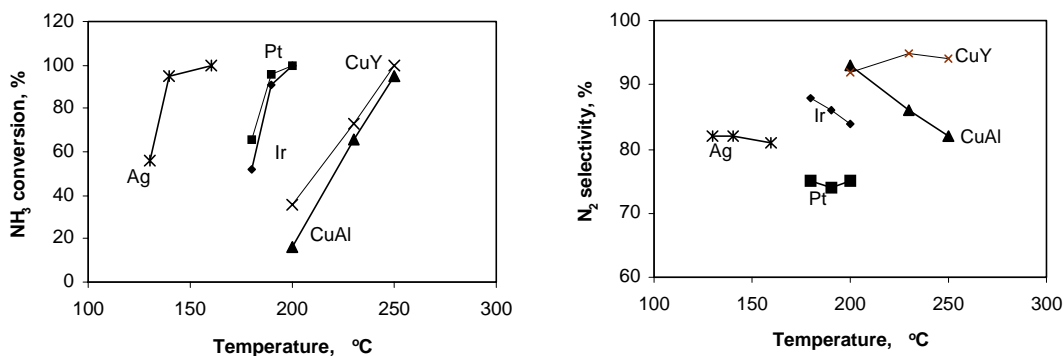


Fig. 5 Comparison of different catalysts for low concentration of ammonia oxidation
(reaction conditions are same as in Table 6)

3.7. Comparison with the noble metal catalysts

For clearly comparison the results of Table 7 and Table 6 are plotted in Fig.4 and Fig.5. It can be seen evidently that noble metal catalysts are very active especially at high ammonia concentration, however their selectivity to nitrogen is very poor at low

ammonia concentration conditions. Since ammonia concentration has less influence on the catalyst activity the noble metal catalysts are suitable for the high ammonia concentration conditions with further improvement of catalyst selectivity. Alumina-supported silver catalysts show comparable activity and slightly better selectivity to noble metal catalysts at high ammonia concentration conditions. At low ammonia concentration and high oxygen concentration conditions the activity of silver-based catalysts is superior to that of the noble metal catalysts, mostly due to the high reaction order in oxygen. With further improving the catalyst selectivity, silver-based catalysts are very promising to be applied to the removal of ammonia in flue gas, where usually excess amount of oxygen exists. By comparison the copper-containing catalysts, especially CuY catalysts, are even more promising. These catalysts may be applied at temperatures below 300 °C and possess high activity and higher selectivity compared with noble metals.

4. Conclusions

The activity of copper ion-exchanged zeolite Y catalysts for ammonia oxidation was shown to be comparable to that of noble metal catalysts at low temperatures. The selectivity to nitrogen was much higher for the zeolite catalysts. Treatment of CuY with NaOH after ion-exchange increased the ammonia oxidation activity. Alumina-supported silver catalysts were also very active for ammonia oxidation, especially at high O₂/NH₃ ratios. With further improving the catalyst selectivity silver-based catalysts are very promising to be applied to the removal of ammonia in flue gas. Co-fed steam dramatically decreased catalyst activity, especially at lower temperatures. Ion-exchanged zeolite Y catalysts were more stable than alumina-supported catalysts at high ammonia concentration conditions. At low ammonia concentration conditions both types of catalysts are stable. The deactivation of the catalyst is thus probably caused by ammonia-induced species. It has been shown that the selectivity to nitrogen was greatly decreased by decreasing the ammonia concentration. At high O₂/NH₃ ratio the activity of all catalysts increased but the selectivity for nitrogen production decreased.

References

- [1] G.B. Barannik, V.F. Lyakhova and A.V. Simakov: Chemistry for Sustainable Development, 1995.
- [2] J.J.P. Biermann, Ph.D. Thesis, University of Twente (1990).
- [3] N.I. Il'chenko, Russian Chem. Rev., 45(12)(1976)1119.
- [4] J.J. Ostermaier, J.R. Katzer and W.H. Manogue, J. Catal., 41(1976)277.
- [5] J.J. Ostermaier, J.R. Katzer and W.H. Manogue, J. Catal., 33(1974)457.
- [6] J.E. Delaney and W.H. Manogue, Proc. Int. Congr. Catal. 5th, 1(1973)267.
- [7] O.V. Al'tshuller and M.Ya. Kushnerev, Problemy Kinetiki i Kataliza, 15(1973)56.
- [8] N.N. Sazonova, A.V. Simakov and H. Veringa, React. Kinet. Catal. Lett., 57(1)(1996)71
- [9] F.J.J.G. Janssen and F.M.G. van den Kerkhof, Selective Catalytic Removal of NO from Stationary Sources, KEMA Sci. & Techn. Reports, 3(6)(1985).
- [10] J.P. Chen and R.T. Yang, Appl. Catal., 80(1992)135.
- [11] G. Tuentner, W.F. van Leeuwen and L.J.M. Sneyers, Ind. Eng. Chem. Prod. Res. Dev., 25(1986)633.
- [12] E.T.C. Vogt, A. Boot, J.W. Geus and F.J.J.G. Janssen, J. Catal., 114(1988)313.
- [13] E.T.C. Vogt, Ph.D. Thesis, University of Utrecht (1988).
- [14] J.J.P. Biermann, F.J.J.G. Janssen and J.W. Geus, J. Mol. Catal., 60(1990)229.
- [15] M. de Boer, A.J. van Dillen and J.W. Geus, Catalysis Letters, 11(1991)227.
- [16] Y. Li and J.N. Armor, Appl. Catal. B, 13(1997)131.
- [17] A. Wollner and F. Lange, Appl. Catal. A, 94(1993)181.
- [18] K.G. Ione, P.N. Kuznetsov and V.N. Romannikov, Application of Zeolite in Catalysis, Akademiai Kiado, Budapest, 87(1979).
- [19] R.A. Schoonheydt, K.G. Ione, P.N. Kuznetsov and V.N. Romannikov, J. Catal., 43(1976)292.
- [20] M. Suzuki, K. Tsutsumi, H. Takahashi and Y. Saito, Zeolites, 8(1988)284.
- [21] M. Suzuki, K. Tsutsumi, H. Takahashi and Y. Saito, Zeolites, 8(1988)387.
- [22] N. Watanabe, H. Yamashita, H. Miyadera and S. Tominaga, Appl. Catal. B, 8(1996)405.
- [23] S.E. Golunski, H.A. Hatcher, R.R. Rajaram and T.J. Truex, Appl. Catal. B, 5(1995)367.
- [24] G. Lu, J. van Grondelle, B.G. Anderson and R.A. van Santen, J. Catal., 186(1999)100.

Chapter 3

Selective low temperature NH₃ oxidation to N₂ on copper-based catalysts

Abstract

TPD, TPR, NEXAFS, UV-visible spectroscopy and HREM have been used to characterize the state and reactivity of NaY and alumina-supported copper-based catalysts for the oxidation of ammonia to nitrogen. The results of HREM and UV spectra show that a CuAl₂O₄ like phase is more active than a CuO phase for the ammonia oxidation reaction. Both surface oxygen and copper lattice oxygen can react with NH₃ to produce N₂ but surface oxygen is much more active than lattice oxygen at low temperature. For copper zeolite catalysts [Cu-O-Cu]²⁺-like species or small copper oxygen aggregates are the likely forms of the catalytically-active centers at low temperature. The activity of CuY was increased by treating the sample with NaOH. This treatment presumably increases the amount of low temperature active centers.

1. Introduction

Gas phase ammonia oxidation to nitrogen may find application in the treatment of ammonia containing industrial flue gases, in the SCR de-NO_x process for ammonia slipstream treatment, in the purification of reformates for fuel-cell systems, in the deodorization of ammonia/amine containing gas and for the small scale production of pure nitrogen as a safety gas. Previous studies show that noble metals such as Pt and Ir are very active for this reaction but are less selective. Significant amounts of nitrous oxide or nitric oxide are produced on these catalysts [1-3]. Supported molybdenum and vanadium catalysts show higher selectivity but the reaction temperature needed is too high for some of the industrial applications [4-6].

Copper oxide is one of the most active catalysts and has been considered as a potential substitute for noble metal-based emission control catalysts. Sazonova et al. [7] investigated the activity of various catalysts for ammonia oxidation at temperatures between 250° and 400°C. They concluded that the most active and selective catalysts are V/TiO₂, Cu/TiO₂ and Cu-ZSM-5. Topsøe of Denmark [8] recently patented a process for catalytic low temperature oxidation of ammonia in off-gas at temperatures between 200° and 500°C. The catalysts used were silica-supported Cu, Co and Ni oxides doped with small amounts of noble metals (100 to 2000ppm). They claimed that the selectivity and activity of the catalysts was improved when the catalysts were sulphated either during or prior to contact with the ammonia-containing gas. Their data show that the selectivity can be improved from 53 % to 99 % by sulphation. Wollner reported that high ammonia conversion (80-100 %) was obtained over mixed copper-manganese oxides supported on titania catalysts at temperatures greater than about 300 °C [9]. However the selectivity was not reported clearly. The results of Hodnett [10] show that Cu/Al₂O₃, which is a very active SCR catalyst, is also very active and selective for ammonia oxidation at a temperature of about 325 °C. A pulse reaction study of various transition metal-exchanged zeolite Y catalysts revealed CuY as the most active catalyst for ammonia oxidation at low temperature [11].

The aforementioned studies show that copper oxides supported on alumina, SiO₂, TiO₂ or zeolites are all active ammonia oxidation catalysts. The operating temperature for these catalysts is still rather high (greater than 300 °C). Little is known about the relationship between catalyst preparation and the active phase for these copper-based ammonia oxidation catalysts. In the present study various kinds of copper oxides supported on alumina and on zeolite Y have been prepared and tested as catalysts for the ammonia oxidation reaction. TPD, TPR, UV-visible spectroscopy

and HREM were used to characterize these catalysts in an attempt to shed light on the optimal preparation for active and selective low-temperature ammonia oxidation catalysts.

2. Experimental

2.1. Catalyst preparation

The starting zeolite was a commercial NaY zeolite from Akzo with a Si/Al ratio of 2.4 (Na₅₆Al₅₆Si₁₃₆O₃₈₄.249H₂O). NaY was ion-exchanged in an aqueous solution of copper nitrate at room temperature for 24 hours. After filtration, it was washed with deionized water three times, dried at 110 °C and then calcined at 400 °C for 2 hours. The copper contents were 3.7 and 8.4 wt% respectively. The samples will be referred to as CuY-3.7 and CuY-8.4 in the subsequent discussion.

Three Cu/Al₂O₃ samples with Cu loadings of 5, 10 and 15 wt% respectively were prepared by incipient wet impregnation. A commercial γ -Al₂O₃ (Akzo/Ketjen 000 1.5E) with a specific surface area of 235 m²/g and a BET pore volume of 0.55 ml/g was used as support. The precursor for these catalysts was Cu(NO₃)₂.3H₂O. The samples were calcined in air at 500 °C for 24 hours before testing. These samples will be referred to as Cu-Al-5, Cu-Al-10 and Cu-Al-15.

2.2. Catalyst testing

Catalytic activity measurements were carried out in a quartz, fixed-bed reactor (4 mm internal diameter). The amount of catalyst used was about 0.2 gram (250-425 μ m particles). Ammonia, oxygen and helium flow rates were controlled by mass flow meters. Water vapor was introduced by passing the helium flow through a water saturator at elevated temperature. The inlet and outlet gas compositions were analyzed using an on-line gas chromatograph equipped with a thermal conductivity detector. A quadrupole mass spectrometer was also used to monitor the different products.

2.3. Catalyst characterization

High resolution transmission electron microscopy (HREM) measurements were done on a Philips CM30-T electron microscope at the National Centre for HREM at the Delft University of Technology. Diffuse reflectance UV-visible spectra were recorded at room temperature using a Shimadzu UV-2401PC spectrometer, in the 190-900 nm

wavelength range. The Kubelka-Munk function $F(R)$ was plotted against the wavelength (in nm).

NH₃ and O₂ TPD experiments were performed using a fixed-bed flow reactor system equipped with a computer interfaced quadrupole mass spectrometer. After adsorption of NH₃ or O₂ at room temperature the TPD data were recorded by mass spectrometer while the temperature was increased from 50° to 500 °C at a heating rate of 5 °C/min. The TPR data were obtained on a typical computer-controlled temperature programmed reduction apparatus. The hydrogen consumption was measured using a thermal conductivity detector. The temperature was ramped from 25° to 800 °C at a rate of 5 °C/min.

In situ NEXAFS (near edge X-ray absorption fine structure) measurements were performed in BESSY I and BESSY II, the Berlin electron storage ring for synchrotron radiation. The instrument consists of a two chamber UHV system, of which one chamber with a base pressure of $<5 \times 10^{-9}$ mbar was connected to the U49/1-SGM beamline. The second chamber used as reactor is separated from the first by a 300 nm polyimide window, withstanding a pressure of at least 100 mbar in the reaction chamber. The detector system, which is described in detail in refs. [31-34], mainly consists of an aluminum plate facing the sample (collector) and a shielded gold mesh, both working in total-electron-yield (TEY) mode. Due to their different shape and spatial arrangement, the collector signal is a mixture of electrons from the sample and the gas phase, whereas the gold mesh provides an almost pure gas phase signal. Therefore the gas phase spectrum must be subtracted from the collector spectrum to obtain the resonances only from the sample surface. The evaluation procedure for copper L-edge is less difficult due to a lack of any resonances in the gas phase, so that only a normalization to the beam intensity and a pre-edge background subtraction is needed.

3. Results

3.1. Catalytic oxidation of NH₃ on copper based catalysts

The results of Table 1 show that the performance of the copper alumina catalysts is comparable to copper zeolite catalysts at high temperature (>300 °C). At lower temperature, the copper zeolite catalysts become superior. An optimal copper loading exists for the copper alumina catalysts. For CuY catalysts, increased loading led to higher activity.

Table 1. Ammonia oxidation over various copper catalysts

Catalyst	Temperature (°C)	NH ₃ conversion (%)	N ₂ selectivity (%)
Cu-Al-5	250	0	--
	300	21	97
	350	75	96
Cu-Al-10	250	12	96
	300	90	97
	350	100	90
Cu-Al-15	250	9	97
	300	46	96
	350	100	94
CuY-3.7	250	16	97
	300	54	98
	350	100	97
CuY-8.4	250	23	97
	300	88	98
	350	100	98
CuY-3.7 (with after-treatment)	200	21	97
	250	56	98
	300	100	98
CuY-8.4 (with after-treatment)	200	35	95
	250	68	97
	300	100	98

Reaction condition: NH₃ = 1.14%; O₂ = 8.21%;
flow rate = 74.7 Nml/min; cat. weight = 0.2g

Ione et al.[12] and Schoonheydt et al.[13] reported that the polynuclear nickel or copper ions were formed in the framework of zeolite Y when NaY was ion exchanged with an aqueous Ni(NO₃)₂ or Cu(NO₃)₂ solution at pH 6-7. These polynuclear cations gave a higher activity for CO oxidation than the mononuclear state. Suzuki et al.[14,15] successfully prepared a highly dispersed nickel oxide catalyst, which was also a very good CO oxidation catalyst, by hydrolysing the Ni²⁺ exchanged zeolite Y with an aqueous solution of NaOH or ammonia at various pH values. In this research the effect of NaOH aftertreatment has also been examined. We have used the procedure reported by Suzuki et al [14,15] to study the effect of NaOH aftertreatment on CuY catalysts. The results are included in Table 1.

As can be seen in Table 1, the activity of the two copper zeolite catalysts for ammonia oxidation increased significantly following NaOH treatment. This significantly higher activity was probably induced by the formation of small metal oxides in the zeolite. It should be noted that the CuY catalysts are active at temperatures as low as 200 °C. Temperatures of at least 250 °C are necessary for reaction on Cu alumina catalysts.

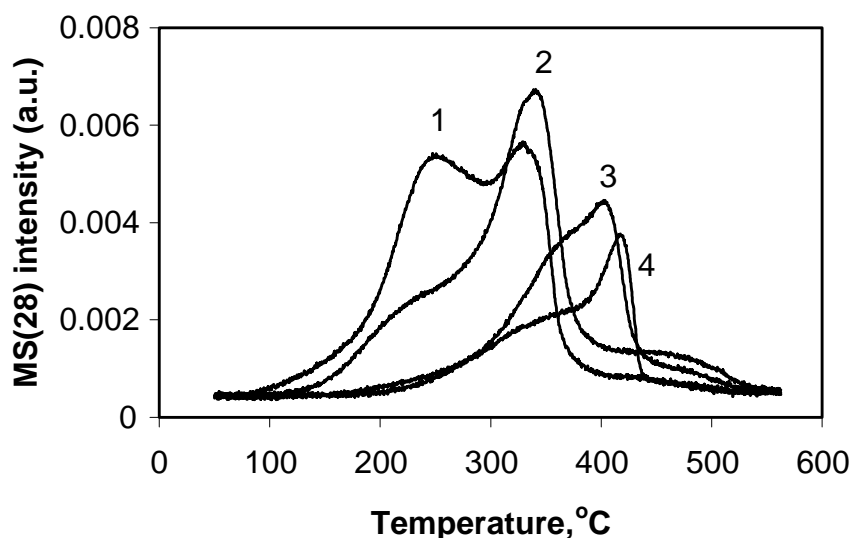


Fig.1 N_2 profiles on oxidized Cu-Al-10 catalyst during NH_3 TPD as a function of repeated NH_3 exposures (1,2,3,4 represent cycles)

3.2. TPD and TPR profiles for copper based catalysts

Four successive cycles consisting of isothermal NH_3 adsorption at 50 °C followed by TPD up to 500 °C were carried out on an oxidized Cu-Al-10 catalyst. The catalyst was heated in O_2/He flow at 500 °C for 2 hours before the first cycle. After a TPD run the sample was cooled in flowing helium to 50 °C. NH_3 was then readsorbed and the N_2 TPD spectrum was measured. The nitrogen production profiles for four such successive cycles of NH_3 TPD experiments are shown in Fig.1. It can be seen that there are two peaks around 250° and 330 °C for the first cycle TPD. In second cycle, the first peak almost disappeared while the second peak shifted to a slightly higher temperature. In the third and fourth cycles, the peak moved to even higher temperatures. As copper is dispersed very well on alumina (see HREM results) and since no nitrogen is produced during NH_3 TPD on alumina alone, the possibility of different active centers for the two peaks is very unlikely. We propose that the first peak is caused by the reaction of adsorbed surface oxygen with NH_3 and that the second peak is caused by reaction of ammonia with sub-surface or possibly with lattice oxygen. After the first TPD cycle the surface oxygen is almost totally consumed. This explains the disappearance of the first peak in the latter cycles.

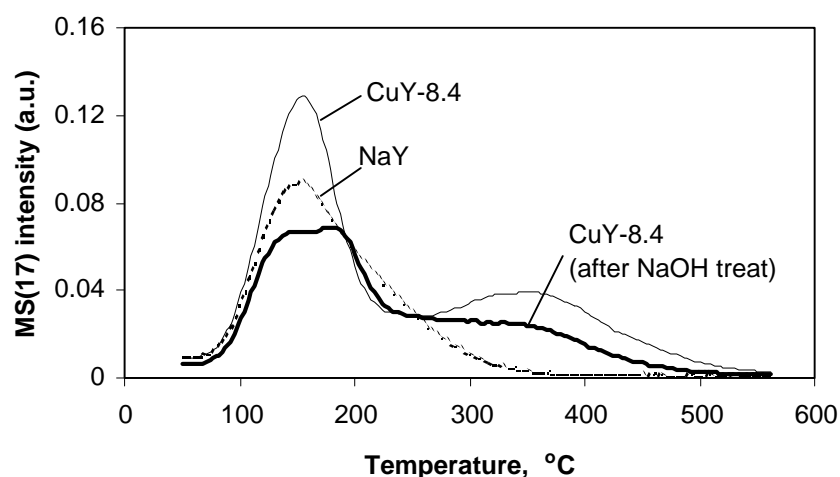


Fig.2 NH_3 TPD profiles on copper zeolite catalysts
(catalyst pretreatment: 400 °C in O_2 heated for 2 hr)

Fig.2 and Fig.3 compares NH_3 and N_2 desorption profiles measured during NH_3 TPD experiments on copper zeolite catalysts that had been subjected to NaOH aftertreatment. The zeolite catalysts were pretreated in O_2 at 400 °C for 2 hours prior to the experiments. The amount of catalyst is same for all the samples used in these experiments. Only one cycle of NH_3 TPD data are shown in Fig.2 and Fig.3 since the successive cycles measured on these zeolite catalysts showed no N_2 production. This means that either no oxygen existed on the copper zeolite catalysts or that the copper was completely reduced after the first cycle of the NH_3 TPD experiment. The desorption of NH_3 on NaY showed only one peak at 150 °C whereas two peaks (at 150° and 350 °C) were observed on the CuY-8.4 catalyst. The introduction of Cu into NaY not only creates a more strongly bonded NH_3 adsorption center but it also increases the amount of weakly bonded NH_3 centers. After NaOH treatment, a third ammonia adsorption center seemed to be produced, although this center is not very strong. There was almost no N_2 produced on NaY whilst on CuY-8.4 there were two N_2 peaks at the temperature at which ammonia desorption occurred. This shows that apparently there were some active ammonia oxidation centers created by the introduction of Cu into NaY. The first active center (at around 150 °C) is very interesting as it indicates that ammonia oxidation at low temperature on copper catalysts is possible. A third peak (at around 190 °C) for ammonia oxidation is created following NaOH treatment. Comparison of the N_2 production profiles measured on the alumina-based catalyst (Cu-Al-10) and on the zeolite-based catalyst shows that CuY is apparently much more active than Cu- Al_2O_3 at low temperature (<200 °C).

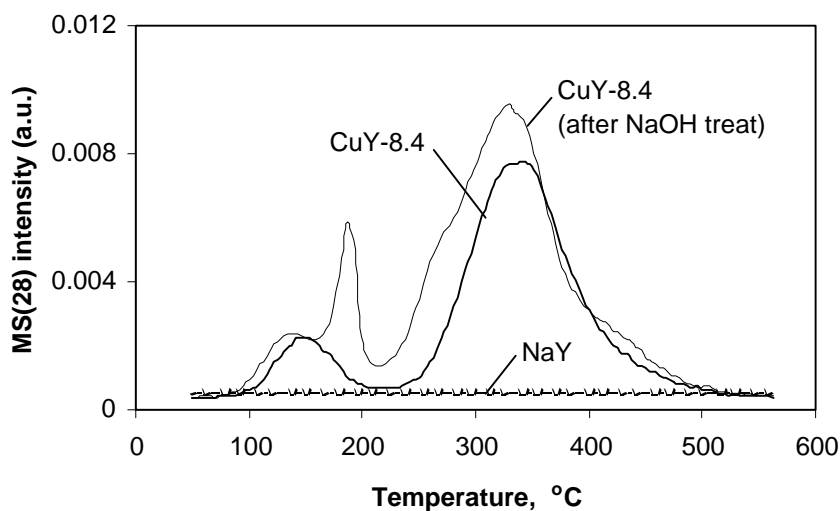


Fig.3 N_2 production profiles on CuY catalysts during NH_3 TPD (catalyst pretreatment: 400 °C in O_2 heated for 2 hr)

Catalysts used in O_2 TPD and H_2 TPR were all treated in O_2 at 400 °C for 2 hours and then cooled to room temperature. The amount of catalyst used for all O_2 TPD and H_2 TPR experiments is same, so the peak areas of different catalysts can be compared directly with each other. It can be seen from Fig.4 that two peaks exist in the O_2 TPD profiles on the CuY-8.4 catalyst. Since no O_2 desorption was observed on NaY, these two O_2 desorption peaks must be caused by the Cu in the zeolite. After the NaOH treatment the amount of O_2 desorbed was greatly increased. Many investigations[16,17] on the complete oxidation of CO and hydrocarbons have shown that their reactivities directly depend on the capacity of oxygen adsorption. Here it also appears that oxygen adsorption relates to the rate of ammonia oxidation. Fig.5 shows the TPR profiles of the CuY catalyst with and without the aftertreatment. Integration of the peaks reveals that the amount of reducible copper ions increased greatly when the CuY catalyst was treated with NaOH.

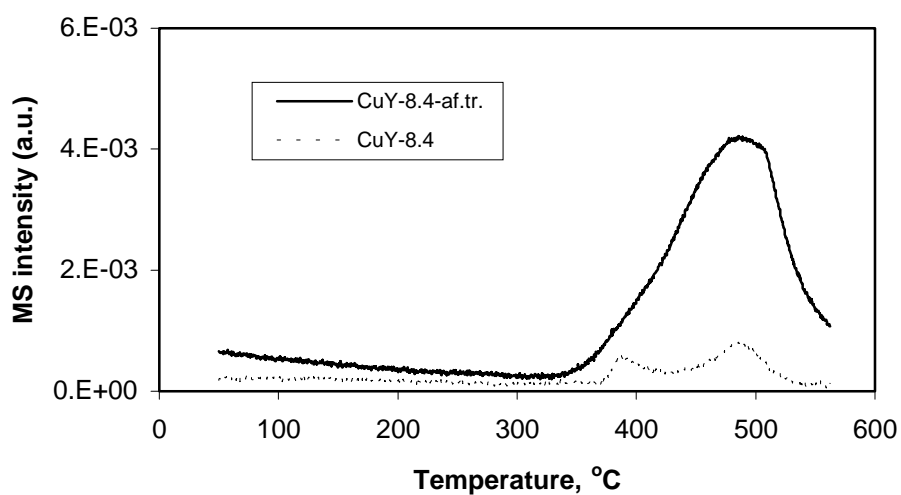


Fig.4 O_2 desorption on CuY catalyst with and without aftertreatment

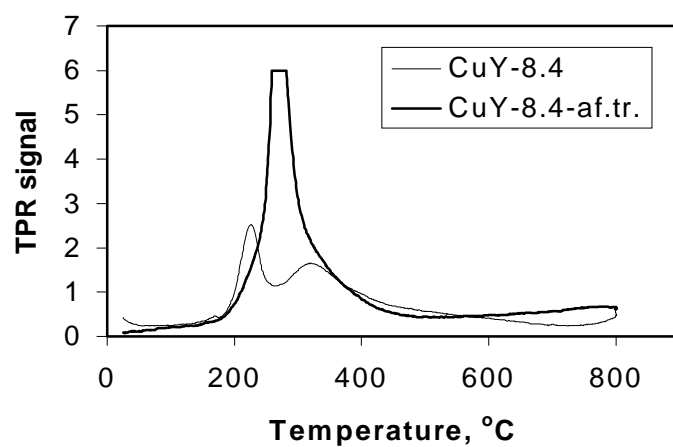


Fig.5 TPR by H_2 profiles for CuY with and without aftertreatment

3.3. HREM results



Fig.6 HREM image of Cu-Al-10

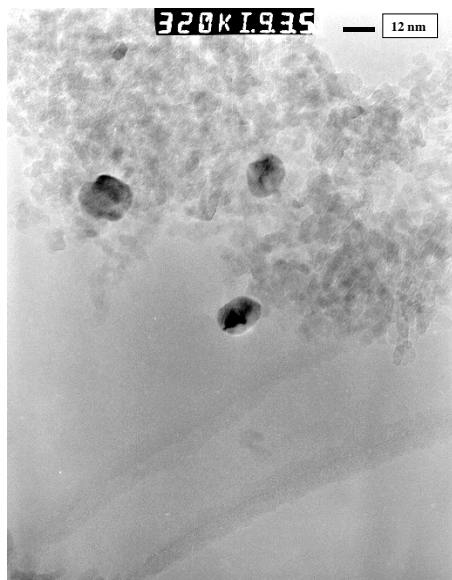


Fig.7 HREM image of Cu-Al-15

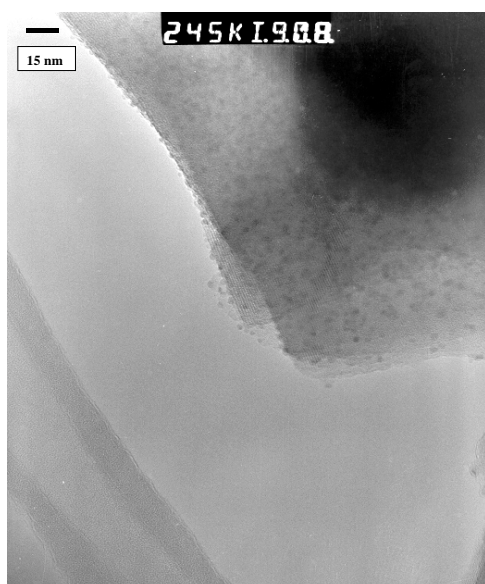


Fig.8 HREM image of CuY-8.4
(without aftertreatment)

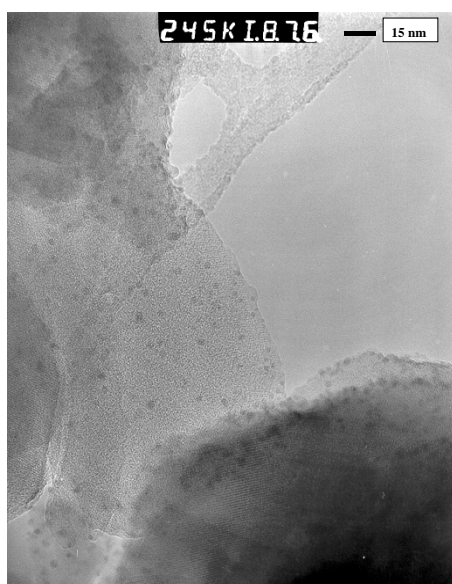


Fig.9 HREM image of CuY-8.4
(with NaOH aftertreatment)

No metal oxide particles were observed on the alumina surface of the Cu-Al-5 and the Cu-Al-10 catalysts with TEM (see Fig. 6). Metal particles with diameters ranging between 5 and 10 nm were observed on the Cu-Al-15 catalyst (see Fig. 7). The Cu-Al-15 catalyst was black in colour, probably due to the formation of these CuO particles on the alumina surface. By contrast the catalysts with lower copper loadings

(Cu-Al-5 and Cu-Al-10), on which no particles could be detected, were green in colour.

No differences in the HREM images were observed on samples of the catalyst CuY-3.7 before and after NaOH treatment. However, a very small amount of particles was discovered on the outer surface of the zeolite crystals for CuY-8.4 samples (see Fig. 8 and Fig. 9). Again there was no big difference observed before and after NaOH treatment.

3.4. UV-visible spectroscopy

The Cu²⁺ ion has a 3d⁹ electronic structure. In the presence of a crystal field generated by ligands or oxygen ions, d-d transitions appear in the visible or near-infrared range. For an octahedral environment, transitions appear between 600 and 800 nm depending on the crystal-field strength. Table 2 shows the summary of our assignments of the UV spectral bands measured on different kind of catalysts.

Table 2 Summary of the UV spectrum for different copper catalysts

Absorption wavelength	copper species	support
840 nm	Cu ²⁺ ions	Zeolite Y
740-750 nm	CuAl ₂ O ₄ like phase or [Cu-O-Cu] ²⁺ species	Al ₂ O ₃ , Zeolite Y
650 nm	CuO phase	no support or Al ₂ O ₃
560 nm	Cu ⁰ metal phase	no support or Zeolite Y

Fig.10 shows the UV spectra measured on copper-alumina catalysts with different copper loadings. It can be seen that there is a weak absorption band at about 740 nm for Cu-Al-5 and Cu-Al-10 catalysts. This band shifts to 650 nm for the Cu-Al-15 catalyst. According to previous studies [18] the band at 650 nm corresponds to a CuO phase. A UV spectrum measured on CuO showed indeed that a broad band around 650 nm exists (see Fig.11). The shift of this band to higher wavelength indicates that the distance between Cu²⁺ and the ligands or oxygen ions increases, i.e. the Cu²⁺-O²⁻ bond should exhibit greater ionic character.

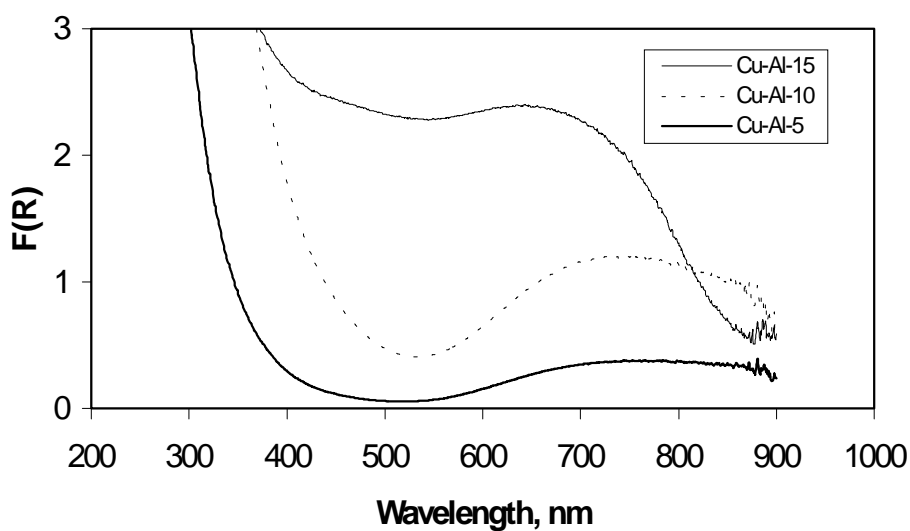


Fig.10 UV spectra for copper alumina catalysts

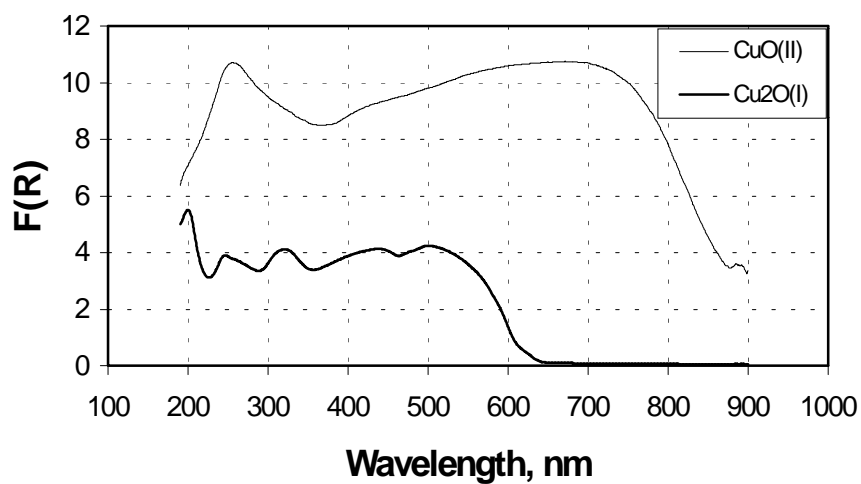


Fig.11 UV spectra for bulk CuO and Cu₂O oxides

It can be seen from Fig.12 that the absorption band appears at about 840 nm for CuY samples without NaOH aftertreatment. This indicates the existence of isolated Cu^{2+} ions of square pyramid symmetry [19-21]. After NaOH treatment, this band shifts to

about 750 nm, similar to the bands observed on the alumina-based copper catalysts (Cu-Al-5 and Cu-Al-10).

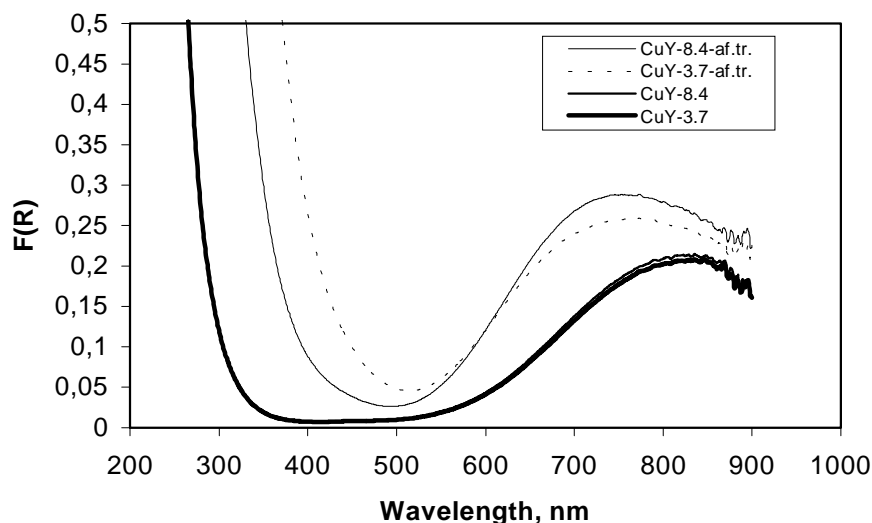


Fig.12 UV spectra for CuY based catalysts

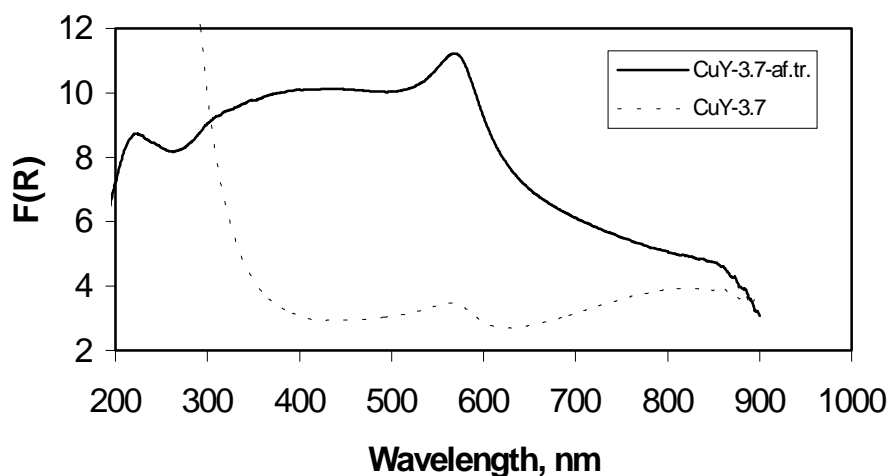


Fig.13 UV spectra for reduced CuY samples

CuY-3.7 samples with and without aftertreatment, were reduced in H_2/He at 500 °C for 2 hours before measuring the UV spectra (see Fig.13). The appearance of an absorption maximum at 560 nm indicates the creation of a metallic copper phase[21]. The absorption band at 840 nm measured on CuY-3.7 means that some Cu^{2+} ion can not be reduced. The intensity of the absorption band at 560 nm (Cu^0) did increase at the expense of 840 nm band (Cu^{2+}) indicating that some further reduction of copper is possible following NaOH treatment.

3.5. NEXAFS measurements

NEXAFS is known to contain a wealth of chemical and structure information, such as valence state, site symmetry, bond distances and coordination geometry [35]. Particularly, the presence of pre-edges, which arise because of promotion of inner-shell electrons to unoccupied states, is used as an information source for the symmetry of the absorber. Fig.14 shows the NEXAFS Cu L-edge spectra measured on CuY-8.4 catalysts with and without NaOH treatment after heating at 400 °C under vacuum. It is well known that most of isolated Cu²⁺ ions on zeolite Y will be auto-reduced to Cu⁺ after high temperature heating in vacuum [24]. The spectrum in Fig.14 for CuY-8.4 without NaOH treatment also shows the existence of large amount of Cu⁺ after high temperature treating in vacuum. When the CuY-8.4 catalyst was treated by NaOH, the NEXAFS spectrum showed that only a small part of Cu²⁺ could be auto-reduced to Cu⁺ by high temperature vacuum treating. This indicates that new copper species are formed from isolated Cu²⁺ ions after NaOH treatment for CuY catalyst.

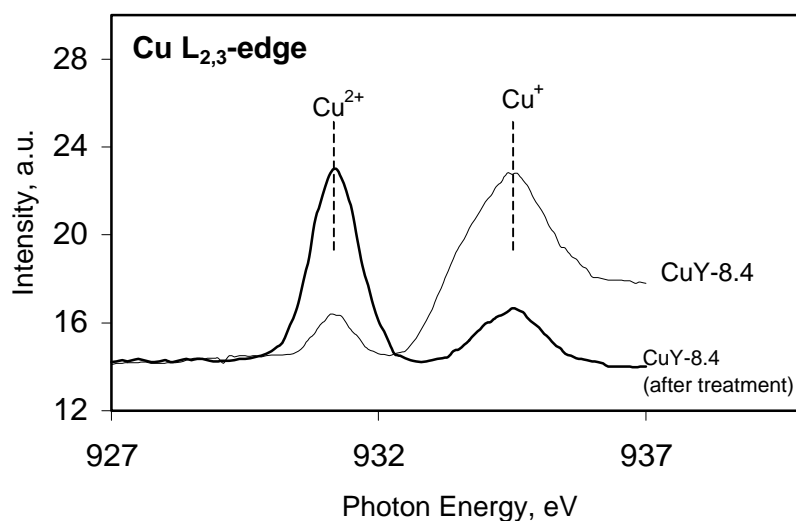


Fig.14 NEXAFS spectra at the copper L-edge for CuY based catalysts

Both catalyst are pretreated at 400 °C for 2 hours in vacuum and then measured in vacuum

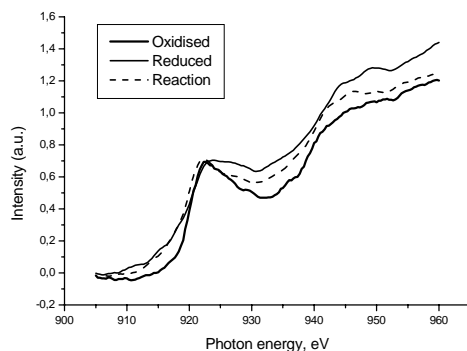


Fig.15 In situ NEXAFS Cu L-edge spectra of CuY-8.4 catalyst
Reaction conditions: $\text{O}_2/\text{NH}_3=3$, $T=200\text{ }^\circ\text{C}$, $P_{\text{abs}}=4\text{ mbar}$

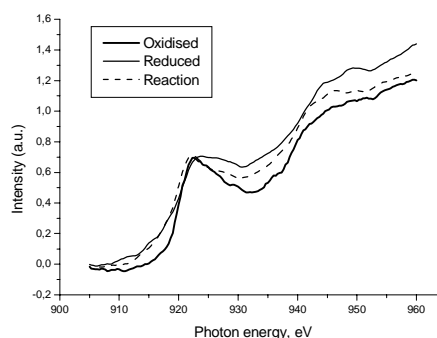


Fig.16 In situ NEXAFS Cu L-edge spectra of CuY-8.4-af.tr. catalyst
Reaction conditions: $\text{O}_2/\text{NH}_3=3$, $T=200\text{ }^\circ\text{C}$, $P_{\text{abs}}=4\text{ mbar}$

Fig.15 and Fig.16 show a plot of a selection of in situ NEXAFS spectra of CuY-8.4 catalysts taken at the copper L-edge at $200\text{ }^\circ\text{C}$. A gas flow ratio $\text{O}_2/\text{NH}_3=3$ is used. The signals in these figures are very weak due to the pressure effect and old equipment used in BESSY I. However, qualitative analysis of these spectra is still possible. During ammonia oxidation reaction conditions, the copper on both CuY-8.4 catalysts with and without NaOH treatment is partially reduced, most probably in the state of Cu^+ .

4. Discussion

The most extensive investigation of $\text{Cu}/\text{Al}_2\text{O}_3$ catalysts has been performed by Friedman et al.[22]. By applying several techniques and combining results with previous work, a coherent model of the surface structure was developed, resulting in the following conclusions [22,23]: 1. At low metal loadings and at calcination temperature below $500\text{ }^\circ\text{C}$ the formation of a surface spinel (which resembles CuAl_2O_4) predominates. Most of the Cu^{2+} ions are in a distorted octahedral geometry, unlike bulk CuAl_2O_4 where about 60% are tetrahedral and 40% octahedral. 2. At higher metal loadings, segregation of bulk-like CuO may also occur. 3. Calcination at $900\text{ }^\circ\text{C}$ leads to formation of bulk CuAl_2O_4 . Our HREM and UV measurements also show that no CuO particles form on the alumina surface for Cu-Al-5 and Cu-Al-10 catalysts but that particles are present on the Cu-Al-15 sample. The fact that the performance of Cu-Al-10 is better than that of the Cu-Al-15 catalyst supports the conclusion that a CuAl_2O_4 -like phase is more active than bulk CuO phase in the ammonia oxidation reaction.

At least three types of copper species in CuY have been described in the literature: 1. Isolated ions interacting with the framework Al, either without an extraframework ligand, or with an extraframework O or OH ligand. These species show a different reactivity [24]. 2. Polymeric chains or multinuclear species (often called small copper-oxygen aggregates), for instance $[\text{Cu-O-Cu}]^{2+}$ inside the zeolite supercage [25-27]. 3. CuO particles on the external surface of zeolite crystals [28]. Although at high loadings the HREM results show some CuO particles on the outer surface of the zeolite, the UV spectra show no apparent CuO adsorption band intensity at 650 nm. This means that only a small amount of copper is on the surface of the zeolite crystals as CuO as compared with the amount of copper inside the pores of zeolite.

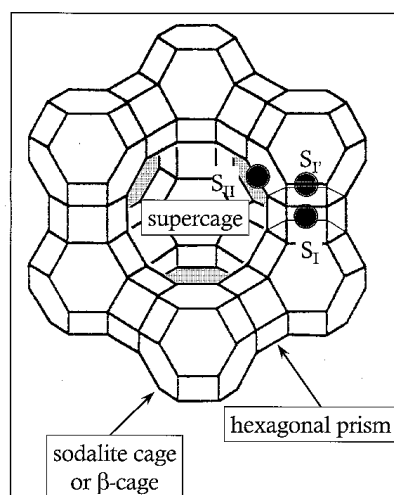


Fig.17 Structure of Zeolite Y

In Y-type zeolites X-ray diffraction studies by Gallezot et al. [37] indicated that Cu^{2+} ions occupy mainly S_I and S_F sites (see Fig.17). This means that at moderate exchange levels, the Cu^{2+} ions are unavailable for catalysis, unless they can be induced to take up positions in the supercages. Although ammonia may readily enter the sodalite cage, molecules such as molecular oxygen are apparently too large to enter the 2.2 Å aperture at moderate temperatures. Therefore copper centers that are accessible to ammonia oxidation have to be located in the supercages. According to earlier studies [29] they are localized at S_{II} sites i.e. near the centers of six-membered rings of the sodalite cages. The results of NH₃ TPD on different zeolite samples show that only one weakly bonded NH₃ adsorption center exists on NaY. The introduction of Cu into NaY not only creates a more strongly bonded NH₃ adsorption center but it also increases the amount of weakly bonded NH₃ centers. Isolated Cu^{2+} ions are believed to be responsible for the strongly bonded NH₃ adsorption centers since they can easily react with ammonia forming comparatively stable $[\text{Cu}(\text{II})(\text{NH}_3)_4]^{2+}$.

complex [38]. This complex can decompose at a moderate temperature to produce NH₃ and [Cu(II)(NH₃)₃]²⁺ complex according to following equation:



This may explain the increase of weakly bonded NH₃ adsorption centers after introducing Cu into the NaY. At even higher temperatures the [Cu(II)(NH₃)₃]²⁺ complex can be completely decomposed. After NaOH treatment, another weakly bonded NH₃ adsorption centers appeared and the amount of strongly bonded NH₃ adsorption centers decreased. This may attribute to the fact that some of the isolated Cu²⁺ ion migrated from the sodalite cages to the supercages of the zeolite Y. Some copper clusters such as [Cu-O-Cu]²⁺, can also be formed during this process. These copper clusters might be another type of centers for weakly bonded NH₃ adsorption.

The results of O₂ TPD and TPR strongly indicate this migration. The UV spectra for reduced CuY samples also indicate that more Cu²⁺ ions are reduced to Cu⁰ after NaOH treatment. Comparison of the UV spectra for CuY samples with and without aftertreatment shows that there are mainly isolated copper ions in the zeolite before NaOH treatment. The shift of the absorption band from 840 nm to 750 nm after treatment indicates the creation of [Cu-O-Cu]²⁺ inside the zeolite supercage or the presence of small copper-oxygen aggregates [25-27]. Perhaps copper ions are first deposited as Cu(OH)₂ by hydroxylation both in the supercages and in the sodalite cages. Part of the Cu(OH)₂ then moves to the S_{II} sites in the supercages during this hydroxylation process. Upon dehydration of Cu(OH)₂, [Cu-O-Cu]²⁺ complexes are produced which are thought to be the active centers for low temperature ammonia oxidation. Actually [Cu-O-Cu]²⁺ already exists in CuY prior to NaOH treatment. According to prior studies [30], [Cu-O-Cu]²⁺ species are present even at low ion-exchanged levels in CuY. The concentration of [Cu-O-Cu]²⁺ species increases with the Cu-loading. This is in agreement with the finding that low temperature active centers for ammonia oxidation exist on an untreated CuY catalyst.

The results of NEXAFS measurements also indicates that mainly isolated copper ions exist in CuY before NaOH treatment. These isolated copper ions can be changed into other copper species or clusters by NaOH treatment. In situ NEXAFS studies on ammonia oxidation over un-supported copper catalysts showed that mainly N₂ was produced when copper was in the state of Cu⁺ during reaction. When copper was in the state of Cu²⁺ during reaction, the main product was NO or N₂O [36]. It has been shown by our in situ NEXAFS measurements that copper on CuY catalysts is in the state between Cu⁰ and Cu²⁺, most likely Cu⁺ during ammonia oxidation reaction. This

may explain that good selectivity to nitrogen is always obtained on CuY-based catalysts.

5. Conclusions

HREM and UV-visible spectral measurements showed that no metal oxide particles form on alumina at copper loadings below 10 % (by weight). At higher loadings a CuO phase was detected. The fact that the performance of 10 wt.% Cu / Al₂O₃ was better than 15 wt% (Cu-Al-15) supports the conclusion that a “CuAl₂O₄”-like surface phase is more active than a CuO phase in the ammonia oxidation reaction. NH₃ TPD profiles on Cu-Al-10 indicate that both surface oxygen and lattice oxygen can react with NH₃ to produce N₂. However, surface oxygen is much more active than lattice oxygen at low temperature.

NH₃ TPD on CuY catalysts shows three types of active centers. Two of these are active at low temperature (below 200 °C) and one is active at a higher temperature (above 300 °C). The existence of low temperature active centers indicates that ammonia oxidation at low temperature on copper catalysts is possible. According to the UV and NEXAFS spectra, the [Cu-O-Cu]²⁺-like species or small copper oxygen aggregates are responsible to the low temperature active centers. However the amount of low temperature active centers or the concentration of [Cu-O-Cu]²⁺ species is small prior to NaOH treatment. The NaOH treatment of CuY increases the amount of low temperature active centers.

The above results apparently indicate that the environment or the type of active copper species is very important for low temperature ammonia oxidation and is strongly related with different supports and preparation methods.

References

- [1] Li, Y. and Armor, J.N., *Appl. Catal. B*, **13**, 131(1997).
- [2] Delaney, J.E. and Manogue, W.H., *Proc. Int. Congr. Catal. 5th*, **1**, 267(1973).
- [3] Ostermaier, J.J., Katzer, J.R. and Manogue, W.H., *J. Catal.*, **41**, 277(1976).
- [4] Boer, M. de, van Dillen, A.J. and Geus, J.W., *Catalysis Letters*, **11**, 227(1991).
- [5] Biermann, J.J.P., Janssen, F.J.J.G. and Geus, J.W., *J. Mol. Catal.*, **60**, 229(1990).
- [6] Vogt, E.T.C., *Ph.D. Thesis*, University of Utrecht(1988).
- [7] Sazonova, N.N., Simakov, A.V. and Veringa, H., *React. Kinet. Catal. Lett.*, **57**(1), 71(1996).
- [8] Dannevang, F., *US Patent* 5,587,134 (1996).
- [9] Wollner, A. and Lange, F., *Appl. Catal. A*, **94**, 181(1993).
- [10] Deconinck, C., Knuttel, N., Curtin, T. and Hodnett, B.K., to be published.
- [11] Al'tshuller, O.V. and Kushnerev, M.Ya., *Problemy Kinetiki I Kataliza*, **15**, 56(1973).
- [12] Ione, K.G., Kuznetsov, P.N. and Romannikov, V.N., *Application of Zeolite in Catalysis*, Akademiai Kiado, Budapest, 87(1979).
- [13] Schoonheydt, R.A., Ione, K.G., Kuznetsov, P.N. and Romannikov, V.N., *J. Catal.*, **43**, 292(1976).
- [14] Suzuki, M., Tsutsumi, K., Takahashi, H. and Saito, Y., *Zeolites*, **8**, 284(1988).
- [15] Suzuki, M., Tsutsumi, K., Takahashi, H. and Saito, Y., *Zeolites*, **8**, 387(1988).
- [16] Watanabe, N., Yamashita, H., Miyadera, H. and Tominaga, S., *Appl. Catal. B*, **8**, 405(1996).
- [17] Golunski, S.E., Hatcher, H.A., Rajaram, R.R. and Truex, T.J., *Appl. Catal. B*, **5**, 367(1995).
- [18] Marion, M.C., Garbowski, E. and Primet, M., *J. Chem. Soc. Faraday Trans.*, **86**(17), 3027(1990).
- [19] Lever, A.B.P., *Inorganic Electronic Spectroscopy*, Elsevier, Amsterdam, 1984.
- [20] Strohmeier, B.R., Leyden, D.E. and Hercules, D.M., *J. Catal.*, **94**, 514(1985).
- [21] Praliaud, H., Mikhailenko, S., Chajar, Z. and Primet, M., *Appl. Catal. B*, **16**, 359(1998).
- [22] Friedman, R.M., Freeman, J.J. and Lytle, F.W., *J. Catal.*, **55**, 10(1978).
- [23] Park, P.W. and Ledford, J.S., *Appl. Catal. B*, **15**, 221(1998).
- [24] Centi, G., Perathoner, S., *Appl. Catal. A*, **132**, 179(1995).
- [25] Wang, Z., Sklyarov, A.V., Keulks, G.W., *Catal. Today*, **33**, 291(1997).
- [26] Beutel, T., Sarkany, J., Lei, G.D., Yan, J.Y., Sachtler, W.M.H., *J. Phys. Chem.*, **100**, 845(1996).
- [27] Dedeczek, J., Wichterlova, B.N., *J. Phys. Chem.*, **98**, 5721(1994).
- [28] Praliaud, H., Mikhailenko, S., Chajar, Z., Primet, M., *Appl. Catal. B*, **16**,

- 359(1998).
- [29] Breck, D.W., *Zeolite Molecular Sieves*, A Wiley-Intersci. Publ., New York-London-Sydney-Toronto, 1974.
- [30] Conesa, J.C. and Soria, J., *J. Chem. Soc. Faraday Trans. I*, **75**, 406(1979).
- [31] M. Havecker, A. Knop-Gericke, T. Schedel-Niedrig and R. Schlögl, *Angew. Chem. Int. Ed.*, **37** (1998) 1939.
- [32] A. Knop-Gericke, M. Havecker, T. Neisius and T. Schedel-Niedrig, *Nucl. Instr. and Meth.*, A **406** (1998) 311.
- [33] M. Havecker, A. Knop-Gericke and T. Schedel-Niedrig, *Appl. Surf. Sci.*, **142** (1999) 438.
- [34] A. Knop-Gericke, M. Havecker, T. Schedel-Niedrig and R. Schlögl, *Topics in Catalysis*, **10** (2000) 187.
- [35] J. Stöhr., *NEXAFS spectroscopy*, Springer Series in Surface Science, Vol. 25 (Springer, Berlin, 1992).
- [36] R.W. Mayer, M. Havecker, A. Knop-Gericke and R. Schlögl, to be published.
- [37] P. Gallezot, Y. Ben Taarit and B. Imelik, *J. Catal.*, **26** (1972) 295.
- [38] W.B. Williamson, D.R. Flentge and J.H. Lunsford, *J. Catal.*, **37** (1975) 258.

Chapter 4

Intermediate species and reaction pathways for the oxidation of ammonia on powdered silver catalysts

Abstract

Ammonia oxidation reaction pathways on high surface area silver powder has been studied by TPD, TPR, FT-Raman and by transient as well as by steady-state ammonia oxidation experiments. NO was found to be the main reaction intermediate yielding N_2O as well as N_2 . NO could be formed even at room temperature and when oxidized to NO_x became adsorbed to the silver surface, thus blocking the active sites for oxygen dissociation. The dissociation of oxygen is thus believed to be the rate-controlling step for ammonia oxidation. The selectivity for N_2 , N_2O and NO are mainly determined by the surface oxygen coverage and by reaction temperature. The adsorbed NO_x , N_2O_x species are actually inhibitors for ammonia oxidation but these adsorbed species lower the surface oxygen coverage. Hence the selectivity to nitrogen is improved with the increasing amount of these adsorbed species.

1. Introduction

The selective catalytic oxidation of ammonia to nitrogen and water (SCO process) has been proposed as an effective ammonia abatement process [1-3]. Among the catalysts published in the open literature noble metals such as Pt, Ir are the most active catalysts at low temperatures. However the selectivity of these metal catalysts is not satisfying, especially at the condition of very high O_2/NH_3 ratios. Silver was also found in our laboratory to be one of the most active ammonia oxidation catalysts but

also showed a poor selectivity to nitrogen, also forming N_2O as a main product. In order to improve the selectivity of these catalysts it is essential to develop a clear understanding of the reaction pathways for ammonia oxidation on these catalysts.

The majority of mechanistic studies on ammonia oxidation have been done on platinum catalysts. Three reaction mechanisms have been proposed in earlier studies. The nitroxyl (HNO) mechanism suggests that the first step is the formation of a nitroxyl species which will further react to give N_2 , N_2O and NO [4]. Bodenstein [5,6] extended this mechanism by suggesting that the formation of hydroxylamine (NH_2OH) was the first step. This NH_2OH is converted to HNO in a next reaction step. An imide mechanism in which the first step yields imide (NH) was postulated by Raschig and Zawadzki [7,8]. Based on the data of secondary ion mass spectrometry (SIMS) Fogel et al. concluded that the intermediate species HNO, NH_2OH , HNO_2 and N_2O were not formed during ammonia oxidation at partial pressures of 10^{-4} Torr [9]. The only intermediate species was NO. The formation of N_2 was proposed to be a result of the NO reacting with NH_3 .

New insights in the reaction mechanism of ammonia oxidation were obtained from surface science experiments [10-13]. Single crystals of platinum were used in these experiments and the reaction was carried out under high vacuum conditions. The first step of ammonia oxidation was believed to be the formation of NH_x species through oxydehydrogenation of ammonia. Mieher and Ho [11] concluded that NO and N_2 were formed by the combination of nitrogen atoms with adsorbed oxygen atoms or with two nitrogen atoms respectively. However Bradley and King [13] suggested that NO was directly produced by reacting NH_a with O_a . The formation of N_2 resulted from the consecutive dissociation of NO. Since only NO and N_2 were produced under the reaction conditions of these studies, the formation of N_2O was not discussed. The recent study of Van den Broek and van Santen [14,15] showed that NH and OH were the main surface species adsorbed on Pt and Ir sponge catalysts after ammonia oxidation. The reaction of NH and OH was thought to be the rate-determining step under their reaction conditions. They argued that N_2O was produced by NO reacting with adsorbed N. The STM technique was used by the group of M.W. Roberts [16-18] to study ammonia oxidation on copper surfaces. They observed that at very low temperatures ammonia could be oxidized to adsorbed NH_2 and NH species. At higher temperature NO formation was also observed. On metal oxide catalysts a mechanism based on the recombination of two NH_x species giving rise to a hydrazinium intermediate was also proposed [19-21].

Ammonia adsorption on Ag(110) has been studied previously by TPD, TPRS and by EELS with and without coadsorption of molecular and atomic oxygen[22]. It was concluded that a diffusing nitrogen adatom was the reactive intermediate in NO and N₂ formation. On the basis of a combination of XPS and VEEL spectra a dioxygen-NH₃ complex had been suggested to be a key intermediate in the oxidation of ammonia on Ag(111) surfaces [35,36]. No report has been published to-date on the intermediate species and reaction mechanisms on polycrystalline silver at atmospheric pressure. In this study the ammonia reaction pathways were studied by TPD, TPR, FT-Raman and by pulsed ammonia reactions on high surface area silver powder at high O₂/NH₃ ratios.

2. Experimental

Polycrystalline silver was prepared from Ag₂O (>99.99%) powder. The powder was first reduced in flowing H₂/He overnight at 400 °C and then oxidized in flowing O₂/He at 400 °C for 2 hours. This process was repeated three times to remove any carbon species and to maintain a stable surface area. The surface area of reduced silver powder determined by krypton BET was 0.67 m²/g with an average particle size of 0.43 μm. Catalytic activity measurements were carried out in a quartz, fixed-bed reactor (4 mm internal diameter). The amount of silver powder catalyst was about 0.2 g. Ammonia, oxygen and helium flow rates were controlled by mass flow meters.

NH₃, NO and NO₂ were analyzed by a ThIs Analytical Model 17C Chemiluminescence NH₃ Analyzer using the reaction of nitric oxide (NO) with ozone (O₃) as its basic principle (NO+O₃→ NO₂+O₂+hv). To measure the NO_x (NO+NO₂) concentration, NO₂ must be transformed to NO in a molybdenum converter heated to approximately 325 °C prior to reaching the reactor chamber. To measure the N_t (NO+NO₂+NH₃) concentration, both the NO₂ and NH₃ must be transformed to NO prior to reaching the reaction chamber. This transformation took place in a stainless steel converter heated to approximately 750 °C. The NO₂ concentration was determined by subtracting the signal obtained in the NO mode from the signal obtained in the NO_x mode (NO₂=NO_x-NO). The NH₃ concentration was determined by subtracting the signal obtained in the NO_x mode from the signal obtained in the N_t mode (NH₃=N_t-NO_x). Other substances such as N₂O, N₂ and H₂O were analyzed by a quadrupole mass spectrometer (Baltzers OmniStar). The nitrogen mass balance was calculated based on combination of these two analysis techniques. It attained a balance of 90 ± 10% for all the measurements.

NH₃ TPD and TPR experiments were performed using a fixed-bed flow reactor system equipped with a computer interfaced quadrupole mass spectrometer. After adsorption of NH₃ at room temperature the TPD or TPR data were monitored with a mass spectrometer while the temperature was increased from 50 °C to 500 °C at a heating rate of 10 °C/min. FT-Raman spectra were obtained with a Bruker FRA 106 Raman Spectrometer equipped with an in-situ reaction chamber. The standard laser is an air-cooled, diode-pumped Nd:YAG operating at 1.064 μm with a maximum laser power of 500 mW. Usually a laser power of 150 mW was used for measures under atmospheric conditions. Detection was performed by a liquid-nitrogen-cooled InGaAs detector. One hundred scans were co-added at a resolution of 2 cm⁻¹.

3. Results

3.1 NH₃ oxidation on silver powder at high O₂/NH₃ ratios

Ammonia oxidation at high O₂/NH₃ ratios was carried out on silver powder at temperatures below 400 °C. Fig.1 shows the results of NH₃ conversion and products selectivity versus reaction temperatures. It can be seen that silver is very active for ammonia oxidation and shows high conversion even below 160 °C. At low ammonia conversion the N₂ selectivity decreases with increasing temperature. At high ammonia conversion the N₂ selectivity increases with increasing temperature. When the temperature is over 300 °C the N₂ selectivity decreases again because of the formation of NO.

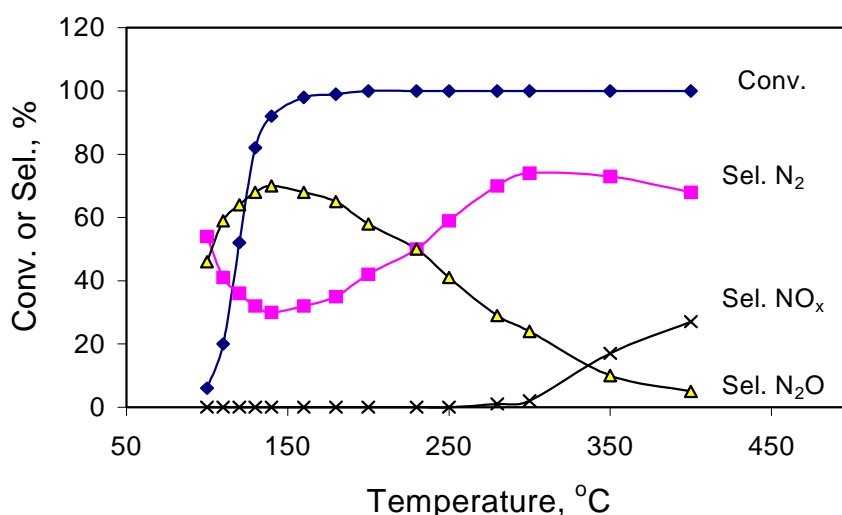


Fig.1 Ammonia oxidation on silver powder at various temperatures

Reaction conditions: NH₃=1000 ppm; O₂=10 vol%;

Total flow rate=50 Nml/min; Cat. Weight=0.1 g

3.2 TPD and TPR of ammonia on reduced and on oxygen-covered silver powder

Fig.2 shows the NH₃ TPD profile measured on completely reduced silver powder. Apparently a small amount of water in the helium or in the ammonia can be adsorbed on Ag and is desorbed at about 150 °C. Trace ammonia also desorbs at this temperature. This is mostly from water-coupled ammonia. This result shows that a clean silver surface can not adsorb ammonia above room temperature. This is in accordance with literature [22]. Fig.3 shows the NH₃ TPD profile measured on oxygen pre-covered silver powder. There are two water production peaks at 150 °C and 280 °C respectively. The peak at 150 °C is similar to the water desorption peak shown in Fig.2. The peak at 280 °C can be caused by the reaction of adsorbed OH species according to the following reactions:

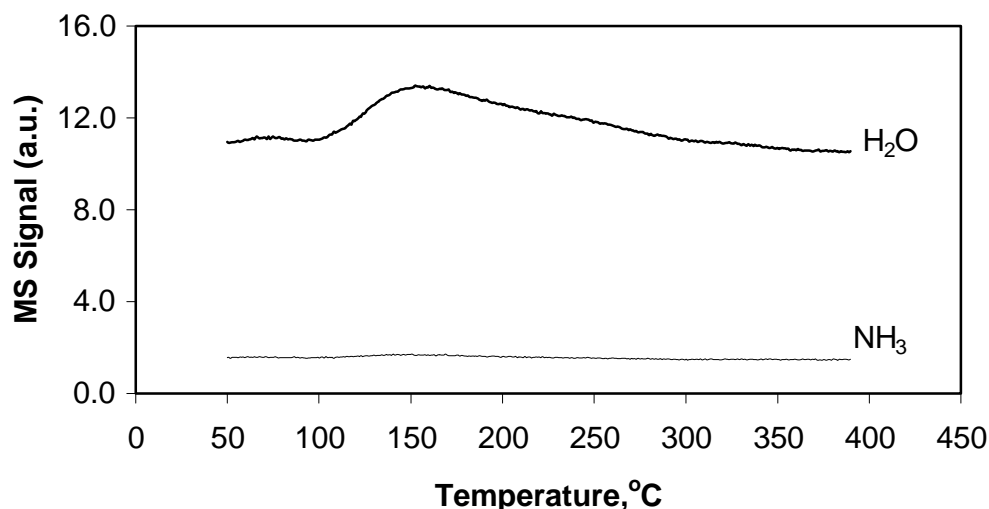
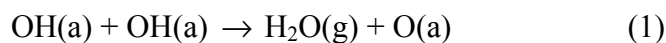


Fig.2 NH₃ TPD on reduced silver powder

(Silver powder was reduced at 400 °C for 2h and then in NH₃/He flow for 0.5 h at 50 °C. TPD was performed in He=20 Nml/min flow. Temperature was increased from 50 °C to 400 °C at a rate of 10 °C/min.)

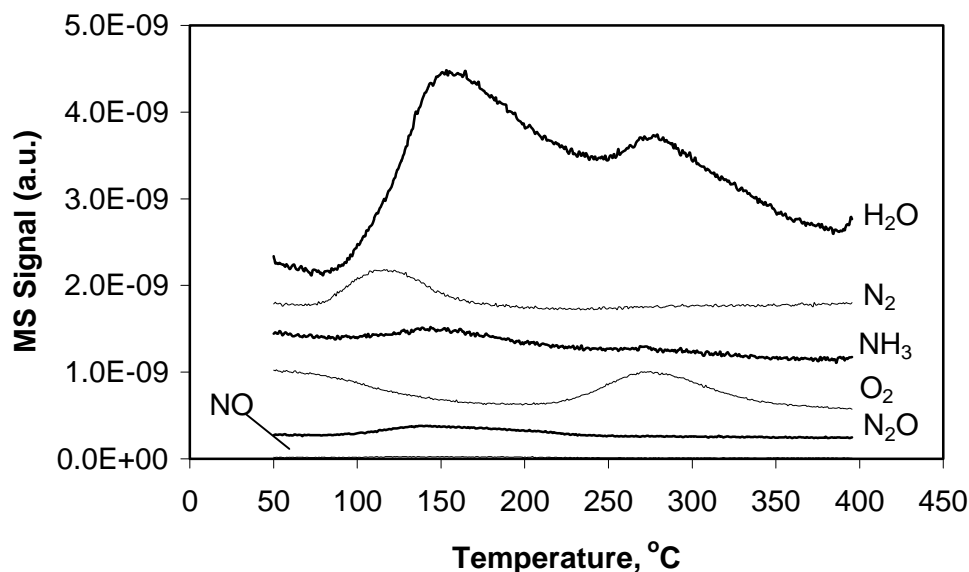
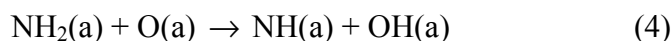
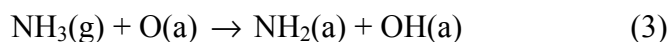


Fig.3 NH₃ TPD on oxygen-covered silver powder

(The reduced silver was first oxidized at 200 °C for 10 min in flowing O₂(10%)/He followed by NH₃ adsorption at RT and TPD as described in Fig.2)

The oxygen peak appears at the same position as the water peak. This strongly suggests that reaction step (1) is rate-limiting. There is still a trace of NH₃ desorbed at 150 °C. Significantly more N₂ is produced at a temperature of 120 °C. This N₂ production must come from adsorbed nitrogenous species on the silver surface. On Ag(111) surfaces a dioxygen-NH₃ complex has been detected by XPS and EELS at -193 °C which is suggested to be a key intermediate in the oxidation of ammonia [35]. When temperature is increased to -63 °C the di-oxygen are not present and NH species appear. A study on Ag(110) surfaces for ammonia oxidation shows that NH groups persist on the surface at temperature corresponding with the water desorption peak at 37 °C and possibly at significantly higher temperatures [22]. Thus the adsorbed nitrogen species may be NH_x(a) or NO(a) produced by oxygen abstraction of hydrogen from NH₃:



Besides N₂ there is also some N₂O produced. The maximum production temperature for N₂O production is higher than that of N₂. This indicates that the selectivity of ammonia oxidation depends on the surface N/O ratio. With the production of N₂ the amount of NH_x decreases and the O/N ratio increases, leading to an increased N₂O production and the observed maximum.

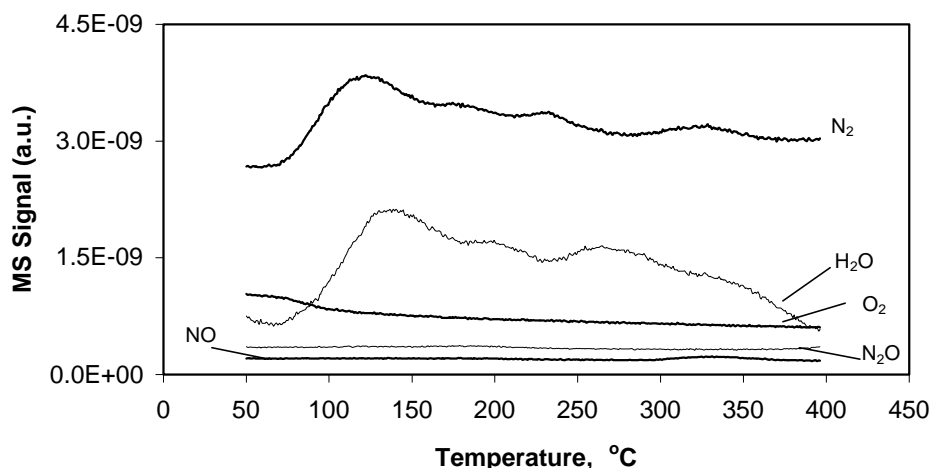
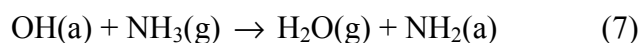
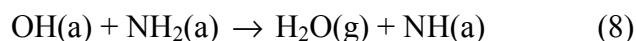


Fig.4 NH₃ TPR profiles on oxygen-covered silver powder

(Silver pretreatment as in Fig.3. TPR performed in NH₃/He=20 Nml/min flow with NH₃ concentration of 1000 ppm from 50 to 400 °C at 10 °C/min)

Fig.4 shows the NH₃ temperature programmed reaction (TPR) profiles on an oxygen pre-covered Ag powder. NH₃/He was flowing constantly over the silver powder during the increase of temperature. With increasing temperature the rate of reaction (3) and (4) are greatly increased and the surface N/O ratio increases accordingly. So over the entire temperature range the only product is nitrogen. There are four N₂ production maxima at 120 °C, 170 °C, 240 °C and 330 °C respectively. The first one is apparently caused by adsorbed surface atomic oxygen. The later two appear coincidentally after water production has reached a minimum. It is possible that water inhibits the migration of subsurface oxygen onto the surface. When water desorbs, more subsurface oxygen may become accessible for the ammonia oxidation reaction. It also can be seen from the water production profile that a new peak at about 200 °C appears in addition to the two already mentioned. This peak surely is not the result of reaction (1). It may originate from the following reactions:





The possibility of reactions (7), (8), (9) cannot be excluded at low temperature but at least one of these reactions, most probably reaction (9), will probably occur only at higher temperatures (>150 °C) since NH(a) is most stable adsorbed species compared with NH₂(a) and NH₃. There is also a new peak at about 330 °C in the H₂O profile which is in the nearly same position as the fourth N₂ peak in the N₂ profile. This may be caused from the ammonia oxidation by bulk dissolved oxygen which is migrated on to the silver surface at high temperature.

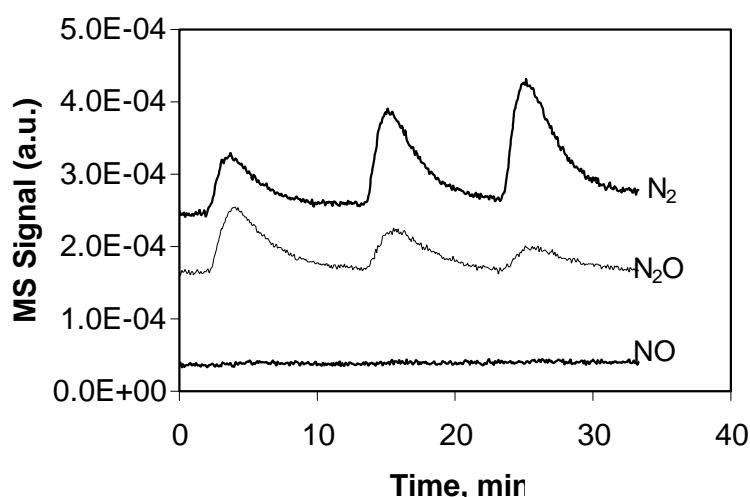


Fig.5 NH₃ pulse reaction profiles on silver powder at 200 °C
(Silver first reduced at 400 °C in flowing H₂(10%)/He=40 Nml/min for 2 h and then in flowing O₂(10%)/He=20 Nml/min at 200 °C. Each pulse contained 5 :l NH₃)

3.3 Ammonia pulse reaction studies

In order to further clarify the reaction mechanism pulse reactions were carried out at different temperatures. Pulses of NH₃ (circa 0.22 :mol) were made into a flow of O₂(10 vol%)/He. It can be seen from Fig.5 that during the first ammonia pulse large amounts of N₂O were produced simultaneously with N₂ production. During the following ammonia pulse the amount of N₂O production was greatly reduced while N₂ production increased. When the reaction temperature was raised from 200 °C to 400 °C the situation changed completely. Large amounts of NO were produced during each NH₃ pulse but the N₂ selectivity changed little (see Fig.6). These results indicate that some adsorbed nitrogen species were produced during the first NH₃ pulse that greatly changed the reaction selectivity of the following NH₃ pulse reaction at 200 °C but had less effect on selectivity at 400 °C.

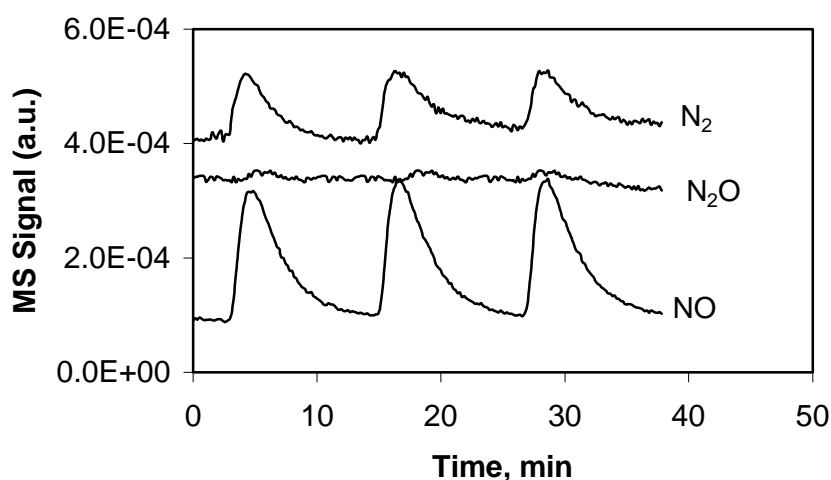
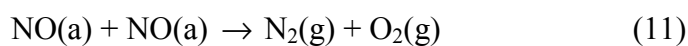
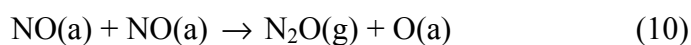


Fig.6 NH₃ pulse reaction profiles on silver powder at 400 °C
(Reaction conditions were the same as in Fig.5)

3.4 Reaction intermediates

In order to clarify the nature of the adsorbed species TPD experiments were done on a silver powder catalyst after reaction under different conditions. Fig.7 shows the TPD profiles measured on a Ag powder catalyst after reaction for 1 h in excess oxygen at 200 °C. It can be seen that the production profile patterns for N₂O, N₂ and O₂ are almost the same. This may indicate that these products originate from the same species. It is well known that NO can react to give N₂O, N₂ and O₂ according to the following reactions [23,24]:



To assess the importance of NO adsorption on Ag powder TPD experiments were carried out. When NO was co-adsorbed with O₂ on reduced silver powder at 200 °C the TPD profiles were nearly the same as that obtained after NH₃ oxidation reaction (see Fig.8). This strongly suggests that the adsorbed intermediate nitrogen species are mainly NO induced species.

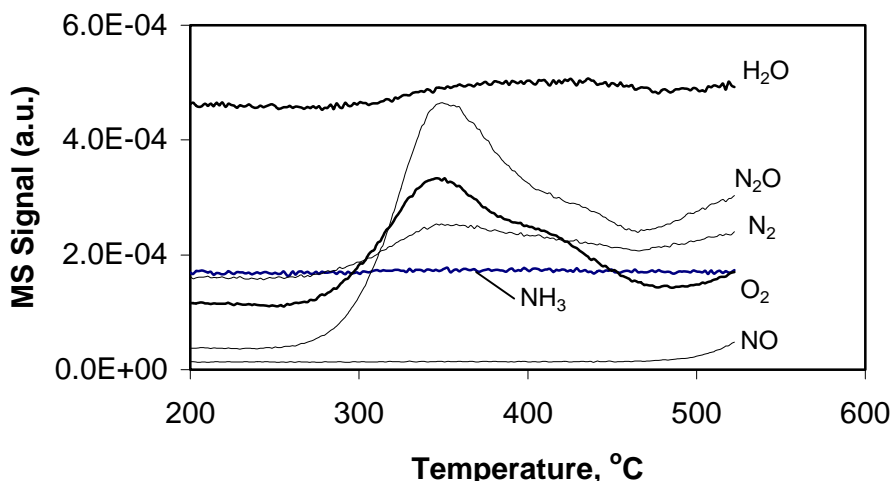
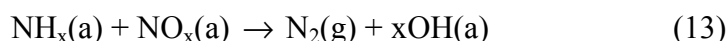


Fig.7 TPD profiles after NH₃ oxidation reaction at 200 °C on silver powder
(Reaction conditions: NH₃=1000 ppm; O₂=10%; Flow rate=50 Nml/min;
Cat. Weight=0.1 g. TPD was performed in flowing He=20 Nml/min from
200 to 550 °C at 10 °C/min)

It also can be seen from Fig.7 that there is some water produced. This may indicate the presence of some OH or NH_x species but the quantity is small. The fact that there is a trend to desorb N₂, NO, N₂O and O₂ at higher temperature (>500 °C) suggests the existence of more than one NO induced species. This species may be NO₃⁻ since it is the most stable species on the silver surface.

When the reaction was carried out at low O₂/NH₃ ratios (eg. 1/1) the TPD profile after reaction was totally different (see Fig.9). Much more water was produced and only N₂ desorbs at low temperature. As most of the OH species can be desorbed as H₂O at 280 °C, according to reaction (1), the comparatively large amount of water must come from NH_x species. Most probably N₂ and H₂O result from the following reaction:



Thus, apparently there are more NH_x species on the surface when the O_2/NH_3 ratio decreases.

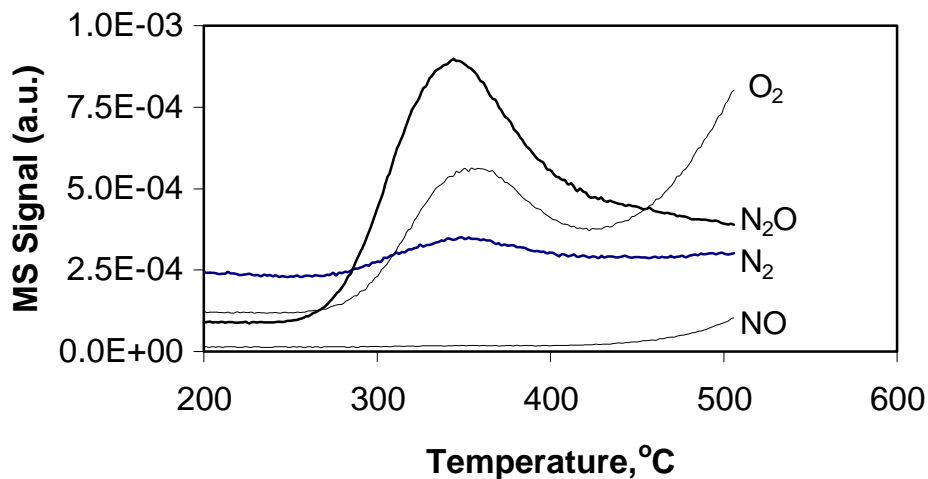


Fig.8 TPD profiles after $\text{NO}+\text{O}_2$ adsorption at 200 °C for 5 min

($\text{NO}=1000$ ppm; $\text{O}_2=10\%$; $\text{NO}/\text{O}_2/\text{He}=20$ Nml/min. TPD performed in flowing $\text{He}=20$ Nml/min from 200 to 550 °C at 10 °C/min)

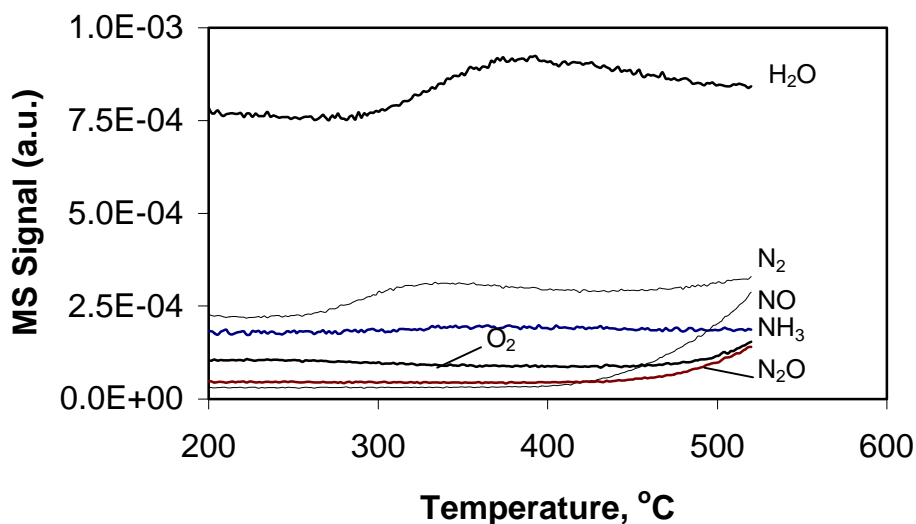


Fig.9 TPD profiles after NH_3 oxidation at 200 °C on silver powder

(Reaction conditions: $\text{NH}_3=1\%$; $\text{O}_2=1\%$; flow rate=50 Nml/min;
Cat. Weight=0.1 g. TPD performed in flowing $\text{He}=20$ Nml/min from 200 to 550 °C at 10 °C/min)

3.5 FT-Raman spectroscopy

FT-Raman measurements were carried out on a silver powder with pre-adsorbed NO, NO₂ or NH₃. For NO or NO₂ adsorption a completely reduced silver powder was used and the adsorption temperature was 50 °C. For NH₃ adsorption the reduced silver powder was first oxidized in O₂ at 200 °C for one hour and then NH₃ was adsorbed at 100 °C to increase the Raman signal. All of the measurements were done at room temperature to avoid heat effects. The resulting spectra are shown in Fig.10. Bao et al. have studied NO adsorption on Ag(110) by Raman and XPS [25]. They concluded that NO was not stable on a silver surface. NO was quickly oxidized to NO₂⁻ and NO₃⁻ which were strongly adsorbed on silver surface. SERS (Surface Enhanced Raman Spectroscopy) spectra of NO₂ adsorbed on silver powder were also reported in the literature [26,27]. Peaks at 815, 1045 and 1285 cm⁻¹ after exposure of silver powder to several nitrogen dioxide pulses added into the He gas stream were observed. They assigned the peaks at 815 and 1285 cm⁻¹ to adsorbed NO₂⁻ and the peak at 1045 cm⁻¹ to adsorbed NO₃⁻ on silver surface. Comparing the Raman spectrum of NH₃ adsorption with NO and NO₂ adsorption spectra in Fig.10, it is obvious that a similar spectrum to that of NO, NO₂ adsorption appears upon adsorption of NH₃ on oxygen-covered silver powder. This strongly indicates that NH₃ can be quickly oxidized to NO which will consequently be oxidized to NO₂⁻ and NO₃⁻ species. The remaining peaks in Fig.10, such as in the positions of 615 cm⁻¹, 670 cm⁻¹ and 985 cm⁻¹, are assigned to the different oxygen species on the silver surface [29].

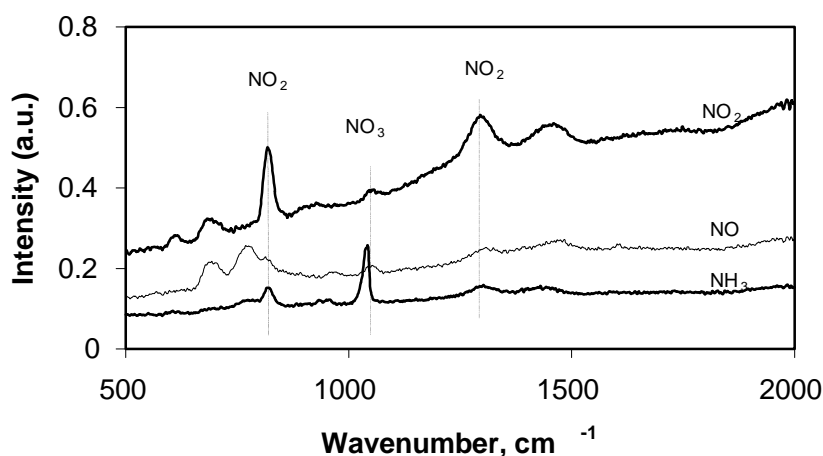


Fig.10 Raman spectra for NO, NO₂ and NH₃ adsorbed on silver powder
(NO and NO₂ adsorption at 50 °C on reduced silver powder; NH₃ adsorption at 50 °C on oxygen-covered silver powder)

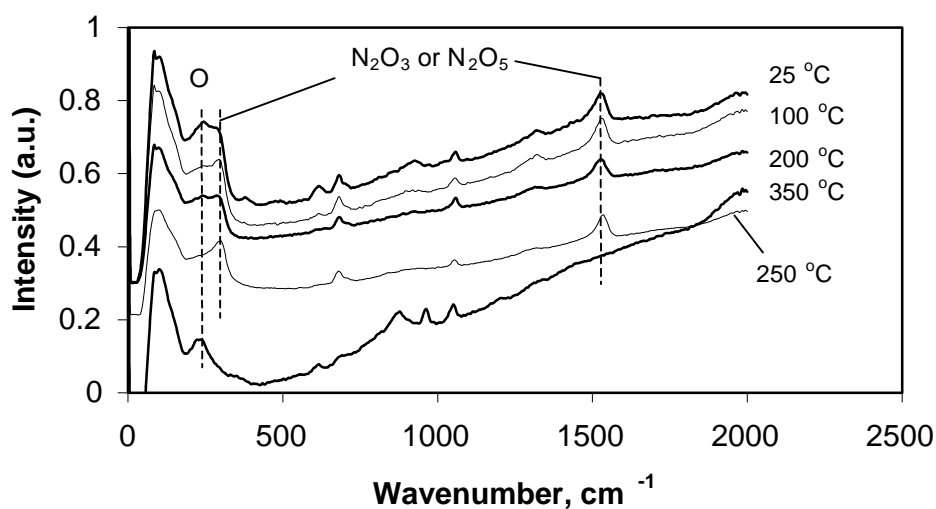


Fig.11 Raman spectra measured at room temperature after ammonia oxidation on silver powder at different temperatures
(Reaction conditions: NH₃=1000 ppm O₂=10 %; NH₃/O₂/He=50 Nml/min)

Raman measurements were carried out on silver powder at different temperatures following in-situ ammonia oxidation to observe the changes of surface species. The resulting spectra are shown in Fig.11. Based on previously published Raman data on the silver oxygen interaction [28,29] and on Raman and IR measurements of adsorbed

N_2O_x [30-33], the peak at 245 cm^{-1} is assigned to surface adsorbed atomic oxygen and the peaks at 266 and 1540 cm^{-1} are assigned to the N-N stretching Raman band of N_2O_x . The x can be 2, 3, 4 or 5. Unambiguous determination of x is difficult since these N_2O_x species often show intensities at nearly the same positions in Raman and IR spectra. It can be seen from Fig.11 that the intensity of surface atomic oxygen decreases with increasing temperature. The intensity of the N_2O_x peaks increased slightly as heating began but stayed unchanged afterwards. The NO_2 peak intensity decreased but NO_3^- adsorption signal stayed unchanged as the temperature increased. When the temperature was increased to $300\text{ }^\circ\text{C}$ the signals of N_2O_x disappeared and the surface atomic oxygen adsorption signal recovered again.

3.6 Reaction of NO and NO_2 with NH_3

The reactions between NO_x and NH_3 were also tested on powdered silver catalyst to probe the possibilities of different reactions between these reactants.

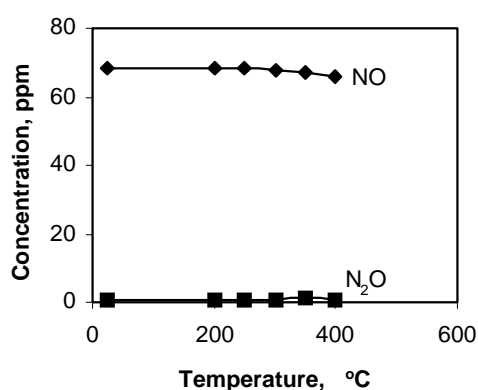


Fig.12 $\text{NO}+\text{H}_2$ reaction on reduced silver powder ($\text{NO}=74\text{ ppm}$, $\text{H}_2=5\%$, $\text{NO}/\text{H}_2/\text{He}=100\text{ Nml/min}$ Cat. Weight= 0.1 g)

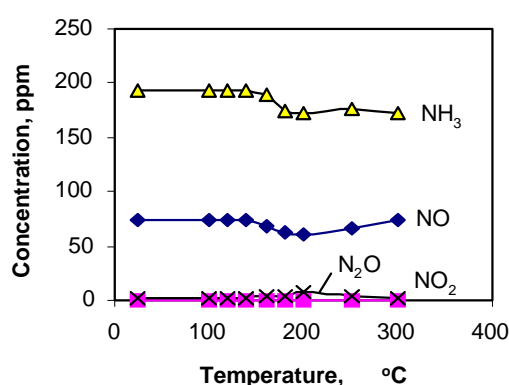


Fig.13 $\text{NO}+\text{NH}_3$ reaction on reduced silver ($\text{NH}_3=194\text{ ppm}$, $\text{NO}=74\text{ ppm}$, Cat. Weight= 0.1 g , $\text{NH}_3/\text{NO}/\text{He}=100\text{ Nml/min}$)

It can be seen from Fig.12 that under steady state reaction conditions the NO cannot be reduced by H_2 . This indicates that N_2 and N_2O cannot be directly formed from NO alone on silver powder catalysts. Fig.13 shows the results of reaction between NO and NH_3 . Only a small fraction of NO can react with NH_3 directly to produce N_2 and N_2O on silver powder catalysts. It can be from Fig.14 that the SCR reaction of NO with NH_3 is greatly increased by introducing O_2 . Fig.15 shows the results of reaction between NO_2 and NH_3 on silver powder catalyst. The NO_2 was first decomposed into NO and then reacted with NH_3 to produce N_2 and N_2O . At higher temperatures the NO concentration increases again because of the direct ammonia oxidation. This

experiment clearly indicates that NO₂ is not a reaction intermediate species to produce N₂O on silver catalysts.

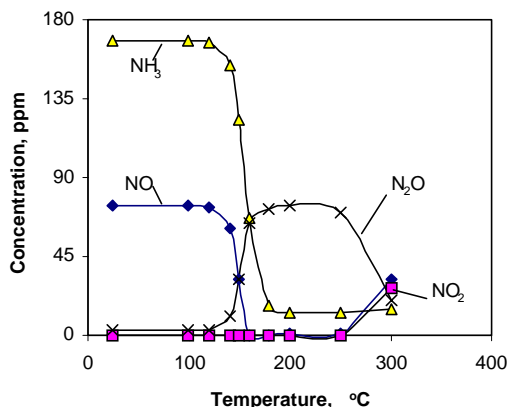


Fig.14 NH₃+NO+O₂ reaction on silver powder
(NO=74 ppm, NO/NH₃/O₂/He=100 Nml/min
NH₃=168 ppm, Cat. Weight=0.1 g)

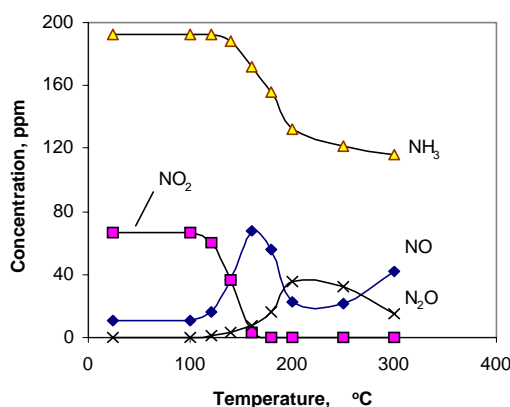
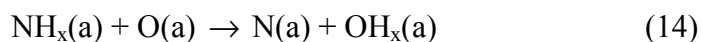


Fig.15 NO₂+NH₃ reaction on silver powder
(NH₃=194 ppm, NO₂=70 ppm, Cat. Weight=
0.1 g, NH₃/NO₂/He=100 Nml/min)

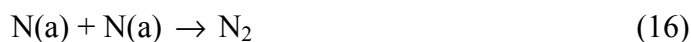
4. Discussion

NH₃ TPD and TPR results show that NH₃ does not adsorb on clean silver surface above room temperature. On an oxygen pre-covered silver surface NH₃ dissociatively adsorbs only as NH_x with one or two hydrogen abstracted by oxygen according to reaction (3) and (4). This is considered to be the initial step for ammonia oxidation. Reaction (3) and (4) can be enhanced by either increasing the temperature or by increasing the oxygen coverage on silver surface [17,18].

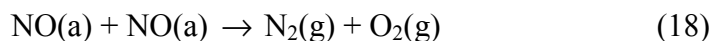
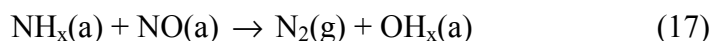
NH_x species can subsequently react with either O or OH according to reaction (9) to give N:



The N is very reactive and gives NO or N₂ according to:

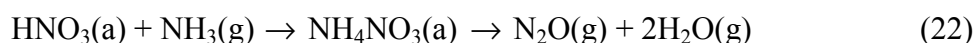
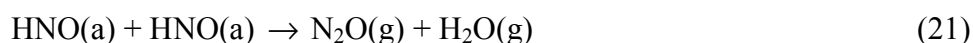


When there is pre-adsorbed oxygen on the silver surface the probability of reaction (16) occurring is low due to the high rate of reaction (15). The Raman experimental results clearly showed that NO_x species appeared even at room temperature upon ammonia adsorption. There was no evidence for the formation of molecular nitrogen at room temperature on silver powder. The fact that reactions (14) and (15) can take place at room temperature indicates that reaction (14) is not the rate-controlling step for gas phase NO formation as suggested by many authors [11,15,21]. Actually the NO formed can not desorb at low temperatures and quickly reacts with other adsorbed oxygen to produce NO_x which will strongly adsorb on the silver surface and block the active sites for oxygen dissociation. Since reaction (16) is not significant at high O₂/NH₃ ratio conditions, the formation of nitrogen may occur as follows:



The reaction (18) actually involves the NO dissociation and atomic nitrogen combination as in reaction (16). This occurs only at low temperatures on reduced silver and oxygen is a strong inhibitor of this reaction.

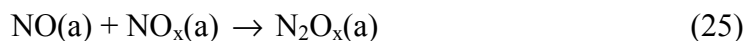
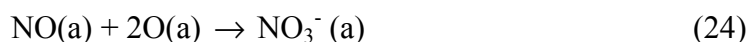
The mechanism of N₂O formation from ammonia is not very clear. In low pressure ammonia oxidation studies on Pt and Ag single crystals no N₂O formation was found over a large temperature interval and a large range of NH₃/O₂ ratios[13,22]. On Pt and Ag polycrystals, however, large amounts of N₂O are produced at low temperatures. At higher temperatures NO, instead of N₂O, is produced. The possible N₂O formation pathways proposed in the literature are as follows [4,15,23,34]:



Reaction (21) and (22) involve the intermediate HNO, HNO₃ species which were not observed on the silver surface. Thus, these two reactions are unlikely to occur on silver catalysts. The difference between reaction (19) and (20) is that the dissociation of NO is required in order that reaction (20) can proceed. This can only happen at

very low surface oxygen coverage. The chemisorption of nitric oxide at a Ag(111) surface has been reported to form N₂O at 80 K. However at 295 K this surface is unreactive to NO(g) under the same condition [37]. Our experiments on silver powder also show that N₂O can be produced only on reduced silver at initial stage of NO adsorption. When NO is introduced continuously to a reduced silver powder catalyst at temperature from 50-400 °C no N₂O is produced except for the initial time. Hence reaction (19) is the most likely reaction candidate for the formation of N₂O. To give further evidence for this theory, the SCR reaction was also carried out on reduced silver powder. The results show that the production of N₂O is not significant when NO reacts with NH₃ alone on silver catalyst. In the presence of oxygen NO can react quickly with NH₃ to give rise to N₂O and N₂. These experiments clearly indicate that N₂ and N₂O are not formed mainly from NO alone. NO cannot react directly with NH₃ on silver either. The role of O₂ is actually to produce adsorbed NH_x and N species which can then react readily with NO to produce N₂ and N₂O.

Apparently NO₂⁻, NO₃⁻ and N₂O_x species are produced by NO reacted with O or O₂:



Thus the overall ammonia reaction pathway on silver powder in an oxygen-rich atmosphere can be described schematically as in Fig.16.

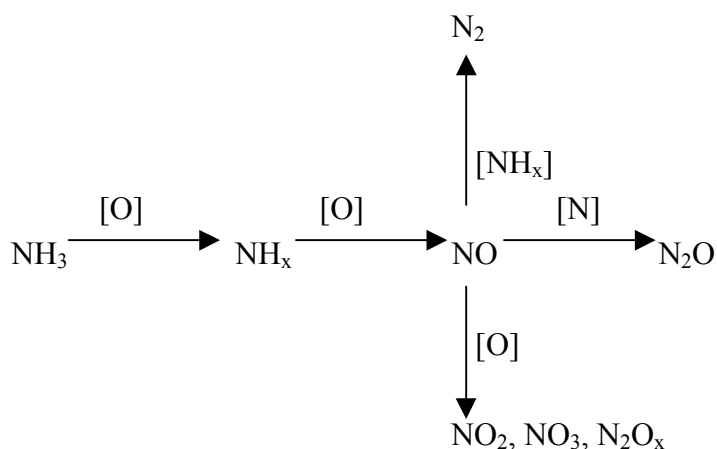


Fig.16 Scheme illustrating the pathways of NH₃-O₂ reactions

It can be seen clearly from this scheme that NO is the key intermediate. Even at room temperature NO can be quickly produced. Since NO cannot desorb at low temperature, it blocks the active sites for oxygen dissociation. So the reaction can continue only when the adsorbed NO is removed. At moderate temperatures (below 300 °C) NO can only be removed either as N₂O or N₂ through surface reaction (17) and reaction (15) respectively. At even higher temperature NO can directly desorb as one of the products. The rate-controlling step is thus the oxygen dissociation rate which is determined by the rate of NO removal. The selectivities to N₂ and to N₂O are also controlled by the relative rates of reaction (17) and (19). Actually, the relative rates of these two reactions are controlled by the surface oxygen coverage. At high surface oxygen coverage the reaction from NH_x to NO and N is very fast so that the surface NH_x concentration will decrease and the rate of reaction (17) will decrease accordingly. The selectivity is thus mainly towards N₂O. On the contrary the reaction becomes more selective to nitrogen when the surface oxygen coverage decreases.

As the surface NO₂, NO₃⁻ and N₂O_x species block some of the active sites for oxygen dissociation, they become inhibitors for ammonia oxidation. However the adsorption of these species on silver surface decreases the oxygen coverage. So the selectivity to nitrogen increases with increasing amounts of these adsorbed species. The Raman spectra for ammonia oxidation clearly showed that atomic surface oxygen intensity decreased with increasing temperature from 50 °C up to 300 °C. This is due to the fact that the amount of adsorbed N₂O_x species increases with increasing temperature. At a temperature higher than 350 °C N₂O_x decomposes and is removed from the surface so the oxygen coverage again increases. The steady-state tests for ammonia oxidation on silver powder at different temperatures (Fig.1) also show that the nitrogen selectivity increases with increasing temperature up to 300 °C. With further increase of temperature, the selectivity to nitrogen decreases due to the increasing rate of NO desorption. Ammonia pulse reactions again indicated the effect of adsorbed NO_x, N₂O_x species on the product selectivity. After the first ammonia pulse at 200 °C some adsorbed NO_x, N₂O_x species were produced which partially block the surface and decreased the surface oxygen coverage. In subsequent ammonia pulse reactions the selectivity to nitrogen was improved due to the lower surface O/N ratio. At higher temperature (400 °C) the desorption rate of NO became high, so that NO is formed instead of N₂O. Since little NO_x can be adsorbed on silver surface at this temperature there is almost no selectivity difference among three consecutive ammonia pulses.

5. Conclusions

Silver is a very active catalyst for ammonia oxidation. At low temperature (below 300 °C) mainly N_2 and N_2O are produced. At higher temperature NO instead of N_2O becomes one of the products. NO is an important reaction intermediate for this reaction. Even at room temperature NO can be produced and adsorbed on silver surface in the form of NO_x . Since NO can not desorb at low temperature it blocks the active sites for oxygen dissociation. The dissociation of oxygen is thus believed to be the rate-controlling step for ammonia oxidation. The selectivity to N_2 , N_2O and NO is determined by surface oxygen coverage and temperature. Low surface oxygen coverage favors nitrogen formation. Adsorbed NO_x , N_2O_x species are actually inhibitors for ammonia oxidation but they also lower the surface oxygen coverage. Hence, the selectivity to nitrogen is improved by increasing the amount of these adsorbed species on silver surface.

Generally speaking, silver alone, like Pt, is not a good catalyst for selective ammonia oxidation to nitrogen because too much N_2O is produced. It follows from the above conclusions that blocking of the sites for oxygen dissociation is an effective way to improve the nitrogen selectivity, but also would result in a loss of catalyst activity.

References

1. Li, Y., and Armor, N., Appl. Catal. B **13**, 131(1997).
2. Wollner, A., Lange, F., Schmelz, H., and Knozinger, H., Appl. Catal. A **94**, 181(1993).
3. De Boer, M., Huisman, H.M., Mos, R.J.M., Leliveld, R.G., Dillen, A.J., and Geus, J.W., Catal. Today **17**, 189(1993).
4. Andrussow, L., Z. Ang. Ch. **39**, 321(1926).
5. Bodenstein, M., Z. Elektroch. **41**, 466(1935).
6. Bodenstein, M., Z. Electroch. **47**, 501(1935).
7. Raschig, F., Z. Ang. Ch. **40**, 1183(1927).
8. Zawadzki, J., Disc. Faraday Soc. **8**, 140(1950).
9. Fogel, Ya.M., Nadykto, B.T., Rybalko, V.F., Shvachko, V.I., and Korobchanskaya, I.E., Kinet. Catal. **5**, 431(1964).
10. Gland, J.L., and Korchak, V.N., J. Catal. **53**, 9(1978).
11. Mieher, W.D., and Ho, W., Surf. Sci. **322**, 151(1995).
12. Asscher, M., Guthrie, W.L., Lin, T.H., and Somorjai, G.A., J. Phys. Chem. **88**, 3233(1984).
13. Bradley, J.M., Hopkinson, A., and King, D.A., J. Phys. Chem. **99**, 17032(1995).
14. Van den Broek, A.C.M., Van Grondelle J., and Van Santen, R.A., J. Catal. **185**(2), 297(1999).
15. Van den Broek, A.C.M., Ph.D. Thesis, Eindhoven University of Technology, 1998.
16. Carley, A.F., Davies, P.R. and Roberts, M.W., Chem. Commun., 1793(1998).
17. Carley, A.F., Davies, P.R., Kulkarni G.U., and Roberts, M.W., Catal. Lett. **58**, 97(1999).
18. Afsin, B., Davies, P.R., Pashusky, A., Roberts, M.W., and Vincent, D., Surface Science. **284**, 109(1993).
19. Amores, J.M.G., Escribano, V.S., Ramis, G., and Busca, G., Appl. Catal. B **13**, 45(1997).
20. Trombetta, M., Ramis, G., Busca, G., Montanari, B., and Vaccari, A., Langmuir **13**, 4628(1997).
21. Ramis, G., Yi, L., and Busca, G., Catal. Today **28**, 373(1996).
22. Thornburg, D.M., and Madix, R.J., Surf. Sci. **220**, 268(1989).
23. Otto, K., and Shelef, M., J. Phys. Chem. **76**(1), 37(1972).
24. Otto, K., Shelef, M., and Kummer, J.T., J. Phys. Chem. **74**(13), 2690(1970).
25. Bao, X., Wild, U., Muhler, M., Pettinger, B., Schlogl, R., and Ertl, G., Surf. Sci. **425**, 224(1999).

26. Von Raben, K.U., Dorain, P.B., Chen, T.T., and Chang, R.K., Chem. Phys. Letters **95**, 269(1983).
27. Matsuta, H., and Hirokawa, K., Surf. Sci. **172**, L555(1986).
28. Mcbreen, P.H., and Moskovits, M., J. Catal. **103**, 188(1987).
29. Stencel, J.M., "Raman Spectroscopy for Catalysis", Van Nostrand Reinhold, New York, 1990.
30. Hisatsune, I.C., Devlin, J.P., and Wada, Y., J. Chem. Phys. **33(3)**, 714(1960).
31. Hisatsune, I.C., Devlin, J.P., and Wada, Y., Spectrochimica Acta **18**, 1641(1962).
32. Kugler, E.L., Kadet, A.B., and Gryder, J.W., J. Catal. **41**, 72(1976).
33. Bibart, C.H., and Ewing, E., J. Chem. Phys. **61(4)**, 1293(1974).
34. Andrussow, L., Z. Elektroch. **36**, 756(1930).
35. Carley, A.F., Davies, P.R., Roberts, M.W., Thomas, K.K. and Yan, S., Chem. Commun., 35(1998).
36. Carley, A.F., Davies, P.R. and Roberts, M.W., Current Opinion in Solid State and Materials Science, **2(5)**, 525(1997).
37. Carley, A.F., Davies, P.R., Roberts, M.W., Santra, A.K. and Thomas, K.K., Surface Science, 406, L587(1998).

Chapter 5

Low Temperature Selective Oxidation of Ammonia to Nitrogen on Silver-based Catalysts

Abstract

The low temperature gas phase oxidation of ammonia to nitrogen has been studied over alumina-supported, silica-supported and unsupported silver catalysts. TPD, TPR, TEM, XRD and FT-Raman were used to characterize the different silver catalysts. The results showed alumina-supported silver to be the best catalyst due to the interaction of silver with alumina. Pretreatment had a great effect on the catalyst performance. Reduction in hydrogen at 200 °C without any pre-calcination gave the best activity while reduction at higher temperatures showed little difference from calcination pretreatment. At least four types of oxygen species were produced when silver was oxidized at high temperature. These species are adsorbed molecular oxygen, adsorbed atomic oxygen, strongly adsorbed atomic nitrogen and subsurface oxygen respectively. Ammonia oxidation activity at low temperature is related to the catalyst's ability to adsorb oxygen either dissociatively or non-dissociatively. In addition, a good correlation existed between the N₂ selectivity for the SCO reaction and the SCR performance of NO with NH₃ for the silver-based catalysts, i.e., the higher SCR yield of nitrogen, the higher the SCO selectivity to N₂.

1. Introduction

Low temperature selective catalytic oxidation (SCO) of ammonia with oxygen to nitrogen and water is a potentially efficient method to abate ammonia pollution [1-3]. Previous studies showed that noble metals such as Pt and Ir are active for this reaction at low temperature but deactivate rapidly with time. Dependent on reaction conditions significant amounts of nitrous oxide or nitric oxide can also be produced on these catalysts [4-6]. Metal oxide catalysts such as Co₃O₄, MnO₂, CuO, Fe₂O₃, V₂O₅ and MoO₃ have also been studied in the literature [7-12] but ammonia conversion levels are not high enough at low temperatures to be of practical use.

Silver is an industrially used catalyst for epoxidation of ethylene to ethylene epoxide and for oxi-dehydrogenation of methanol to formaldehyde. Recently it was reported that alumina-supported silver catalysts can also be extremely active for abating NO_x in lean-burning gasoline engine exhaust [13-15]. In this Chapter we report that silver is also a very active ammonia oxidation catalyst. At low temperature (<200 °C) the performance of supported silver catalysts is even superior to noble metal catalysts in both selectivity and activity.

2. Experimental

Ag/ γ -Al₂O₃, Ag/SiO₂ samples with different Ag loadings were prepared by incipient wet impregnation. The precursors for these catalysts are AgNO₃ impregnated on the γ -Al₂O₃ (Akzo/Ketjen 000 1.5E, surface area 235 m²/g) or SiO₂ (Grace 332, surface area 270 m²/g) support. The samples were calcined in air at 500 °C for 24 hours before testing. Polycrystalline silver was prepared from Ag₂O (>99.99%) powder. The powder was first reduced in flowing H₂/He (10% H₂, 50 ml/min) overnight at 400 °C and then oxidized in flowing O₂/He (10% O₂, 50 ml/min) at 400 °C for 2 hours. This process was repeated three times to remove any carbon species and to achieve a stable surface area (surface area 0.67 m²/g, average particle size 0.43 μ m).

Catalytic activity measurements were carried out in a tubular quartz, fixed-bed reactor (4 mm internal diameter). The amount of catalyst used was about 0.2 gram (250-425 μ m particles). Ammonia, oxygen and helium flow rates were controlled by mass flow controllers. The inlet and outlet gas compositions were analyzed by an on-line Chemiluminescence NH₃ and N₂O Analyzer. A quadruple mass spectrometer was also used to monitor the different products (Balzers OmniStar).

NH₃ TPD or TPR experiments were performed using a fixed-bed flow reactor system equipped with a computer-interfaced quadrupole mass spectrometer. After adsorption of NH₃ at room temperature the TPD or TPR data were recorded by mass spectrometer while the temperature was increased from 50° to 500 °C at a heating rate of 5 °C/min. The H₂ TPR and O₂ TPD data were obtained on a typical computer-controlled temperature programmed reduction apparatus. The hydrogen consumption was measured using a thermal conductivity detector. The temperature was ramped from 25° to 800 °C at a rate of 10 °C/min.

FT-Raman spectra were obtained with a Bruker FRA 106 Raman Spectrometer equipped with an in-situ reaction chamber. The standard laser is an air-cooled, diode-pumped Nd:YAG operating at 1.064 µm with a maximum laser power of 500 mW. Usually a laser power of 150 mW was used for measurements at atmospheric pressure. Detection was performed by a liquid-nitrogen-cooled InGaAs detector. One hundred scans were co-added at a resolution of 2 cm⁻¹. High resolution transmission electron microscopy (HREM) measurements were done on a Philips CM30-T electron microscope at the National Centre for HREM at the Delft University of Technology. X-ray powder diffraction (XRD) patterns were recorded on a Rigaku Geigerflex X-ray powder diffractometer using Cu-Kα radiation. Prior to the experiment the catalysts were ground and pressed into a sample holder containing vaseline. The applied scanning speed was 1° per minute. Background subtraction was not applied.

3. Results

3.1. Ammonia oxidation on silver based catalysts

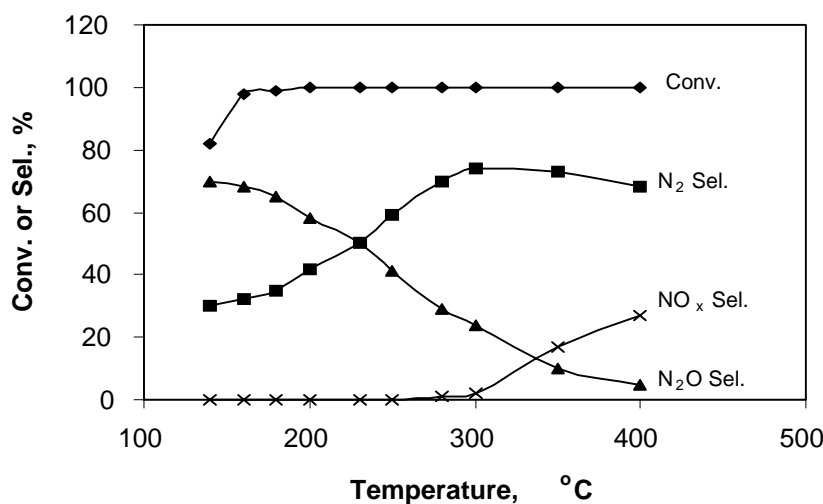


Fig. 1 Ammonia oxidation on silver powder catalyst at different temperature

Reaction conditions: NH_3 =1000 ppm; O_2 =10 vol%;

Total flow rate=50 Nml/min; Cat. Weight=0.1 g

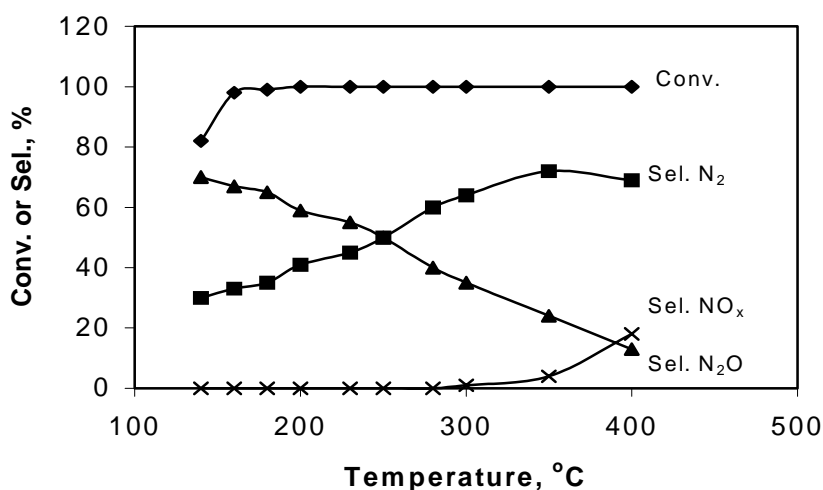


Fig.2 Ammonia oxidation on 10 wt% Ag/SiO₂ catalyst at different temperature

Reaction conditions: NH_3 =1000 ppm; O_2 =10 vol%;

Total flow rate=50 Nml/min; Cat. Weight=0.1 g

In order to elucidate the support effect on ammonia oxidation for the silver system, pure silver powder, silica- and alumina-supported catalysts were prepared and tested

for ammonia oxidation at different temperatures. The results are shown in Fig.1, Fig.2 and Fig.3. It can be seen that pure silver powder catalyst behaves similarly to silica-supported silver catalyst but quite differently from the alumina-supported silver catalyst. The alumina-supported silver catalyst shows better selectivity to N₂ than silver powder or the silica-supported silver catalyst. It is interesting that mainly N₂O is produced on silver powder and silica-supported catalysts at lower temperatures. The selectivity at low temperature (<300 °C) varies little for alumina-supported silver catalyst but decreases abruptly at higher temperature due to the large production of NO (see Fig. 3). Different catalyst pretreatment has a large effect on alumina-supported silver catalysts (see Fig.4). Calcination at high temperature decreases the activity of catalyst. This probably relates to a decrease in surface area at elevated temperature. Reduction in hydrogen at 200 °C without any pre-calcination gives best activity however reduction at higher temperatures shows little difference from the calcined sample.

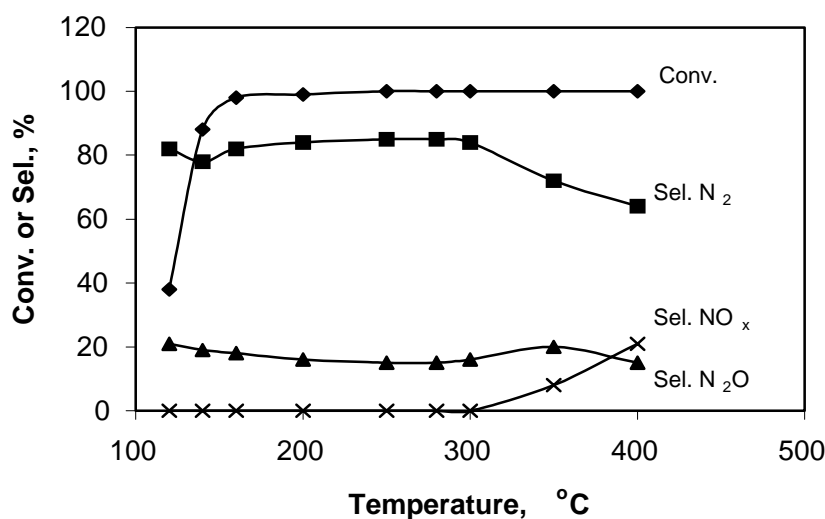


Fig.3 Ammonia oxidation on 10 wt% Ag/Al₂O₃ catalyst at different temperature
 Reaction conditions: NH₃=1000 ppm; O₂=10 vol%;
 Total flow rate=50 Nml/min; Cat. Weight=0.1 g

The above results clearly show that silver-based catalysts are quite active for ammonia oxidation. Alumina-supported silver catalysts are the most selective compared with silver powder and silica-supported catalysts. However the N_2 selectivity is still not very satisfying (around 80%).

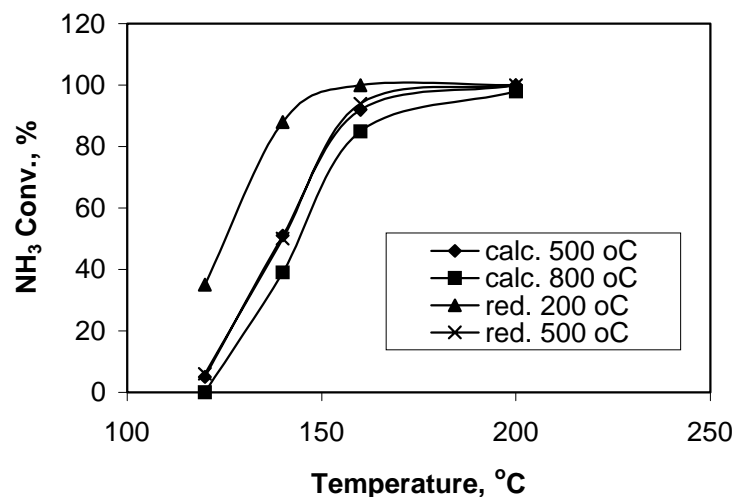


Fig. 4 The effect of pretreatment for 10 wt% Ag/ Al_2O_3 catalyst
Reaction conditions:
 NH_3 =1000 ppm;
 O_2 =10 vol%;
Total flow rate=50 Nml/min;
Cat. weight=0.1 g

Table 1. The activity of various catalysts for ammonia oxidation

catalyst	Temperature	NH_3 conversion	N_2 selectivity
	°C	%	%
Ir/ Al_2O_3 (1.2 wt%) (reduced)	180	52	88
	200	100	84
Pt/ Al_2O_3 (1.2 wt%) (reduced)	180	66	75
	200	100	75
Ag/ Al_2O_3 (10 wt%) (reduced)	120	35	81
	140	88	82
	160	100	82

Reaction conditions: NH_3 = 1000 ppm; O_2 = 10%; O_2/NH_3 = 100
flow rate = 50 Nml/min; cat. weight = 0.1g

Table 1 shows the performance of the $\text{Ag}/\text{Al}_2\text{O}_3$ catalyst compared with the noble metal catalysts. It can be seen that the performance of silver-based catalyst is superior to that of noble metal catalysts in both activity as well as selectivity. With further improvement, this catalyst is promising and could potentially be used instead of noble metal-based catalysts at the temperatures below 200 °C.

3.2. XRD and TEM measurements

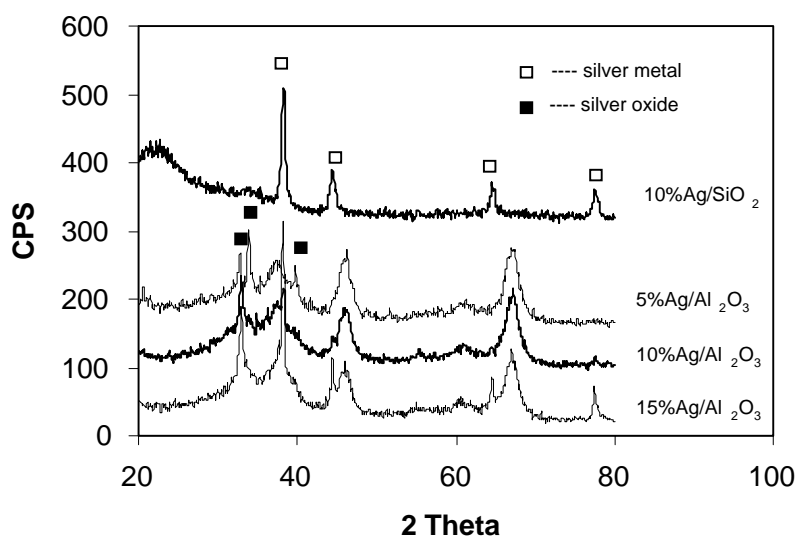


Fig. 5 XRD spectra of supported silver catalysts calcined at 500 °C

XRD and TEM were used to examine the differences between silica- and alumina-supported catalysts. All the catalysts were calcined in air at 500 °C for 24 hours before testing. Fig.5 shows the XRD spectra of the different silica- and alumina-supported catalysts. A distinct XRD pattern attributable to crystallized silver metal was observed for 10 wt% Ag/SiO_2 catalyst. However on 5 wt% $\text{Ag}/\text{Al}_2\text{O}_3$ catalyst no silver metal phase was detected but specific XRD pattern for Ag_2O appeared. As the silver loading on alumina increased the metallic phase increased and the silver oxide phase disappeared except for the peak at diffraction angle of 33.43 degree.

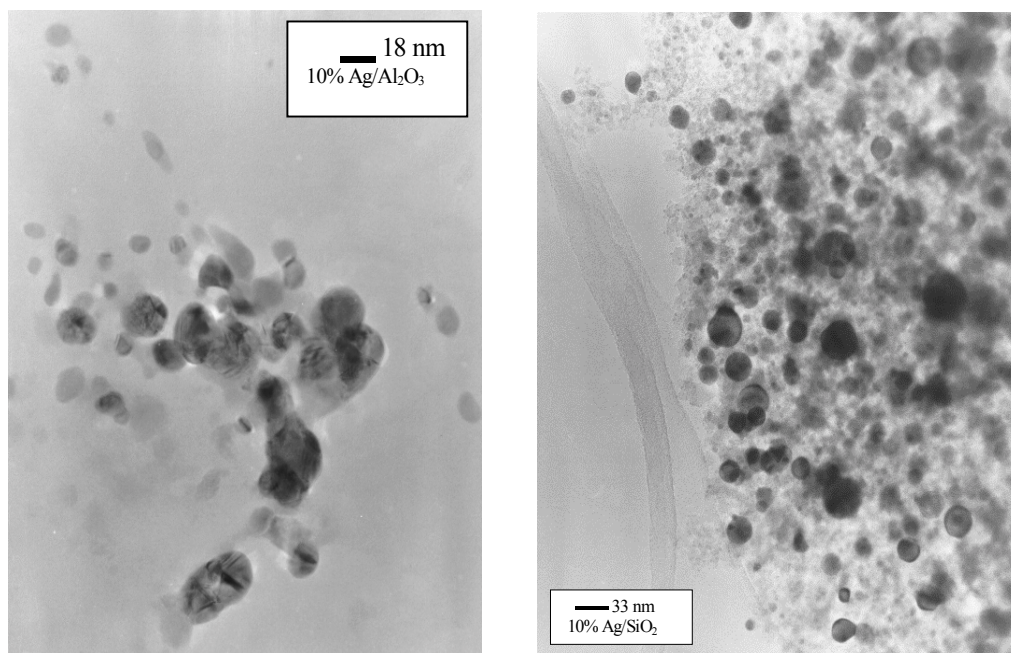


Fig.6 TEM photographs of different supported silver catalysts

Fig.6 shows the TEM photographs of different supported catalysts to demonstrate the distribution of silver particles on the surface of different supports. As shown by Fig.6, the silver was inhomogeneously distributed on both silica and alumina support. The metal particle size distribution on silica-supported silver catalyst seems to be bimodal. Many particles are about 15-40 nm in diameter, whereas many particles of about 1-2 nm diameter are also present. The silver particle size distribution on alumina is very broad. The smallest particles are about 3 nm in diameter and the largest particles found are about 40 nm in diameter. Table 2 shows the silver area and particle size of three silver-based catalysts determined by different techniques.

Table 2 Surface area and particle size of different catalysts

Catalyst	Ag area (m ² /g)	average particle size
Ag powder ^a	0.67	0.43 μm
10 wt% Ag/SiO ₂ ^b	3.27	24 nm
10 wt% Ag/Al ₂ O ₃ ^b	9.48	8.2 nm

^a: determined by BET

^b: determined by O₂ chemisorption

3.3. Interaction of O_2 with silver

FT-Raman measurements were carried out on a silver powder treated in O_2 at different temperatures. All of the measurements were done at room temperature to avoid heating effects. The resulting spectra are shown in Fig.7. McBreen and

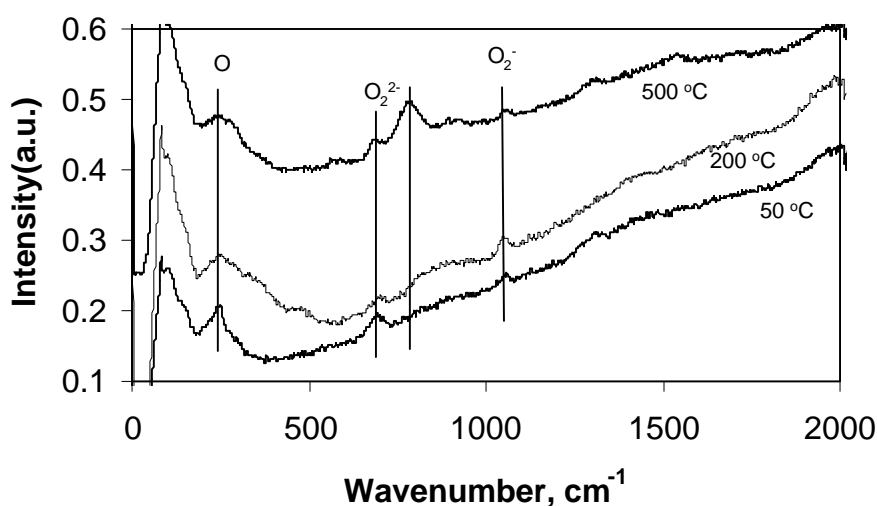


Fig.7 Raman spectra of silver powder oxidized at different temperature

Moskovits [16] examined two types of Ag catalysts by Raman spectroscopy during the adsorption of oxygen and ethylene. These catalysts included a silver colloid and silver electrochemically deposited onto an anodic aluminum oxide. The peak at 238 cm^{-1} in their spectra was assigned to adsorbed atomic oxygen. Relatively weak bands at 670 and 985 cm^{-1} were assigned to adsorbed molecular oxygen. Their results were compared with data from EELS [17] and other Raman experiments [18]. In these references the vibrational frequency of atomic oxygen on Ag was assigned to a band at 312 cm^{-1} , whereas frequencies of peroxidic (O_2^{2-}) and superoxidic (O_2^-) species on Ag were assigned to bands at 697 and 1053 cm^{-1} respectively. Thus in Fig.7 the peak at 245 cm^{-1} can be assigned to atomic adsorbed oxygen. Bands at 680 and 1053 cm^{-1} can be assigned to molecular adsorbed oxygen. It can be seen from Fig.7 that a new feature at 775 cm^{-1} appears after heating in oxygen at $500 \text{ }^\circ\text{C}$. The assignment of this band will be discussed later.

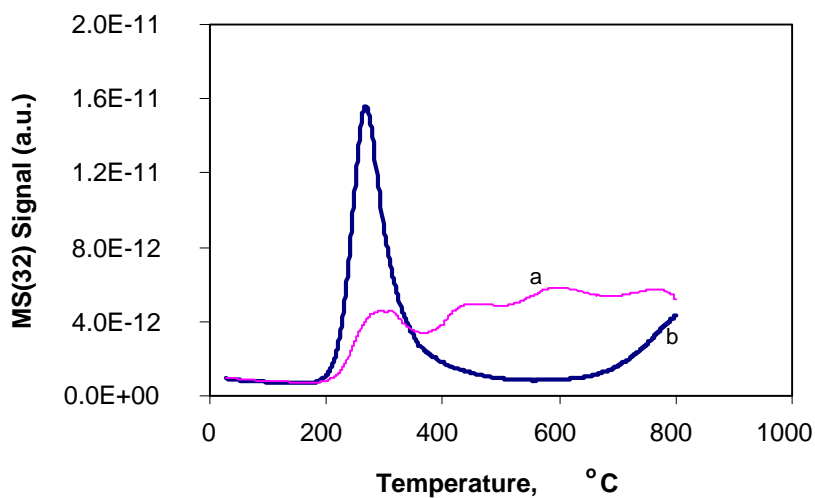


Fig.8 O_2 TPD profile on 10 wt% Ag/SiO₂ catalyst

a—first reduced at 500 °C for 2 hr, then oxidized at 500 °C for 2 hr

b—first reduced at 500 °C for 2 hr, then oxidized at 200 °C for 2 hr

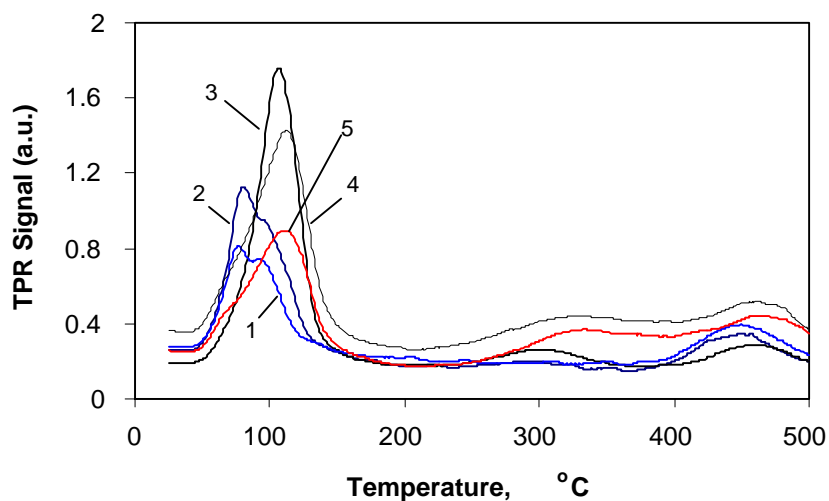


Fig.9 H_2 TPR profiles on 10 wt% Ag/SiO₂ catalyst

1—oxidized at 50 °C; 2—oxidized at 100 °C; 3—oxidized at 200 °C;

4—oxidized at 400 °C; 5—oxidized at 500 °C

O_2 TPD experiments on 10% Ag/SiO₂ were carried out from 25 °C to 800 °C at a heating rate of 10 °C/min. The catalyst was first reduced in H_2/N_2 flow at 500 °C for 2 hours and then pretreated in O_2/He flow at 200 °C or 500 °C for 2 hours and then

cooled down to room temperature in O₂. The O₂ TPD profiles on 10wt% Ag/SiO₂ (see Fig.8) show that two O₂ desorption peaks appear for a catalyst pretreated with oxygen at 200 °C. One is at the temperature of about 280 °C and another at temperature over 800 °C. When the catalyst was pretreated in oxygen at 500 °C, four O₂ desorption peaks were observed at temperatures of 280, 450, 600 and 775 °C respectively. It is well known that atomically adsorbed oxygen desorbs at around 280 °C on a silver surface [19]. High temperature treatment in oxygen decreased the intensity of the atomically adsorbed oxygen peak substantially. This is caused by silver surface reconstruction as argued by many researchers [20-22,30].

The O₂ TPD results above clearly show that pretreatment conditions are extremely important to the silver oxygen interaction. Hence H₂ TPR was carried out on silver catalysts pretreated in oxygen at different temperatures. The catalysts were first reduced at 500 °C for 2 hours before oxygen pretreatment. Fig.9 shows the H₂ TPR profiles on 10 wt% Ag/SiO₂. It can be seen that three peaks exist at temperatures of 80, 97 and 460 °C respectively when the catalyst is pretreated in oxygen at a temperature below 200 °C. When the pretreatment temperature increased to over 200 °C a fourth peak appeared. The position of this peak along with the second peak moved to higher temperatures with the increase of pretreatment temperature.

As H₂ cannot directly go into the silver subsurface or bulk without reacting with the surface oxygen, the first TPR peak must be surface adsorbed molecular or atomic oxygen. As it is well known that adsorbed atomic oxygen can reach a maximum at about 200 °C on silver surface, the second peak can thus be assigned to surface adsorbed atomic oxygen and the first peak can therefore be attributed to molecularly adsorbed oxygen. Compared with the Raman results the peak appeared after high temperature treatment in O₂ can be assigned to atomic oxygen strongly adsorbed on the silver surface defects as discovered by L. Lefferts [30]. The peak at 460 °C thus can be assigned to the subsurface oxygen since this oxygen is the most difficult one to be reduced [23,30].

Fig.10 shows the H₂ TPR profiles on 10 wt% Ag/Al₂O₃. It can be seen that there are also three peaks at temperatures of 75, 130 and 470 °C that can be assigned to molecularly adsorbed oxygen, adsorbed atomic oxygen and subsurface oxygen respectively when catalyst is pretreated in oxygen at the temperature below 200 °C. When the pretreatment temperature increased to over 200 °C, again strongly adsorbed oxygen peak appeared. The position of this peak moved to higher temperatures with the increase of pretreatment temperature.

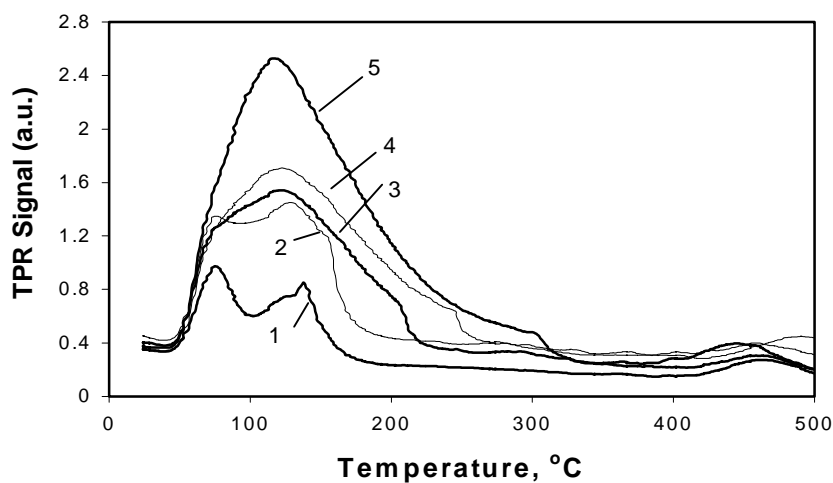


Fig.10 H_2 TPR profiles on 10 wt% $\text{Ag}/\text{Al}_2\text{O}_3$ catalyst

1—oxidized at 50 °C; 2—oxidized at 100 °C; 3—oxidized at 200 °C;
4—oxidized at 400 °C; 5—oxidized at 500 °C

For 5 wt% $\text{Ag}/\text{Al}_2\text{O}_3$ catalyst the TPR profile pattern was almost the same as that of 10 wt% $\text{Ag}/\text{Al}_2\text{O}_3$ but the second peak moved to higher temperatures when the catalyst was treated in oxygen at higher temperature (see Fig.11). Apparently catalysts with low silver loading are even more sensitive to oxygen pretreatment.

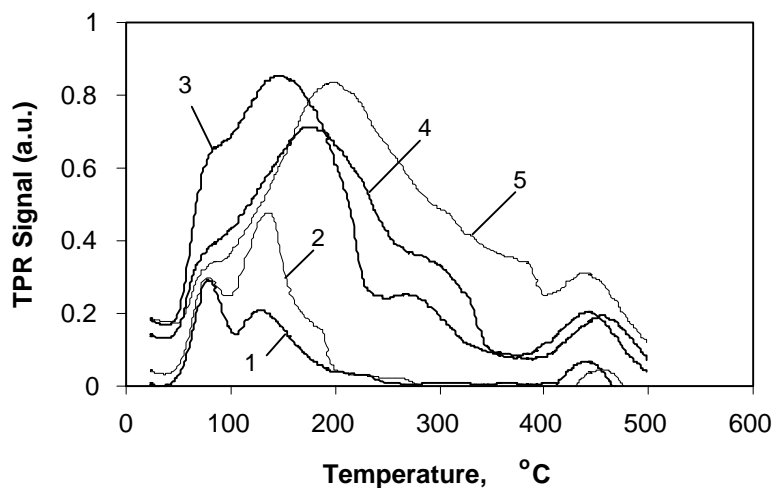


Fig.11 H_2 TPR profiles on 5 wt% $\text{Ag}/\text{Al}_2\text{O}_3$ catalyst

1—oxidized at 50 °C;
2—oxidized at 100 °C;
3—oxidized at 200 °C;
4—oxidized at 400 °C;
5—oxidized at 500 °C

3.4. NH_3 TPR

NH₃ TPR was carried out on different kinds of silver-based catalysts. The catalyst was first reduced in H₂/He flow at 400 °C overnight and then oxidized in O₂/He flow at

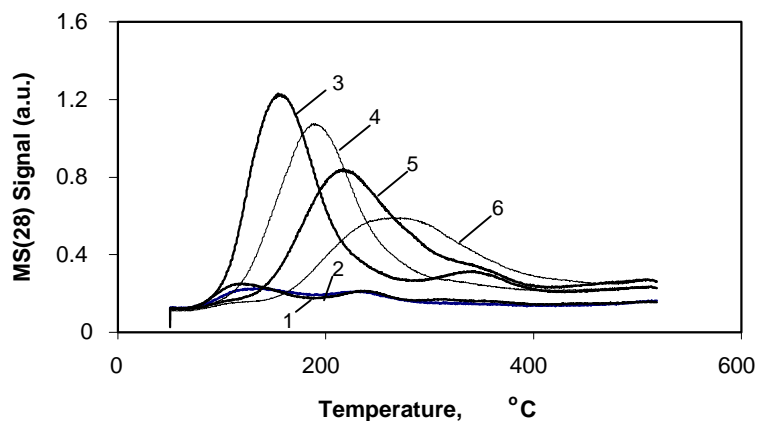


Fig.12 N₂ production profiles on 5 wt% Ag/Al₂O₃ during NH₃ TPR
1—oxidized at 50 °C; 2—oxidized at 100 °C; 3—oxidized at 200 °C;
4—oxidized at 300 °C; 5—oxidized at 400 °C; 6—oxidized at 500 °C

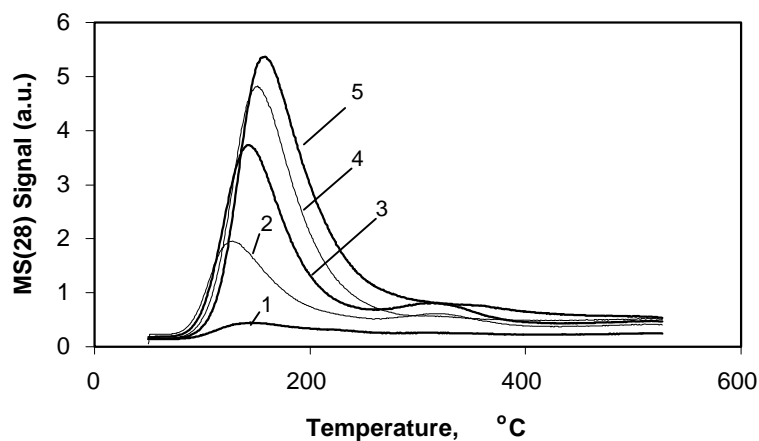


Fig.13 N₂ production profiles on 10 wt% Ag/Al₂O₃ during NH₃ TPR
1—oxidized at 50 °C; 2—oxidized at 100 °C; 3—oxidized at 200 °C;
4—oxidized at 400 °C; 5—oxidized at 500 °C

different temperatures for 2 hours. Fig.12 shows the N₂ production profiles on 5wt% Ag/Al₂O₃ catalyst. The fact that the nitrogen production maximum moved to higher temperature when the catalyst was treated in oxygen at higher temperature again indicated the large effect of oxygen pretreatment. For the 10 wt% Ag/Al₂O₃ catalyst

the effect of the oxygen pretreatment on the position of the nitrogen production maximum was observed to be less (see Fig.13).

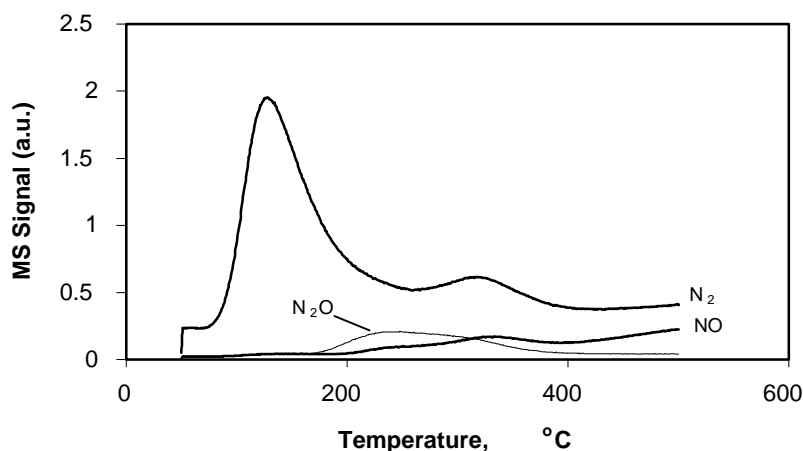


Fig.14 NH₃ TPR profiles on 10 wt% Ag/Al₂O₃ oxidized at 200 °C

Apart from the nitrogen production some N₂O and NO are also produced during NH₃ TPR. The typical profiles are shown in Fig.14. Apparently N₂O and NO formation peaks were behind the nitrogen formation peak. Studies of ammonia oxidation on Pt showed that the selectivity to N₂ or NO was mainly determined by the surface O/N ratio [24,25]. A high O/N ratio favored NO formation. In the present case the surface O/N ratio was always low because there was excess of ammonia in the flow. So a large amount of N₂ was initially produced in NH₃ TPR process. The fact that there was no NO or N₂O formation below 200 °C probably indicates that the NO produced was adsorbed on the silver surface. At higher temperature NO started to desorb and at the same time N₂O was formed from NO through a disproportionation [26] reaction at the silver surface ($\text{NO} + \text{NO} \rightarrow \text{N}_2\text{O} + \text{O}$). The O formed from this reaction will then react with ammonia to produce N₂. That is why there is second nitrogen peak in N₂ formation profile. To obtain evidence of the above hypothesis NO TPD was carried out on reduced silver powder. NO was pre-adsorbed at 50 °C and then a TPD profile was recorded by MS from 50 to 500 °C at a temperature increase of 10 °C/min.

NO TPD profiles in Fig.15 clearly show that NO started to desorb at about 200 °C and N₂O also formed during NO desorption. Since there is no NH₃ in the stream N₂ production is not observed.

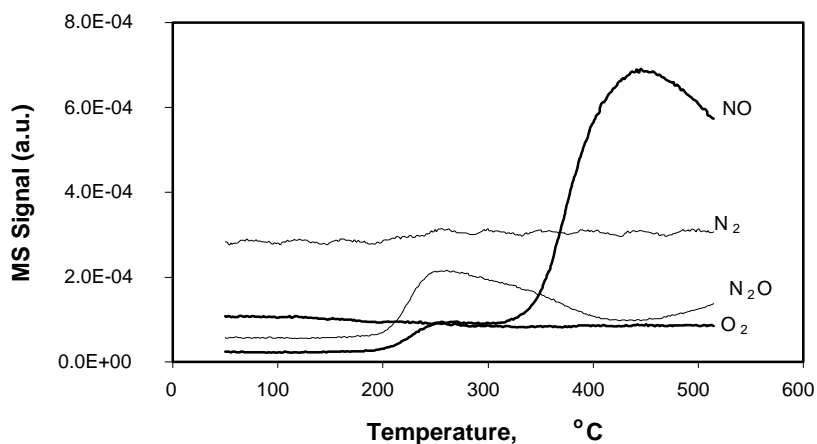


Fig.15 NO TPD profiles on 10 wt% Ag/Al₂O₃ catalyst

The catalyst was first reduced in H₂ at 400 °C for 2 hr and then kept in flowing NO at 50 °C for 30 min. The TPD was carried out in flowing He from 50 to 550 °C at a heating rate of 10 °C/min.

The NH₃ TPR profiles on 10 wt% Ag/SiO₂ catalyst are very complicated (see Fig.16). Clear explanation for these nitrogen production profiles seems to be impossible. Generally this catalyst is also greatly affected by the high temperature pretreatment in oxygen.

Table 3. SCR (NO+NH₃) reaction on different silver-based catalysts

Catalyst	Temperature °C	NO conversion %	N ₂ selectivity %
Ag powder	140	17	33
	150	57	36
	160	98	40
	180	99	54
	200	100	56
Ag/SiO ₂ (10 wt%) (reduced)	140	25	34
	150	66	38
	160	99	41
	180	100	52
	200	100	55
Ag/Al ₂ O ₃ (10 wt%) (reduced)	140	32	67
	150	70	68
	160	98	70
	180	100	74
	200	100	72

Reaction conditions: NO = 75 ppm; NH₃ = 170 ppm; O₂ = 2 vol%;
flow rate = 110 Nml/min; catalyst weight = 0.025g

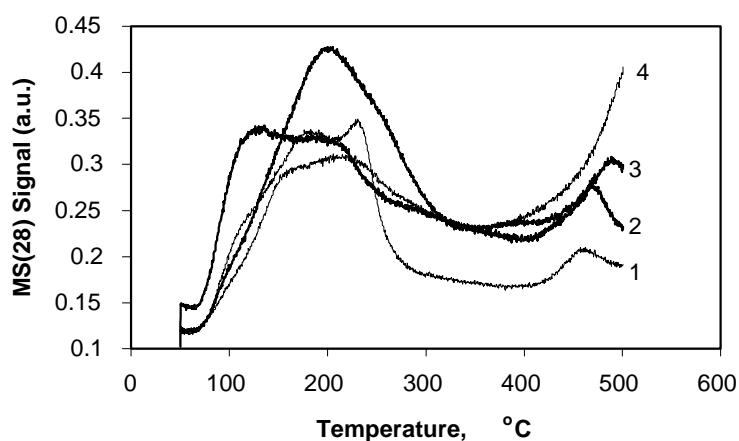


Fig.16 N₂ production profiles on 10 wt% Ag/SiO₂ during NH₃ TPR
1—oxidized at 50 °C; 2—oxidized at 100 °C; 3—oxidized at 200 °C;
4—oxidized at 400 °C

3.5. SCR reaction on silver-based catalysts

Selective catalytic reduction of NO by ammonia (SCR) was also tested on various silver-based catalysts to demonstrate the relationship between the SCR reaction and the ammonia oxidation reaction. The results are shown in Table 3. It can be seen from Table 3 that the activity for the SCR reaction on alumina-supported silver catalyst was a little higher than that on silver powder or on a silica-supported silver catalyst. However there was a big difference in selectivity among these catalysts. The SCR reaction was more selective to nitrogen on alumina-supported silver catalyst compared with silver powder and silica-supported silver catalysts.

4. Discussion

The interaction of O_2 with Ag was thoroughly studied by many researchers, mostly on single crystals and polycrystalline silver and under high vacuum conditions [19-22]. General conclusions could be obtained from these studies. **1.** For Ag(110): Molecular adsorbed oxygen desorbed at about 200K. Atomic-bound oxygen desorbed at about 600K. The adsorbed atomic oxygen can diffuse into the sub-surface region above 423K. Bulk-dissolved oxygen was formed above 723K. **2.** For Ag(111): Compared with (110) this surface showed very low sticking coefficient for oxygen adsorption. Adsorption at (111) was believed to occur primarily at defect sites. Adsorbed molecular and atomic oxygen was also found on this surface. A third oxygen species which was intercalated in the uppermost silver layers was shown to be formed at temperature in excess of 773K. **3.** For polycrystalline Ag: Molecular, atomic, sub-surface, strongly adsorbed atomic oxygen and bulk oxygen species were found on silver. High temperature treatment in O_2 might cause surface reconstruction with the formation of facets. Hydrogen treatment however could roughen the silver surface.

Our Raman spectra and H_2 TPR spectra clearly showed that there were at least four types of oxygen species produced when silver was oxidized at high temperature. These species are adsorbed molecular oxygen, adsorbed atomic oxygen, strongly adsorbed atomic oxygen and subsurface oxygen respectively. It is surprising that at room temperature the molecular oxygen, which is expected to desorb below room temperature according to other researches at UHV conditions, still exists on our silver powder catalyst. There may be two explanations: 1. The silver catalysts we used have more structural defects on silver surface which can adsorb oxygen much more

strongly. 2. The atmospheric pressure, used in our study, may have great effect on the adsorption of oxygen which is different from the other studies, using UHV conditions.

High temperature pretreatment in oxygen greatly reduced the amount of adsorbed atomic oxygen but increased the strongly adsorbed atomic oxygen for low loading silver alumina catalyst. This is believed to be caused by a surface morphology change during the oxygen treatment. When the silver loading was high the interaction between O₂ and Ag was less affected by high temperature treatment.

Ammonia temperature programmed reaction results showed that all oxygen species on silver could react with NH₃ to produce N₂ or N₂O but at low temperature only adsorbed molecular oxygen and atomic oxygen were active. For low silver loading catalyst the reactivity at low temperature was decreased when catalyst was pretreated at high temperature in oxygen. Again less effect was found for high silver loading catalysts pretreated by oxygen at high temperature.

The above results strongly indicate that the ammonia oxidation activity at low temperature is related to the catalyst's ability to adsorb oxygen either dissociatively or non-dissociatively. This means that a high surface area silver catalyst with abundant lattice defects is favored for low temperature ammonia oxidation.

The catalytic performance results showed that the activities of ammonia oxidation on silver powder, silica-supported and alumina-supported silver catalysts were almost the same but the selectivity varied remarkably. Though TEM results showed that the silver particle sizes on both silica and alumina were in the same range with a wide particle size distribution, the average particle size of silver on silica measured by O₂ chemisorption was larger than that on alumina. This means that there exist many smaller silver particles on alumina support that cannot be seen by TEM. Distinct XRD pattern attributable to crystallized silver metal was observed for silica-supported silver catalyst. The fact that silica-supported silver catalyst behaved similarly to silver powder catalysts for ammonia oxidation indicated that there was no evidence of direct interaction between silver and silica. However, the XRD spectra on low loading alumina-supported silver catalyst showed the existence of a silver oxide phase. With increasing silver loading the metallic silver phase appeared but the silver oxide phase still existed. It should be pointed out that only metallic silver should be present on the support after high temperature calcination just as in the case of silica-supported silver catalyst. The presence of a silver oxide phase on alumina indicates again that there exist very small silver particles on alumina support which can be oxidised easily even at lower temperature. The fact that these small silver particles are very stable on

alumina support even at 500 °C may also indicate the present of a strong interaction between silver and alumina. This type of interaction may involve Al-O-Ag bonding and much more resistance to the high temperature migration. The silver- alumina interaction was also mentioned in the study of Naoko Aoyama [27]. They observed that an alumina-supported silver catalyst had a rather high catalytic activity for NO_x reduction, but Ag catalysts on other oxides were far less active for the reaction. They concluded that the Ag compounds (not known) formed during catalysis are stabilized on the alumina surface which in turn is responsible for the high catalytic activity exhibited by Ag/Al₂O₃.

The previous Chapter about ammonia oxidation on silver powder catalyst revealed that two steps were involved [28]. Ammonia was first oxidized to NO. This reaction step was very fast on silver. Even at room temperature the NO could be quickly produced and adsorbed on silver surface in form of NO_x. At moderate temperature (below 300 °C) the NO could be removed either as N₂O or N₂ through a surface SCR reaction, the second step of ammonia oxidation. At even higher temperature NO could directly desorb as one of the products. Apparently the SCR performance of the silver-based catalysts was related closely to the ammonia oxidation performance of the catalysts. It was reported that there existed a good correlation between the N₂ selectivity for the SCO reaction and the SCR performance of NO with NH₃ for the Fe-exchanged zeolites, i.e., the higher the SCR yield of nitrogen, the higher the SCO selectivity to N₂ [29]. The results of the SCR reaction on silver-based catalysts showed the similar good correlation between the SCR reaction and the SCO reaction. It seems that the SCR performance (especially the selectivity to nitrogen) of an alumina-supported catalyst was improved due to the interaction of silver with alumina. Therefore the alumina-supported catalyst showed a better nitrogen selectivity compared with silver powder and silica-supported silver catalysts for ammonia oxidation.

5. Conclusions

Based on the above results, it can be concluded that silver-based catalysts are highly active for ammonia oxidation to nitrogen at very low temperature. Due to the interaction of silver with alumina, the alumina-supported silver catalyst showed better activity and selectivity compared to the silica-supported silver catalyst and silver powder catalyst. Different pretreatment had a large effect on alumina-supported silver catalysts. Calcination at high temperature decreased the activity of catalyst. Reduction in hydrogen at 200 °C without any pre-calcination gave the best activity while reduction at higher temperatures showed little difference from calcination pretreatment. There were at least four types of oxygen species produced when silver was oxidized at high temperature. These species are adsorbed molecular oxygen, adsorbed atomic oxygen, strongly adsorbed atomic oxygen and subsurface oxygen respectively. Ammonia oxidation activity at low temperature was related to the catalyst ability to adsorb oxygen either dissociatively or nondissociatively. This means that a high surface area silver catalyst with abundant lattice defects is favored for low temperature ammonia oxidation. In addition, there exists a good correlation for the silver-based catalysts between the N₂ selectivity for the SCO reaction and the SCR performance of NO with NH₃, i.e., the higher the SCR yield of nitrogen, the higher the SCO selectivity to N₂.

References

- [1] M. Amblard, R. Burch, B.W.L. Southward, *Appl. Catal. B*, 22(3) (1999) L159.
- [2] J.J.P. Biermann, Ph.D. Thesis, University of Twente, Twente, 1990.
- [3] M. de Boer, H.M. Huisman, R.J.M. Mos, R.G. Leliveld, A.J. Dillen and J.W. Geus, *Catal. Today*, 17 (1993) 189.
- [4] J.J. Ostermaier, J.R. Katzer and W.H. Manogue, *J. Catal.*, 41 (1976) 277.
- [5] J.J. Ostermaier, J.R. Katzer and W.H. Manogue, *J. Catal.*, 33 (1974) 457.
- [6] J.E. Delaney and W.H. Manogue, in: *Proceedings of the Fifth International Congress on Catalysis*, Vol. 1, 1973, p. 267.
- [7] F.J.J.G. Janssen and F.M.G. van den Kerkhof, *Selective Catalytic Removal of NO from Stationary Sources*, KEMA Sci. & Techn. Reports, 3(6) (1985).
- [8] J.P. Chen and R.T. Yang, *Appl. Catal.*, 80 (1992) 135.
- [9] G. Tuentner, W.F. van Leeuwen and L.J.M. Sneyers, *Ind. Eng. Chem. Prod. Res. Dev.*, 25 (1986) 633.
- [10] E.T.C. Vogt, A. Boot, J.W. Geus and F.J.J.G. Janssen, *J. Catal.*, 114 (1988) 313.
- [11] J.J.P. Biermann, F.J.J.G. Janssen and J.W. Geus, *J. Mol. Catal.*, 60 (1990) 229.
- [12] M. de Boer, A.J. van Dillen and J.W. Geus, *Catalysis Letters*, 11 (1991) 227.
- [13] A. Abe, N. Aoyama, S. Sumiya, N. Kakuta and K. Yoshida, *Catal. Lett.*, 51 (1998) 5.
- [14] T. Miyadera and K. Yoshida, 63th Annual Meeting of Chem. Soc. Jpn., 2C447 (1992), in Japanese.
- [15] N. Irite, A. Abe, H. Kurosawa, K. Yoshida and T. Miyadera, 65th Annual Meeting of Chem. Soc. Jpn., 3F135 (1993), in Japanese.
- [16] P.H. McBreen and M. Moskovits, *J. Catal.*, 103 (1987) 188.
- [17] C. Backx, C.P.M. De Groot, P. Biloen and W.H.M. Sachtler, *Surf. Sci.*, 128 (1983) 81.
- [18] J. Eickmans, A. Godmann and A. Otto, *Surf. Sci.*, 127 (1983) 153.
- [19] C.T. Campbell, *Surf. Sci.*, 157 (1985) 43.
- [20] R.B. Grant and R.M. Lambert, *Surf. Sci.*, 146 (1984) 256.
- [21] V.I. Bukhtiyarov, I.P. Prosvirin and R.I. Kvon, *Surf. Sci.*, 320 (1994) L47.
- [22] X. Bao, M. Muhler, B. Pettinger and R. Schlögl, *Catal. Lett.*, 22 (1993) 215.
- [23] G.R. Meima, L.M. Knijf, A.J. van Dillen, J.W. Geus, J.E. Bongaarts, F.R. van Buren and K. Delcour, *Catal. Today*, 1 (1987) 117.
- [24] W.D. Mieher and W. Ho, *Surf. Sci.*, 322 (1995) 151.
- [25] J.M. Bradley, A. Hopkinson and D.A. King, *J. Phys. Chem.*, 99 (1995) 17032.
- [26] K. Otto and M. Shelef, *J. Phys. Chem.* 76 (1972) 37.
- [27] N. Aoyama, K. Yoshida, A. Abe and T. Miyadera, *Catal. Lett.*, 43 (1997) 249.

- [28] Lu Gang, J. van Grondelle, B.G. Anderson and R.A. van Santen, J. Catal., 199 (2001) 107.
- [29] R.Q. Long and R.T. Yang, J. Catal., to be published.
- [30] L. Lefferts, Ph.D. Thesis, University of Twente, Twente, 1987.

Chapter 6

Bi-functional alumina-supported Cu-Ag catalysts for ammonia oxidation to nitrogen at low temperature

ABSTRACT

The addition of copper to alumina-supported silver catalysts, by co-incipient wetness impregnation, increased the selectivity to nitrogen during the catalytic oxidation of ammonia at 250 °C without significant decrease in activity relative to that of Ag / alumina alone. An increase in selectivity from 80 % to circa 95 % was observed at 100 % ammonia conversion at the optimum Ag / Cu weight ratio (between 1:1 to 3:1). No increase in activity was observed for mechanical mixtures of Cu / alumina and Ag / alumina catalysts. Based on TEM, EDX, LEIS, XPS and Auger analysis, the catalysts consisted of monolayers of copper oxide on alumina upon which silver particles sat. TEM images and EDX analysis showed that silver particles, with a very large size distribution, existed on all catalysts. EDX also revealed the presence of very small (< 1 nm) silver dispersed in copper everywhere on the alumina surface. Thus intimate contact between copper and silver on alumina-supported Cu-Ag catalysts existed. No indication of the formation of CuAl_2O_4 or of Cu-Ag phases was observed. The promotional effect of copper can be explained by a bi-functional mechanism in which the silver component mainly catalyzes ammonia oxidation to NO, the first step of this reaction, and the copper catalyzes the SCR of NO to nitrogen, thus reducing N_2O formation on silver.

1. Introduction

The increasing problem of air pollution by N-containing compounds, such as NO, NO₂, N₂O and NH₃, has led to more stringent emission control. The removal of ammonia from waste streams is becoming an increasingly important issue. Selective catalytic oxidation of ammonia to nitrogen and water (SCO) could be a solution to pollution caused by various ammonia emission sources such as the SCR process, soda production, and agricultural sources [1-12].

Most studies on ammonia oxidation focus on the high temperature (>800 K) process that selectively produces NO because of its industrial importance. However the low temperature reaction that mainly produces N₂ and N₂O is becoming more important because of the environmental aspect. Various catalysts of different types have been tested for the low temperature ammonia oxidation reaction: biological catalysts [1,2], metal oxide catalysts [3-6], ion-exchanged zeolites [7-9] and metallic catalysts [10-12]. When the various types of catalysts are compared it turns out that the metallic catalysts such as Pt, Ir and Ag are the most active but are the least selective. Significant amounts of N₂O are produced on these catalysts. The metal oxide catalysts such as CuO, V₂O₅ and MoO₃ show very high selectivity to nitrogen, but the reaction temperature needed is too high to be matched with some industrial applications.

We have previously reported that silver was very active for ammonia oxidation [13]. Alumina-supported silver catalysts were superior even to noble metal catalysts in both activity and in selectivity to nitrogen. However the nitrogen selectivity of the silver-based catalysts (circa 80%) is not sufficient as N₂O and NO are still co-produced. As these compounds are even more toxic than NH₃, selectivity to nitrogen of near 100% is required. Intermediate species and reaction pathways for ammonia oxidation on an unsupported silver powder catalyst were studied by TPD, TPR, FT-Raman and by transient as well as steady-state ammonia oxidation experiments [14]. NO was found to be the main reaction intermediate that produced N₂O as well as N₂. NO could even be formed at room temperature. Its subsequent oxidation to NO_x led to adsorption on the silver surface, blocking the active sites for oxygen adsorption. The pathway for ammonia oxidation at low temperature was found to consist of a two-step consecutive reaction. Ammonia was first oxidized to NO. This reaction step was very fast on silver. At moderate temperatures (below 300 °C) NO could then be removed either as N₂O or as N₂ through a surface SCR (selective catalytic reduction) reaction, the second step of the reaction mechanism. At even higher temperatures NO could directly desorb as one of the products. Apparently the ability of silver-based catalysts to perform the SCR reaction was closely related to its ability to oxidize ammonia.

As ammonia oxidation to nitrogen consists of two reaction steps and as it is difficult to find a catalyst that accelerates both of these, a composite catalyst system made of two or more catalyst components, each of which catalyses only a part of the reaction, appeared to be a good alternative to improve the performance of overall reaction. Hence a bi-functional catalytic system was sought.

The bi-functional catalyst required must first contain a component active for ammonia oxidation at low temperatures. The co-production of N_2O can be avoided, or at least further reduced, by the second component that performs the SCR of the intermediate NO species. As stated above, Ag is capable of performing the first step. Copper oxide appeared to be an excellent choice for the second component as it is known to be both active and selective in the selective catalytic reduction of NO by ammonia. Supported copper oxide catalysts are commonly reported in the literature for this purpose [25]. In addition, as previously mentioned, CuO yields a high selectivity to nitrogen in the SCO reaction. Alumina-supported Ag-Cu catalysts were thus prepared and screened for their ability to catalyze both the SCO and the SCR reactions. These materials were also characterized by several spectroscopic techniques in order to determine their physico-chemical compositions and these were compared with catalytic performance. The results are discussed in this article.

2. Experimental

Ag/ Al_2O_3 , Cu/ Al_2O_3 and AgCu/ Al_2O_3 samples with different Ag and Cu loadings were prepared by incipient wetness (co-)impregnation. The precursors for these catalysts were $AgNO_3$ and $Cu(NO_3)_2$ distributed over the γ - Al_2O_3 support (Akzo / Ketjen 000 1.5E, surface area $235\text{ m}^2/\text{g}$). The samples were calcined in air at $500\text{ }^\circ\text{C}$ for 24 hours before testing.

Catalytic activity measurements were carried out in a quartz, fixed-bed reactor (4 mm internal diameter). The amount of catalyst used was about 0.2 gram (250-425 μm particles). Ammonia, oxygen and helium flow rates were controlled by mass flow meters. NH_3 , NO and NO_2 were analyzed by a ThIs Analytical Model 17C Chemiluminescence NH_3 Analyzer. Other substances such as N_2O , N_2 and H_2O were analyzed by a quadrupole mass spectrometer (Baltzers OmniStar). The nitrogen mass balance was calculated based on combination of these two analysis techniques (balance of $90 \pm 10\%$ for all the measurements).

High resolution transmission electron microscopy (HREM) measurements were performed using a Philips CM30/T at the National Centre for HREM at the Delft

University of Technology. Samples were mounted on a microgrid carbon polymer supported on a copper grid, followed by drying at ambient conditions. EDX analysis was performed using a LINK EDX system. This enabled us to obtain information about the relative Ag/Cu ratios in selected areas of the sample.

X-ray powder diffraction (XRD) patterns were recorded on a Rigaku Geigerflex X-ray powder diffractometer using Cu-K α radiation. Prior to the experiment, the catalysts were ground and pressed into a sample holder containing vaseline. The applied scanning speed was 1° per minute. Background subtraction was not applied.

XPS experiments were performed on a VG Ionex system modified with a VG Mg/Al K α X-ray source and a VG Clam II analyzer. The powdered catalyst particles were pressed into indium foil. To correct for the energy shift caused by charging, all peaks were corrected by setting the C1s peak of adsorbed hydrocarbons to a binding energy of 285.0 eV. The peaks were fitted using the XPSPEAK version 4.0 peakfitting program. All peaks were fitted by using a linear background.

Low Energy Ion Scattering (LEIS) experiments were performed in co-operation with Calipso b.v. at the Eindhoven University of Technology. The newly developed ERISS system was used as the ion scattering apparatus. In this apparatus ion doses can be reduced to such a low level that the damage of the surface is negligible, thus enabling the performance of static LEIS [15-20]. To prevent charging of insulating materials, a neutraliser was available to spray low energy electrons to the sample. Samples were prepared by pressing the ground sample with a load of 1600 kg into a tantalum cup (N 1 cm) and subsequently loaded into the pretreatment chamber that was connected to the main UHV chamber. All the samples were pretreated at 300 °C in 214 mbar of oxygen for 20 min. Most LEIS measurements were performed using 5 keV Ne⁺ ions; these provided a good mass resolution for the heavy elements (Ag and Cu). A number of samples were also analyzed using 3 keV ⁴He⁺ ions. This yielded a good sensitivity for the light elements (C, O, Al, Si). In most cases, the samples were mechanically scanned over an area of 1×1 mm². During the measurements, the pressure in the main chamber was determined by the noble gas used in the ion source and was typically around 1×10⁻⁸ mbar. The base pressure of the system was in the 10⁻¹⁰ region. Analysis of the outermost surface layer and at different depths was performed on both the catalysts and on the gamma-alumina carrier. Depth analysis was performed by sputtering the samples with Ne⁺ ions or ⁴He⁺ ions, thus removing up to 8 ML (Ne) and up to 0.8 ML (He).

3. Results

3.1. Catalytic ammonia oxidation tests

Fig.1 shows the dependence of both the ammonia conversion level and the selectivity to nitrogen on the catalyst composition at 250 °C. It can be seen that the conversion of ammonia decreases with increasing copper weight ratio in the catalyst, but that the nitrogen selectivity changes in the opposite direction. It has previously been shown that selectivity is a very weak function of the ammonia conversion level [23]. The optimum Ag/Cu weight ratio seems to be in the range between 1 and 3. Both activity and selectivity to nitrogen are high in this range. Apparently, the nitrogen selectivity can be greatly improved by addition of small amounts of copper to the silver catalyst system with only a small loss in catalyst activity.

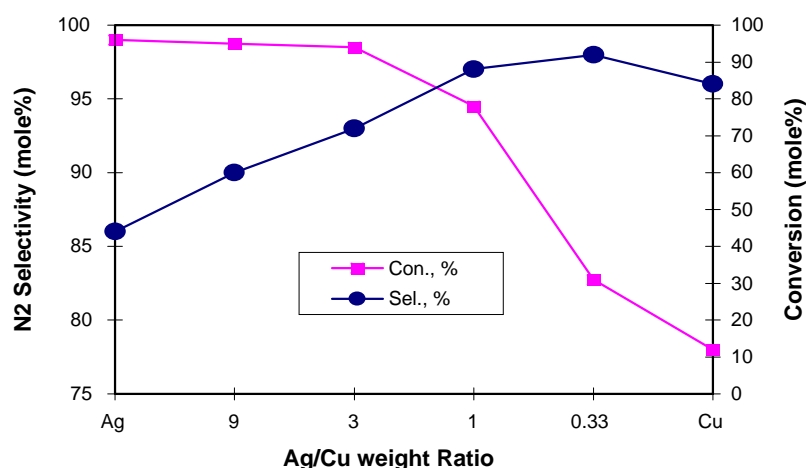


Fig. 1 The effect of Ag/Cu weight ratio on ammonia conversion and on selectivity to nitrogen for Ag-, Cu-, and AgCu/ γ -Al₂O₃ catalysts.

(Reaction conditions: NH₃: 1.14 vol.%; O₂: 8.21 vol.%; flow rate=74.7 Nml/min; catalyst weight=0.2 g; T=250 °C)

For comparison, a mechanical mixture of 10 wt%-Ag/Al₂O₃ and 10 wt%-Cu/Al₂O₃ catalyst with a weight ratio of 3/1 was also tested in the SCO reaction. The results are listed in Table 1. It can be seen that a mechanically mixed silver and copper catalyst behaves similarly to the silver catalyst itself. Neither activity nor selectivity to nitrogen was improved by mechanical mixing of two different catalysts.

Table 1 SCO (NH₃+O₂) reaction on different catalysts

Catalyst	Temperature °C	NH ₃ conversion %	N ₂ selectivity %
10 wt%Cu/Al ₂ O ₃	250	12	97
	300	90	96
	350	100	90
10 wt%Ag/Al ₂ O ₃	200	11	88
	250	98	86
	300	100	83
Ag/Al ₂ O ₃ +Cu/Al ₂ O ₃ (Ag/Al ₂ O ₃ : Cu/Al ₂ O ₃ =3:1)	200	8	89
	250	96	87
	300	100	82

Reaction conditions: NH₃ = 1.14%; O₂ = 8.21 vol%; flow rate = 74.7 Nml/min;
catalyst weight = 0.2 g

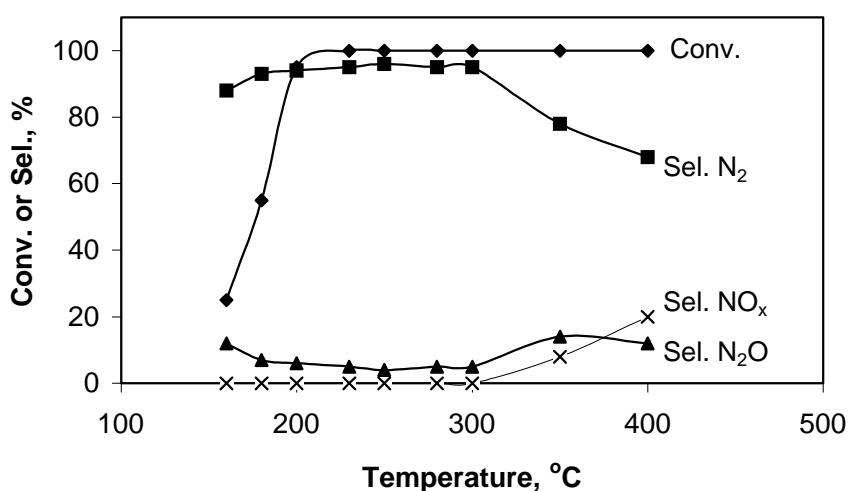


Fig. 2 Ammonia oxidation on 7.5 wt% Ag-2.5 wt% Cu/Al₂O₃ catalyst at various temperatures.

Reaction conditions: NH₃=1000 ppm; O₂=10 vol%; total flow rate=50 Nml/min; catalyst weight=0.1 g.

Fig.2 shows the conversion of ammonia and the selectivity to various products on an alumina-supported 7.5 wt% Ag-2.5 wt% Cu catalyst as a function of temperature. Between 200 -300 °C the catalyst converted 100% of the ammonia with a selectivity to nitrogen of circa 95%. Above 300 °C, more NO_x is produced. The catalyst was quite stable. There was no significant deactivation during a one-day test under these experimental conditions. However, the selectivity did change somewhat with time (see Fig.3). It can be seen from Fig.3 that the selectivity to nitrogen increased with reaction time during the first 40 minutes on stream, whereafter it remained

unchanged. This is mainly caused by adsorbed NO_x , N_2O_x species produced during reaction which can lower the surface oxygen coverage as discussed previously [14].

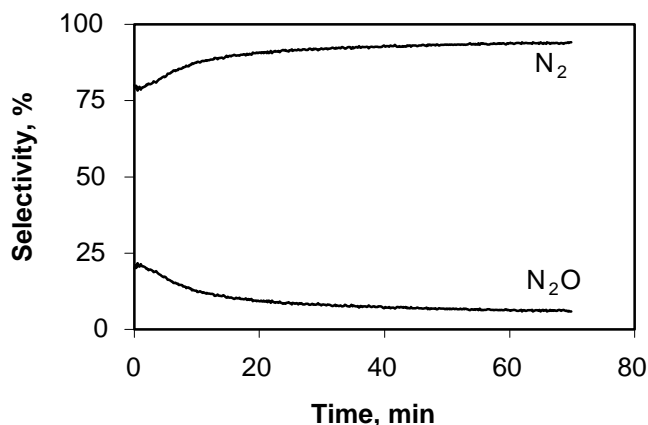


Fig. 3 Selectivity change with time on 7.5 wt% Ag-2.5 wt% Cu/ Al_2O_3 catalyst

Reaction conditions: NH_3 =1000 ppm; O_2 =10 vol%; total flow rate=50 Nml/min; catalyst weight=0.1 g.

Selective catalytic reduction of NO by ammonia (SCR) was also tested on various copper and silver-based catalysts to demonstrate the relationship between the SCR reaction and the ammonia oxidation reaction. Table 2 shows a comparison of the data obtained for the SCR reaction on different catalysts. It can be seen that the activity for the SCR reaction on alumina-supported Cu-Ag catalyst was much higher than that on alumina-supported silver catalyst. The SCR reaction was also more selective to nitrogen on alumina-supported Cu-Ag catalyst as compared with alumina-supported silver catalysts.

Table 2. SCR ($\text{NO}+\text{NH}_3$) reaction on different silver-based catalysts

Catalyst	Temperature °C	NO conversion %	N_2 selectivity %
CuAg/ Al_2O_3 (7.5%Ag-2.5%Cu)	150	27	98
	200	61	95
	250	98	96
10 wt%Cu/ Al_2O_3	150	53	98
	200	97	97
	250	99	98
10 wt%Ag/ Al_2O_3	200	5	67
	250	14	74
	300	25	72

Reaction conditions: NO = 500 ppm; NH_3 = 1000 ppm; O_2 = 8 vol%; flow rate = 100 Nml/min; catalyst weight = 0.2 g

3.2. XRD and XPS

Fig.4 shows the XRD diffractograms of 5 wt% Cu/Al₂O₃, 5 wt% Ag/Al₂O₃ and 7.5 wt% Ag-2.5 wt% Cu/Al₂O₃ catalysts. All the catalysts were calcined at 500 °C in air for 24 hours before measuring. No XRD diffraction lines attributable to crystallized copper metal or other copper compounds were observed on the copper-containing samples. However, diffraction lines attributable to AgO appeared in the XRD spectra of both silver-containing samples. Low intensity diffraction lines due to metallic silver were also observed on the 7.5wt%Ag-2.5wt%Cu catalyst.

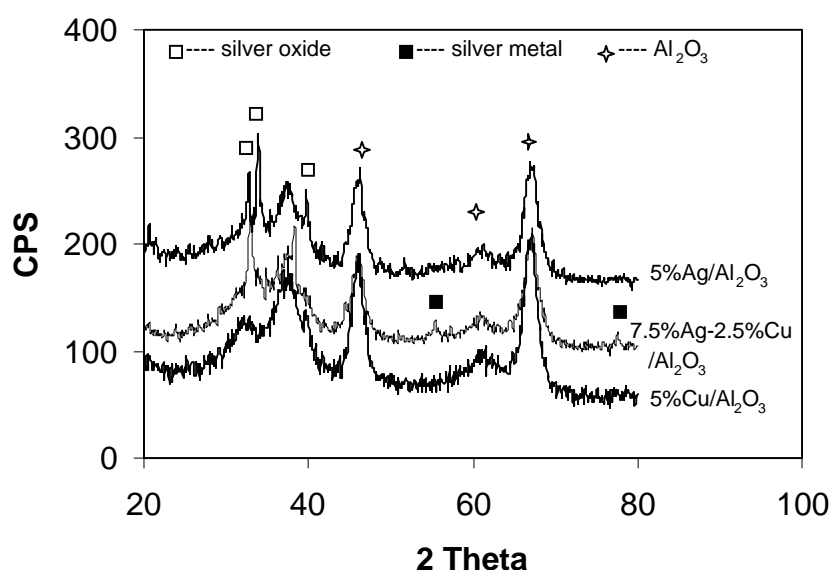


Fig. 4 XRD spectra of alumina-supported Cu-Ag catalysts calcinated at 500 °C

Four samples of Ag and Cu with different loadings of metal were characterized by XPS. The spectra in Fig. 5(a) show the Ag 3d region measured by XPS. Two peaks observed are due to removal of electrons from the 3d_{3/2} and 3d_{5/2} levels. The more intense peak due to removal of 3d_{5/2} core level electrons had a binding energy of 368.3 eV. Unfortunately, according to literature data [21], the binding energies of the 3d electrons in Ag⁰, Ag⁺¹ or Ag⁺² are all very similar. Hence it is impossible to ascertain the oxidation state of silver from this XPS peak alone. However, more information can be obtained by measuring the Auger bands to construct a Wagner plot [26]. Fig. 5(b) shows the Auger spectra obtained on three silver-containing catalysts in the region 370-330 eV. As shown, the peaks are very broad, but the kinetic energy of the Auger electrons is about 350 eV for all three samples. By comparison of these results with the literature [22] it can be concluded that silver is not in a metallic state, but in a state between Ag⁺¹ and Ag⁺².

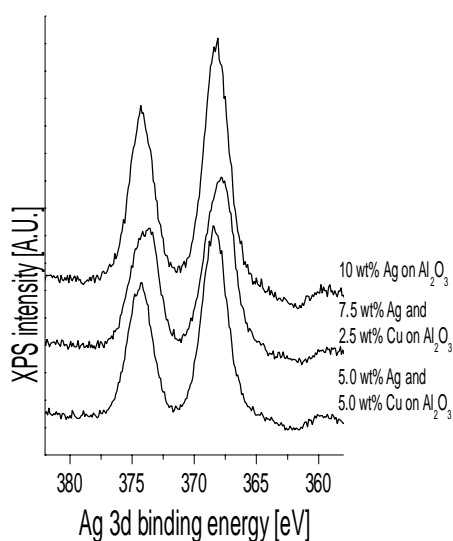


Fig.5(a) Ag 3d XPS spectra of different Cu-Ag/Al₂O₃ catalyst

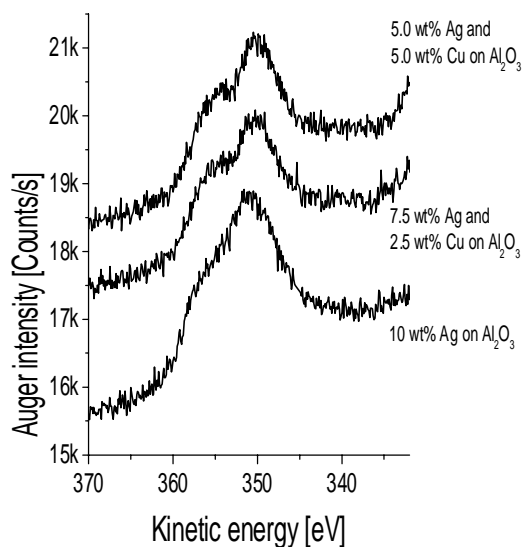


Fig.5(b) Auger bands in Ag region for different Cu-Ag/Al₂O₃ catalyst

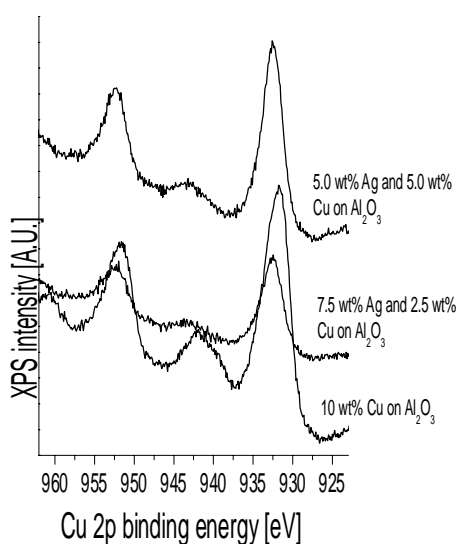


Fig.6(a) Cu 2p XPS spectra of different Cu-Ag/Al₂O₃ catalyst

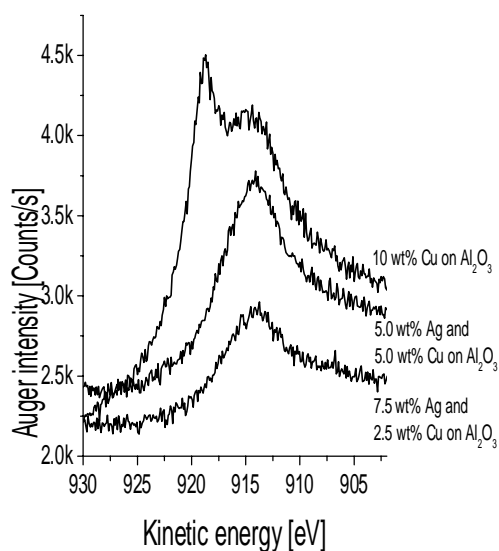


Fig.6(b) Auger bands in Cu region for different Cu-Ag/Al₂O₃ catalyst

Fig. 6(a) shows XPS spectra in the Cu 2p region [925- 960 eV]. The most intense peak occurs at about 932.5 eV. Comparing this result with literature data [21] it seems that Cu is in an oxidization state of +1 if copper is present as copper oxide since the

2p electrons in Cu^{+2} have a much higher binding energy (933.6 eV). Auger bands in the Cu region are shown in Fig. 6(b). The kinetic energies are circa 914 eV, much lower than that of CuO (918.1 eV) and Cu_2O (916.2 eV). The UV-spectra of our γ -alumina-supported copper catalysts [9] and EXAFS studies on other γ -alumina-supported copper catalysts [24] clearly showed that copper was in an oxidation state of +2. The shift of the binding energy may be caused by the interaction of copper with the support. New copper species other than copper oxide are formed due to this interaction. A second possibility is an interaction between Ag and Cu.

In order to be able to exclude any interaction between silver and copper two solid solutions were made of 5 wt% copper in silver and 5 wt% silver in copper. A special procedure was needed to fabricate these solid solutions, as at low temperatures these metals do not mix at all, and will phase-separate into micro-crystallites when cooling down from the melt. Such rough samples were prepared by melting the appropriate amounts together in an alumina crucible by induction in a high-frequency furnace, after which the samples were placed in two evacuated quartz capsules. These were heated for 96 hours at a steady temperature of 800 °C, at which temperature solid solutions of these compositions are possible according to the phase diagram [27]. Subsequent quenching prevented the formation of micro-crystallites. The XPS spectra of the Ag 3d and Cu 2p did not show any difference from the pure metals after polishing. Any direct interaction between copper and silver, either through formation of an alloy or at boundaries is thus very unlikely.

3.3. LEIS measurements

The samples measured with LEIS are listed in Table 3. In addition to the Ag/Cu/ γ -alumina catalysts, we analysed a bare (γ -alumina carrier material and Ag- and Cu foil reference samples. Furthermore, in order to analyse the influence of surface roughness on the results we measured both a quartz sample and a silica carrier (Grace 332). Although these samples had the same elemental composition, quartz had a very smooth surface whereas the carrier material exhibits a much larger surface roughness (specific area of 235 m^2/g). Finally, an “ultra-pure” CuO powder sample was analyzed for quantification purposes. Figures 7(a) and 7(b) show the LEIS spectra of 5 wt% Cu/ γ -alumina and 10 wt% Ag/ γ -alumina samples as obtained with 5 keV Ne^+ ions. At the outermost atom layers of the samples significant Ag- and Cu- signals were detected.

Table 3 Samples analysed by LEIS and their pre-treatments

Sample	Ag %wt	Cu %wt	Pre-treatment (in LEIS reaction chamber)	Ne ⁺ 5 keV	⁴ He ⁺ 3 keV
Cu/γ-alumina		5.0	214 mbar O ₂ , 300°C, 20 min	x	x
Ag/γ-alumina	10.0		213 mbar O ₂ , 300°C, 20 min	x	x
Ag/Cu/γ-alum.	10.0	2.5	212 mbar O ₂ , 300°C, 20 min	x	x
Ag/Cu/γ-alum.	2.5	7.5	201 mbar O ₂ , 300°C, 20 min	x	
Ag/Cu/γ-alum.	5.0	5.0	208 mbar O ₂ , 300°C, 20 min	x	
Ag/Cu/γ-alum	9.0	1.0	210 mbar O ₂ , 300°C, 20 min	x	
γ-alumina			216 mbar O ₂ , 300°C, 20 min		x
Reference Ag	100		sputter-cleaned	x	x
Reference Cu		100	sputter-cleaned	x	x
Quartz					x
Silica			Vacuum, 300°C, 74 min		x
CuO				x	

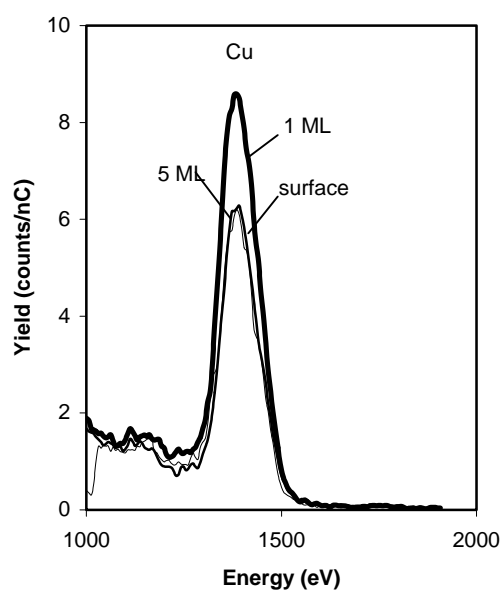


Fig.7(a) 5 keV Ne⁺ spectra of 5 wt% Cu/Al₂O₃ at different depths

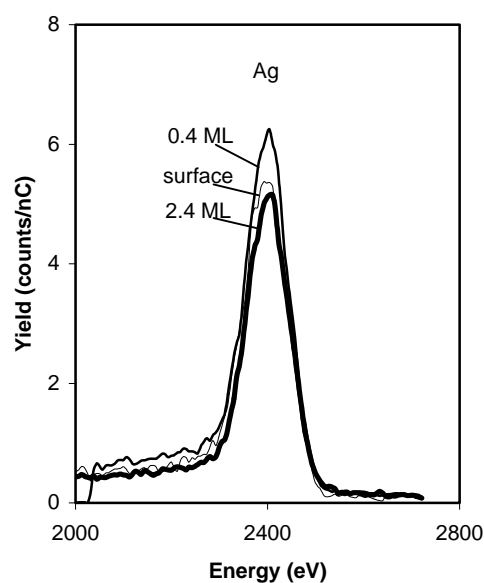


Fig.7(b) 5 keV Ne⁺ spectra of 10 wt% Ag/Al₂O₃ at different depths

The removal of the first (fraction of a) monolayer (ML) results in increased Ag- and Cu signals. After a few ML's the intensities returned to a magnitude on the order of that of the outermost surface (Cu/γ-alumina) or slightly lower (Ag/γ-alumina). Most likely, the first ML removed consisted of contamination that had been deposited on

the surface during the in-situ calcination. The subsequent decrease of the signals suggests that prolonged sputtering resulted in smaller “accessible” silver and copper surfaces. Fig. 8 shows one of the 5 keV Ne^+ spectra recorded for the bi-metallic catalyst (10 wt% Ag-2.5 wt% Cu/ Al_2O_3). In all cases, the removal of the first (fraction of a) ML resulted in increased intensities for both Ag and Cu. Again, we assume that we are dealing with surface contamination that, most likely, originated from the calcination of the samples.

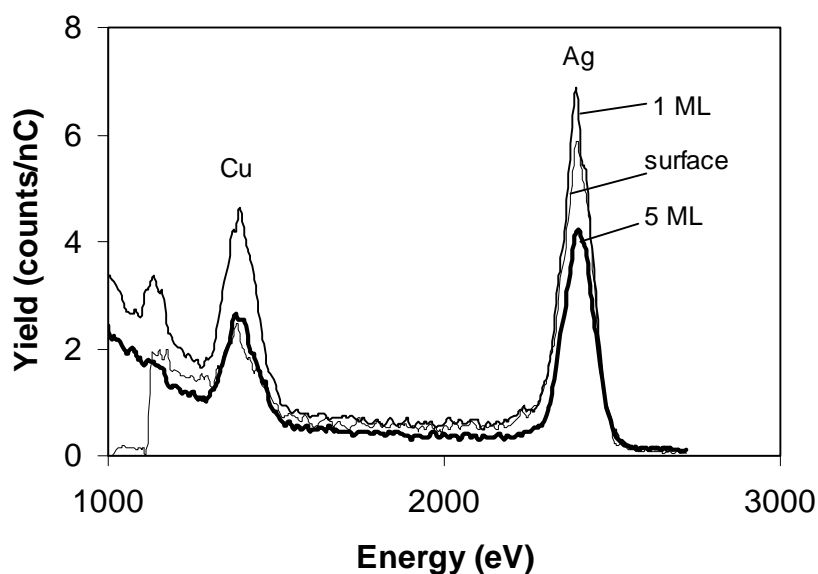


Fig.8 5 keV Ne^+ spectra of Cu/Ag/ γ -alumina (2.5%_w Cu, 10%_w Ag) at different depths

Going deeper, down to 3-5 ML's, the respective Cu signals decreased in a similar fashion for all the copper-containing samples. Concerning Ag, we observed a relatively large intensity drop for the sample shown in Figure 8. The 3 keV $^4\text{He}^+$ spectrum recorded for the catalyst 10 wt% Ag-2.5 wt% Cu/ Al_2O_3 also shows the F peak originating from the bare carrier (Figure 9).

Table 4 Calculation of CuO platelets and Ag particles dispersion from LEIS measurements

Catalysts			CuO platelets			Ag particles		
			depth: 1 ML			depth: 1 ML		
Cu	Ag	Ag/Cu	Cu LEIS signal	Cu visible atoms	CuO platelets	Ag LEIS signal	Ag visible atoms	Ag particles
wt%	wt%	at/at	cnts/nC	atoms/cm ² x10 ³	thickness, #ML's	cnts/nC	atoms/cm ² x10 ³	av. size (nm)
1	9	5.3	231	5.4	0.8	728	4.1	4.1
2.5	10	2.4	352	8.2	1.2	645	3.6	5.2
5	5	0.6	895	20.8	1.0	510	2.8	3.2
7.5	2.5	0.2	1242	28.9	1.0	312	1.7	2.6

The LEIS signals measured at 1 ML depth, i.e. after removal of surface contamination, contain information on the Ag- and CuO dispersions. In order to obtain a (semi) quantitative picture of these dispersions, we have performed some calculations (see Table 4). Starting with the Cu signals, the results indicate that the CuO species are present as thin platelets with a thickness of roughly 1 ML. Between the samples, only minor differences are observed. Obviously, at increasing Cu loading, relatively more (or more extended) rather than thicker CuO platelets are formed. Based on surface tension considerations, Ag is expected to form distinct particles on the γ -alumina support. Assuming (a) that these particles are spherical and (b) that only their upper halves contribute to the LEIS signals, we calculate (from the “1 ML signals”) that the average particle size of Ag ranges between 2.5 and 5.5 nm. Note that the numbers increase with increasing Ag loading.

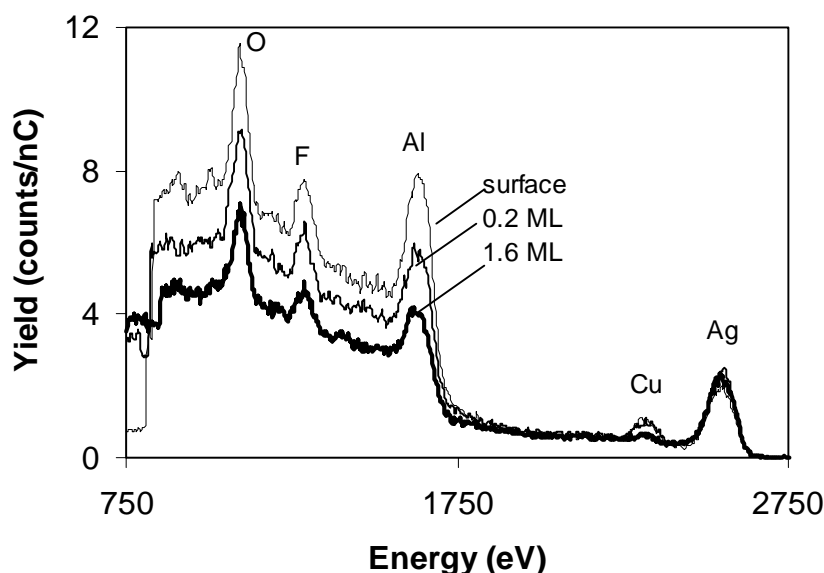


Fig.9 3 keV $^4\text{He}^+$ spectra of Cu/Ag/ γ -alumina (2,5%_w Cu, 10%_w Ag)

3.4. TEM and EDX measurement

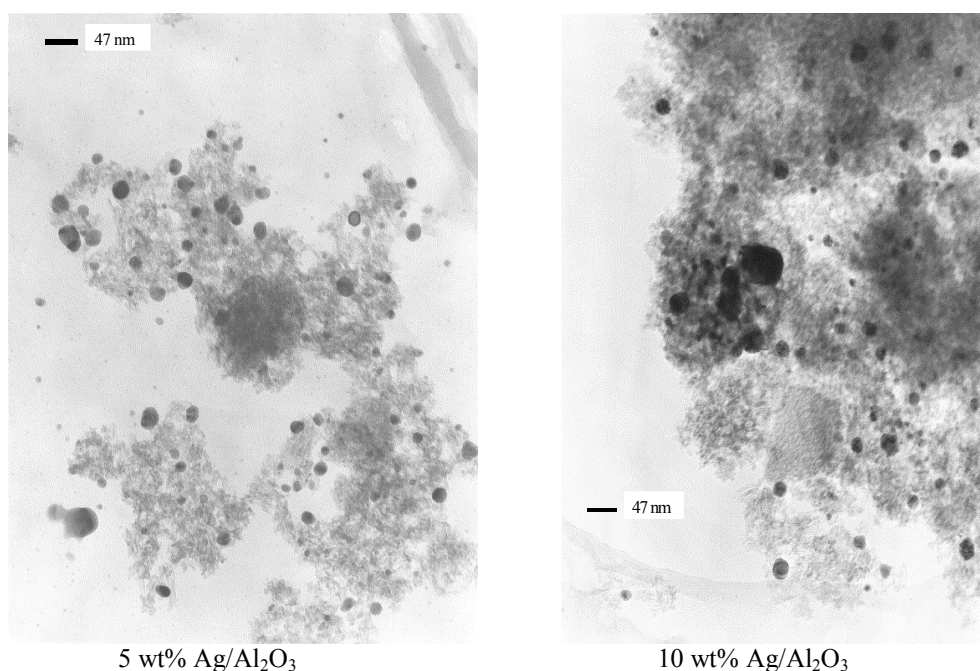


Fig.10 TEM images of alumina-supported silver catalysts

Single component alumina-supported Cu and Ag catalysts with different loading were examined using TEM. No metal oxide particles were observed on the alumina surface of the 5 wt% Cu/Al₂O₃ and 10 wt% Cu/Al₂O₃ catalysts. Particles with diameters ranging between 5 and 10 nm were observed on the 15 wt% Cu/Al₂O₃ catalyst. The TEM images of 5 wt% Ag/Al₂O₃ and 10 wt% Ag/Al₂O₃ catalyst seem to be similar. The silver particle size distribution was very broad. The smallest particles were about 1 nm in diameter, the largest particles found on the images were about 50 nm in diameter (see Fig. 10).

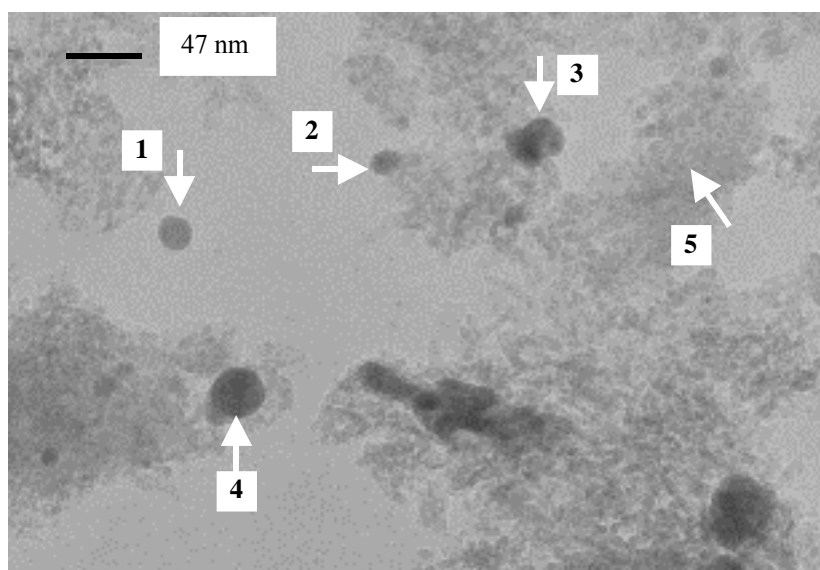


Fig.11(a) TEM image of black particles of 7.5%Ag-2.5%Cu/Al₂O₃ catalyst (the arrows point to the area where the EDX measurement is performed)

Table 5 Relative amounts of copper and silver measured by EDX on different areas of 7.5wt%Ag-2.5wt%Cu/Al₂O₃ (black-particle fraction). Data points refer to numbered arrows in Fig. 11(a).

Data point	atom % Cu	atom % Ag
1	6.90	93.10
2	3.82	96.18
3	3.52	96.48
4	5.97	94.03
5	59.70	40.30
(area without dark particles)		

Two samples of mixed Ag-Cu/alumina catalysts were examined using TEM and EDX elemental analysis. Both samples contained a total metal loading of 10 wt%. One sample contained 7.5 wt% Ag and 2.5 wt% Cu. The other sample contained 2.5 wt% Ag and 7.5 wt% Cu.

7.5 wt% Ag-2.5 wt% Cu/Al₂O₃

This sample clearly consisted of two different macroscopic phases: one containing black particles and the other containing green particles. These two phases were mechanically separated (by hand) and were analyzed separately. Fig. 11(a) shows a representative TEM image that was obtained for the fraction containing black particles. EDX analysis was performed at several different locations on the sample (see numbered arrows). Data points 1 to 4 were chosen to analyze areas containing dark particles. Data point 5 measured an area in which no dark particles were present.

As the relative amounts of copper and silver are of importance these are shown in Table 5. Clearly the areas that include particles visible by TEM (points 1-4) contain very high amounts of silver relative to copper (circa 95:5). By contrast the area containing no visible particles (point 5; and others not shown here) contains relatively more copper than silver (circa 60:40).

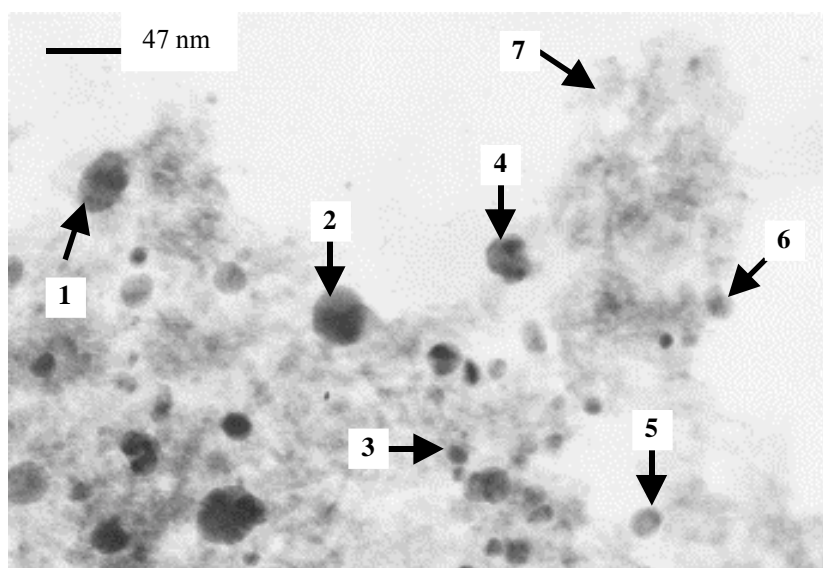


Fig.11(b) TEM image of green particles of 7.5%Ag-2.5%Cu/Al₂O₃ catalyst
(the arrows point to the area where the EDX measurement is performed)

Table 6 Relative amounts of copper and silver measured by EDX on different areas of 7.5wt%Ag-2.5wt%Cu/Al₂O₃ (green-particle fraction). Data points refer to numbered arrows in Fig. 11(b).

Data point	atom % Cu	atom % Ag
1	1.02	98.98
2	1.10	98.90
3	2.10	97.90
4	1.10	98.90
5	1.68	98.32
6	0.86	99.14
7	73.40	26.60
(area without dark particles)		

Fig. 11(b) shows a TEM image that was obtained for the macroscopic green particles of this Ag-rich sample. The relative amounts of copper and silver (by EDX analysis) are listed in Table 6. Similar to the black-coloured particle fraction, this phase also contained a wide distribution of particle size (up to 50 nm). These particles (data points 1-6) were slightly richer in silver relative to copper than were the black

particles. Again although data point 7 shows no particles visible by TEM, both copper and silver were present, copper again being the more abundant.

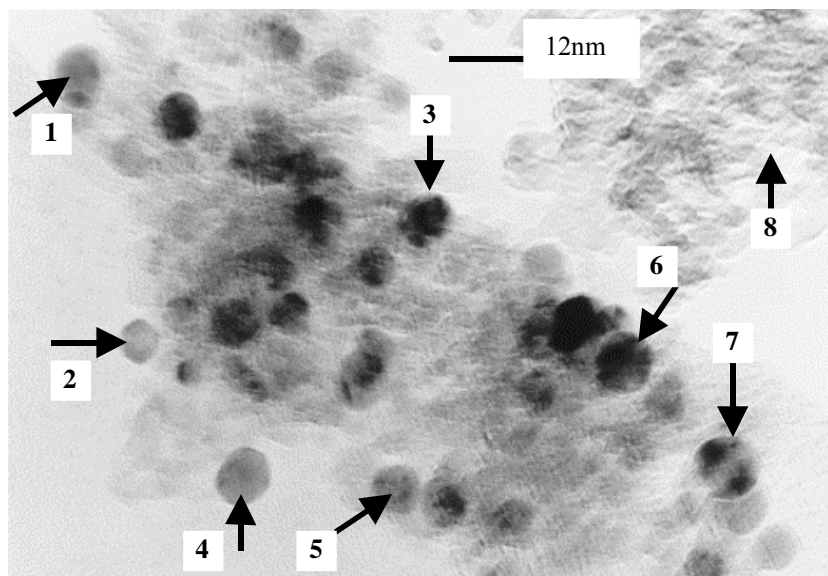


Fig.12 TEM image of green particles of 2.5%Ag-7.5%Cu/Al₂O₃ catalyst (the arrows point to the area where the EDX measurement is performed)

7.5 wt% Cu-2.5 wt% Ag/Al₂O₃

Fig. 12 shows a representative TEM image that was obtained for this Cu-rich sample. Again particles of a large distribution were observed. Table 7 shows the relative

Table 7 Relative amounts of copper and silver measured by EDX on different areas of 2.5wt%Ag-7.5wt%Cu/Al₂O₃. Data points refer to numbered arrows in Fig. 12.

Data point	atom % Cu	atom % Ag
1	3.26	96.74
2	4.56	95.44
3	6.61	93.39
4	4.62	95.38
5	12.89	87.11
6	11.85	88.15
7	13.75	86.25
8	83.28	16.72
(area without dark particles)		

amounts of copper and silver measured at various locations. Again the darker particles visible by TEM (points 1-7) contain a larger abundance of silver. However in several locations the relative amount of copper to silver is higher than was observed in the

previous samples. Data point 8 again shows that copper and a smaller amount of silver are present even in an area without visible dark particles.

4. Discussion

Ammonia oxidation experiments have shown that silver alone supported on alumina has a very high ammonia oxidation activity but with a low selectivity to nitrogen. Alumina-supported copper catalyst has a very high nitrogen selectivity but the activity is low at low temperature. As discussed previously the aim of this study was to determine if alumina-supported binary Cu-Ag catalysts yield a higher selectivity to nitrogen without decrease in activity. The results show that this is indeed the case. Addition of Cu to Ag/Al₂O₃ catalysts, by incipient wetness co-impregnation, showed an increase in N₂ selectivity from 87% to circa 95% at 250 °C whilst the activity was not significantly reduced at Ag/Cu weight ratios greater than unity. An optimum ratio of between 1-3 was observed. The activity and selectivity to nitrogen for the SCR of NO by NH₃ were also increased following the addition of Cu. This is consistent with the previous observation that materials capable of catalyzing the SCO of NH₃ are also able to catalyze the SCR of NO by NH₃. This is due to the fact that the former reaction proceeds through an NO intermediate. Once formed the NO can be selectively reduced by NH₃ to nitrogen rather than being further oxidized to N₂O.

The fact is that a mechanical mixture of Cu/Al₂O₃ and Ag/Al₂O₃ catalysts, with an overall Ag/Cu ratio of 3:1, did not produce an increase in the selectivity to nitrogen as observed in the catalysts prepared by incipient wetness co-impregnation. The above result indicates that either close physical proximity or intimate chemical interaction between the silver and the copper components is necessary in order to increase selectivity. This can be understood by the fact that the intermediate NO cannot desorb from the catalyst surface at temperatures below 300 °C, as shown previously [9]. Thus at low temperatures, transport of NO between Ag and Cu must occur by surface diffusion.

In order to further understand the physico-chemical nature of the Ag-Cu/Al₂O₃ catalysts the results of the various spectroscopic techniques must now be examined. XRD analysis of Cu/Al₂O₃ catalysts revealed that no peaks due to either metallic copper, copper oxide or other copper compounds were present up to loadings as high as 10 wt%. TEM images of these catalysts also showed no visible particles. EDX analysis showed that copper was present on all areas of the alumina catalyst.

Based on the absence of distinct Cu particles in the TEM micrographs, it has been suggested that Cu might have reacted with (surface layers of) γ -alumina and formed CuAl_2O_4 . However, the Cu atoms of this “normal spinel” component are known to occupy tetrahedral, i.e. sub-surface, positions. Consequently, we would not expect CuAl_2O_4 to yield the large copper LEIS signals we actually have obtained. Former LEIS experiments performed on normal spinels yielded much smaller signals. Furthermore, small Cu (oxide) species may simply exhibit insufficient contrast (in TEM) when imaged on γ -alumina. The XRD results also show no diffraction line of CuAl_2O_4 phase for all the copper containing samples. For these reasons, we judge the occurrence of spinels to be rather unlikely. Excluding the presence of spinels, Cu may either be present in metallic- or in oxidic form. Following surface tension considerations, metallic Cu species would form distinct particles whereas CuO species would wet the γ -alumina surface much better. The preparation of the catalysts (through wet impregnation of a mixture of Ag- and Cu nitrates, followed by a reduction step) is expected to yield CuO species rather than metallic Cu particles. Furthermore, the catalysts were calcined prior to be analysed with LEIS analysis. For these reasons, it is very likely that we are dealing with CuO species. Although the expected form of copper oxide is Cu(II) oxide, XPS analysis of Cu/ Al_2O_3 catalyst employing Wagnen plots revealed that copper is in an oxidation state of +1, thus suggesting the presence of Cu_2O .

Analysis of 5 and 10 wt% Ag/ Al_2O_3 catalysts by TEM and EDX showed that Ag was always present as particles on the alumina surface. This is consistent with expectations based on surface tension between Ag and Al_2O_3 . TEM revealed that a very wide particle distribution was always present (1-50 nm). XPS analysis of Ag/ Al_2O_3 employing Wagnen plots showed that Ag was present in an oxidation state between +1 and +2. XRD analysis also showed the presence of AgO besides metallic silver. This is surprising as Ag_2O is very unstable and AgO decomposes at 200 °C, so that following calcination at 500 °C metallic silver was expected.

TEM analysis of binary Cu-Ag catalysts revealed that a very large particle distribution was present (1-50 nm). EDX analysis revealed that the particles contained very large amounts of Ag relative to Cu. Areas in which no particles were present contained relatively more copper but still contained some silver. This suggests again that Cu was highly dispersed and that the particles were of Ag. Silver particles of very small diameters (<1 nm) must also be present. The observations by TEM are consistent with the results of LEIS. A model generated suggested that copper oxide was highly dispersed, as a monolayer, and that the silver particles sit on top of this layer. The average Ag particle size for all silver-containing samples determined by LEIS was

between 2.5 and 5.5 nm. The simple model predicts that the silver particle size distribution is quite narrow and does not vary a lot amongst all the silver-containing catalysts. This distribution is much smaller than was observed by TEM. This probably arises from the fact that LEIS measures the silver content of the entire surface thus including the small particles invisible to TEM.

XPS results show that the valence states of copper and silver are the same for single component catalysts and bi-component catalysts. The TEM images show very broad Ag particle size distributions for all these catalysts. There is no indication for the formation of a new Cu-Ag phase. Indeed, as shown by the phase diagram [27], Ag and Cu have very low solubilities together at temperatures below 780 °C. They tend to phase-separate at lower temperatures. There is no stable region in which a Cu-Ag alloy is formed.

As described previously, the ammonia oxidation on silver is a two-step reaction. Ammonia is first oxidized to NO and then the adsorbed NO is further reacted with NH_x to produce N_2 . In a side reaction, NO can be oxidized to N_2O . The addition of copper to a silver catalyst enhances the selectivity of the SCR reaction. The promotional effect of copper can thus be well explained by a mechanism of bi-functional catalyst.

Since the NO produced in the first step of ammonia oxidation cannot desorb at low temperature, the copper and silver components should be in intimate contact with each other so that the NO produced on the silver surface can migrate to the copper surface easily. Otherwise, NO produced on the silver cannot reach the copper surface and the chances are greater that N_2O is produced rather than nitrogen. The EDX results showed that copper and silver existed together everywhere on the alumina surface. This proved that there was an intimate contact between copper and silver on alumina-supported Cu-Ag catalysts. Our experiments show that the performance of the catalyst, which is a physical mixture of 10 wt% $\text{Ag}/\text{Al}_2\text{O}_3$ and 10 wt% $\text{Cu}/\text{Al}_2\text{O}_3$, behaves similarly to the 10 wt% $\text{Ag}/\text{Al}_2\text{O}_3$ catalyst alone. This again confirms the importance of intimate contact between copper and silver.

In summary, copper was highly dispersed in all catalysts analyzed by LEIS and TEM. Most likely, the catalysts contain copper oxides platelets with a thickness of roughly 1 ML. At increasing copper loading, relatively more (or more extended) rather than thicker platelets are formed. However, silver has a broad particle size distribution. The average size of the Ag species ranges between 2.5 and 5.5 nm measured from LEIS. These numbers increase with increasing silver loading. From TEM images

silver is present as relatively large particles with sizes ranging from 1 nm up to 50 nm. The EDX results also show the existence of silver in the areas without dark particles. This indicates that a fraction of silver is dispersed in the form of platelets or very small particles that cannot be observed by TEM. This fraction of silver may be most interesting from a catalytic point of view. Unfortunately we still cannot unambiguously determine which fraction of silver plays the major role in ammonia oxidation at this stage.

Multi-functional catalysis is not a new concept, but catalyst design deliberately based on the principle of multifunctionality will be inevitable to develop high-performance catalysts which can cope with such difficult problems as in ammonia oxidation. This study only gives one example of such a design. Actually there are more alternatives available. Besides silver, many noble metals such as Pt, Ir are very active for ammonia oxidation with low selectivity to nitrogen due to the low efficiency for SCR reaction. There are also many good SCR catalysts such as vanadium oxide, iron oxide. Opportunities still exist for preparing high-performance bi-functional catalysts from these catalytic components.

5. Conclusions

Alumina-supported silver catalysts are very active for ammonia oxidation but N_2O is also co-produced on these catalysts. The addition of copper to these silver-based catalysts can greatly improve the catalytic selectivity to nitrogen with a negligible loss in activity for ammonia oxidation within the optimum Ag / Cu weight ratio range of between 1 and 3. XPS results show that the valence states of copper and silver are the same for single component catalysts and bi-component catalysts. LEIS and XPS measurements show no indication of formation of a new Cu-Ag phase. Such Cu-Ag alloys have been shown earlier to be thermodynamically unstable.

TEM images show the very broad particle size distributions for all these catalysts. EDX results showed that copper and silver existed together everywhere on the alumina surface thus intimate contact between copper and silver on alumina-supported Cu-Ag catalysts exists. All results seem to be consistent with a model that suggests that the catalyst structure consists of a highly dispersed (monolayer) of copper oxide on alumina upon which silver particles of a very wide particle size distribution sit.

The promotional effect of copper can be explained by a bi-functional mechanism, in which the silver component mainly catalyzes ammonia oxidation to NO, the first step of this reaction, and the copper catalyzes the SCR of NO to nitrogen, thus reducing N_2O formation on silver.

REFERENCES

- [1] M.C.M. van Loosdrecht and S.J. Heijnen, *TIBTECH*, 11 (1993) 117.
- [2] J. Cole, *TIBTECH*, 11 (1993) 368.
- [3] M. Amblard, R. Burch, B.W.L. Southward, *Appl. Catal. B*, 22(3) (1999) L159.
- [4] J.J.P. Biermann, Ph.D. Thesis, University of Twente, Twente, 1990.
- [5] M. de Boer, H.M. Huisman, R.J.M. Mos, R.G. Leliveld, A.J. Dillen and J.W. Geus, *Catal. Today*, 17 (1993) 189.
- [6] A. Wollner and F. Lange, *Appl. Catal. A*, 94 (1993) 181.
- [7] Y. Li and J. N. Armor, *Appl. Catal. B*, 13 (1997) 131.
- [8] N.N. Sazonova, A.V. Simakov and H. Veringa, *React. Kinet. Catal. Lett.*, 57(1) (1996) 71.
- [9] Lu Gang, J. van Grondelle, B.G. Anderson and R.A. van Santen, *J. Catal.*, 186 (1999) 100.
- [10] J.J. Ostermaier, J.R. Katzer and W.H. Manoque, *J. Catal.*, 41 (1976) 277.
- [11] N.I. Il'chenko, *Russian Chemical Reviews*, 45 (1976) 1119.
- [12] A.C.M. van den Broek, Ph.D. Thesis, Technical University of Eindhoven, Eindhoven, 1998.
- [13] Lu Gang, J. van Grondelle, B.G. Anderson and R.A. van Santen, *Appl. Catal. B*, Submitted in 2001.
- [14] Lu Gang, J. van Grondelle, B.G. Anderson and R.A. van Santen, *J. Catal.*, 199 (2001) 107.
- [15] G.J.A. Hellings, H. Ottevanger, S.W. Boelens, C.L.C.M. Knibbeler and H.H. Brongersma, *Surf. Sci.*, 162 (1985) 913.
- [16] C.L.C.M. Knibbeler, G.J.A. Hellings, H.J. Maaskamp, H. Ottevanger and H.H. Brongersma, *Rev. Sci. Instrum.*, 58 (1987) 125.
- [17] P.A.J. Ackermans, P.F.H.M. van der Meulen, H. Ottevanger, F.E. van Straten and H.H. Brongersma, *Nucl. Instr. Meth.*, B35 (1988) 541.
- [18] O. van Kessel, H.H. Brongersma, J.G.A. Hölscher, R.G. van Welzenis, E.G.F. Sengers and F.J.J.G. Janssen, *Nucl. Instr. Meth.*, B64, (1992) 593.
- [19] J.P. Jacobs, A. Maltha, J.G.H. Reintjes, J. Drimal, V. Ponc and H.H. Brongersma, *J. Catal.*, 147 (1994) 133.
- [20] J.C. Fullarton, J.-P. Jacobs, H.E. van Benthem, J.A. Kilner, H.H. Brongersma, P.J. Scanlon and B.C.H. Steele, *Ionics*, 1 (1995) 51.
- [21] J.F. Moulder, W.F. Stickle, P.E. Sobol and K.D. Bomben, "Handbook of X-ray Photoelectron Spectroscopy" (J. Chastain, Ed.), Perkin-Elmer Corporation, Eden Prairie, USA, 1992.
- [22] D. Briggs and M.P. Seah (Editors), "Practical Surface Analysis by Auger and X-Ray Photoelectron Spectroscopy", Wiley, New York, 1983.

- [23] Lu Gang, J. van Grondelle, B.G. Anderson and R.A. van Santen, Catal. Today, 61 (2000) 179.
- [24] R.M. Friedman, J.J. Freeman and F.W. Lytle, J. Catal., 55 (1978) 10.
- [25] J.N. Armor, Appl. Catal., 1 (1992) 221.
- [26] C.D. Wagner, L.H. Gale and R.H. Raymond, Anal. Chem., 51(4) (1979) 466.
- [27] P.M. Hansen, "Constitution of Binary Alloys", MCGRAW-HILL BOOK COMPANY, INC., 1958.

Summary

The selective catalytic oxidation (SCO) of ammonia with oxygen to nitrogen and water recently is considered to be an efficient method to abate ammonia pollution. Previous studies show that noble metals such as Pt, Ir are very active for this reaction at low temperature but less selective. Significant amounts of nitrous oxide or nitric oxide are produced on these catalysts, especially under the condition of very high O_2/NH_3 ratios. Metal oxide catalysts such as Co_3O_4 , MnO_2 , CuO , Fe_2O_3 , V_2O_5 and MoO_3 are also studied in the literature but the efficiencies are not enough at low temperature for a practical use. The research described in this thesis was aimed at the development of new, active and selective catalysts for low temperature selective ammonia oxidation to nitrogen.

In Chapter 2 an elementary catalyst screening study was performed in order to find new catalytic components and composites for SCO reaction. The emphasis was on zeolite-based and alumina-supported metal or metal oxide catalysts. The activity of copper ion-exchanged zeolite Y catalysts for ammonia oxidation was shown to be comparable to that of noble-metal catalysts at low temperatures. The selectivity to nitrogen was much higher for the zeolite catalysts. Treatment of CuY with NaOH after ion exchange increased the ammonia oxidation activity. Alumina-supported silver catalysts showed very high activity for ammonia oxidation, even superior to noble metal catalysts. But the selectivity to nitrogen was comparable to other noble-metal catalysts. Co-fed steam dramatically decreased catalyst activity, especially at lower temperatures. Ion-exchanged zeolite Y catalysts were more stable than alumina-supported catalysts. At high O_2/NH_3 ratios the activity of all catalysts increased but the selectivity for nitrogen production decreased. In all, CuY and silver-based catalysts were found to be the most promising catalysts for low temperature SCO process.

In Chapter 3 various kinds of copper oxides supported on alumina and on zeolite Y have been prepared and studied in detail. TPD, TPR, UV-vis spectroscopy and high-resolution electron microscopy (HREM) were used to characterize these catalysts in an attempt to shed light on the optimal preparation for active and selective low-temperature ammonia oxidation catalysts. The HREM and UV-vis measurement results showed that a $CuAl_2O_4$ -like phase was more active than a CuO phase for SCO reaction. NH_3 TPD profiles on Cu-Al-10 indicated that both surface oxygen and

lattice oxygen can react with ammonia to produce N_2 . However, surface oxygen was much more active than lattice oxygen at low temperature. NH_3 TPD on CuY catalysts showed three types of active centers. Two of these were active at low temperature (below 200 °C) and one was active at a higher temperature (above 300 °C). The existence of low temperature active centers indicated that ammonia oxidation at low temperature on copper catalysts was possible. According to the UV spectra, the $[Cu-O-Cu]^{2+}$ -like species or small copper oxygen aggregates were responsible to the low temperature active centers. However the amount of low temperature active centers or the concentration of $[Cu-O-Cu]^{2+}$ species was small prior to NaOH treatment. The NaOH treatment of CuY increased the amount of low temperature active centers. These studies apparently indicate that the environment or the type of active copper species is very important for low temperature ammonia oxidation and is strongly related with different supports and preparation methods.

In Chapter 4 ammonia oxidation reaction pathways on high surface area silver powder has been studied by TPD, TPR, FT-Raman and transient as well as steady-state ammonia oxidation experiments. Silver is a very active catalyst for ammonia oxidation. At low temperature (below 300 °C) mainly N_2 and N_2O are produced. At higher temperature NO instead of N_2O becomes one of the products. NO is an important reaction intermediate for this reaction. Even at room temperature the NO can be produced and adsorbed on silver surface in the form of NO_x . Since NO can not desorb at low temperature it blocks the active sites for oxygen dissociation. The dissociation of oxygen is thus believed to be the rate-controlling step for ammonia oxidation. The selectivity to N_2 , N_2O and NO is mainly determined by surface oxygen coverage and temperature. Low surface oxygen coverage favors nitrogen formation. Adsorbed NO_x , N_2O_x species are actually inhibitors for ammonia oxidation but they also lower the surface oxygen coverage. Hence, the selectivity to nitrogen is improved by increasing the amount of these adsorbed species on silver surface.

The pathway of ammonia oxidation on silver at low temperature is actually a two-step reaction. Ammonia was first oxidized to NO. This reaction step was very fast on silver. At moderate temperature (below 300 °C) the NO could be removed either as N_2O or N_2 through surface SCR reaction, the second step of ammonia oxidation. At even higher temperature NO could directly desorb as one of the products. Apparently the SCR performance of the silver-based catalysts was related closely to the ammonia oxidation performance of the catalysts. Unfortunately the silver-based catalysts are not good catalysts for SCR reaction. Therefore a large amounts of N_2O is produced. Generally speaking, silver alone, like Pt, is not a good catalyst for selective ammonia oxidation to nitrogen because too much N_2O is produced. It follows from the above

conclusions that blocking of the sites for oxygen dissociation is an effective way to improve the nitrogen selectivity, but also would result in a loss of catalyst activity.

In Chapter 5 low temperature gas phase oxidation of ammonia to nitrogen has been studied over alumina-supported, silica-supported and unsupported silver catalysts to distinguish the support effect on silver-based catalysts. TPD, TPR, TEM, XRD and FT-Raman were used to characterize the different silver catalysts. The results showed alumina-supported silver to be the best catalyst due to the interaction of silver with alumina. Pretreatment had a great affect on the catalyst performance. Reduction in hydrogen at 200 °C without any pre-calcination gave the best activity while reduction at higher temperatures showed little difference from calcination pretreatment. At least four types of oxygen species were produced when silver was oxidized at high temperature. These species are adsorbed molecular oxygen, adsorbed atomic oxygen, subsurface oxygen and bulk dissolved oxygen respectively. Ammonia oxidation activity at low temperature is related to the catalyst's ability of dissociatively or non-dissociatively adsorption of oxygen. In addition, a good correlation existed between the N₂ selectivity for SCO reaction and the SCR performance of NO with NH₃ for the silver-based catalysts, i.e., the higher SCR yield of nitrogen, the higher the SCO N₂ selectivity.

In Chapter 6 a new bi-functional Cu-Ag/Al₂O₃ catalyst was developed based on the previous reaction mechanism study, which showed not only high activity but also high selectivity for ammonia oxidation. The catalysts have been characterized by XRD, XPS, LEIS, TEM and EDX. In all catalysts analyzed by LEIS and TEM, copper has a very high dispersion. Most likely, the catalysts contain copper oxides platelets with a thickness of roughly 1 monolayer. At increasing copper loading, relatively more (or more extended) rather than thicker platelets are formed. However, silver has a broad particle size distribution. The average size of the Ag species ranges between 2.5 and 5.5 nm measured from LEIS. These numbers increase with increasing silver loading. The XRD and XPS results show that the valence states of copper and silver are the same for single component catalysts and bi-component catalysts. The TEM images and LEIS measurements also show no big difference in the particle size distribution for all these catalysts. There is no indication for the formation of a new Cu-Ag phase or the formation of Cu-Ag alloy. So the remarkable change for selectivity with addition of copper is not due to the synergic effect between copper and silver, or the particle size effect. The EDX results show that copper and silver exist together anywhere on the alumina surface. This proves that there is an intimate contact between copper and silver on alumina-supported Cu-Ag catalysts. The promotion effect of copper can thus be well explained by a mechanism of bi-

functional catalyst, in which the silver component mainly catalyzes ammonia oxidation to NO, the first step of this reaction, and the copper catalyzes NO SCR reaction to nitrogen, the second step of ammonia oxidation on silver.

Multi-functional catalysis is not a new concept, but catalyst design deliberately based on the principle of multifunctionality will be inevitable to develop high-performance catalysts which can cope with such difficult problems as in ammonia oxidation. This study only gives one example of such a design. Actually there are more alternatives available. Besides silver, many noble metals such as Pt, Ir are very active for ammonia oxidation with low selectivity to nitrogen due to the less efficiency for SCR reaction. There are also many good SCR catalysts such as vanadium oxide, iron oxide. Opportunities still exist for preparing high-performance bi-functional catalysts from these catalytic components.

Samenvatting

De selectieve katalytische oxidatie (SCO) van ammoniak met zuurstof naar stikstof en water is bekend als een doelmatige oplossing voor de vermindering van de NH_3 uitstoot. Tussen de katalysatoren die genoemd worden als mogelijke materialen voor dit proces, zijn edelmetaal katalysatoren zoals Pt, Ir heel actief bij lage temperatuur maar niet selectief naar stikstof. Bovendien produceeren ze significante hoeveelheden N_2O . Metaaloxides zoals Co_3O_4 , MnO_2 , CuO , Fe_2O_3 , V_2O_5 en MoO_3 zijn ook actief voor ammoniak oxidatie maar de activiteit is niet hoog genoeg om te worden toegepast als industriële katalysator. Het onderzoek, beschreven in dit proefschrift, is gericht op de ontwikkeling van een nieuwe, actieve en selectieve katalysator voor de lage temperatuur selectieve oxidatie van ammoniak naar stikstof.

In hoofdstuk 2 is de screening van een aantal katalysatoren gebaseerd op zeoliet Y en alumina gedragen metaal of metaaloxides voor ammoniak oxidatie beschreven. De resultaten vertoonden een vergelijkbare activiteit tussen de CuY en edelmetaal katalysatoren voor ammoniak oxidatie bij lage temperatuur. Maar de CuY katalysatoren blijken veel selectiever naar stikstof te zijn. De behandeling van CuY met NaOH na ionenwisseling toont toegenomen activiteit voor ammoniak oxidatie. Alumina gedragen zilver katalysatoren zijn actiever dan edelmetaal katalysatoren maar met een vergelijkbare selectiviteit. Er is gevonden dat het effect van water over het algemeen negatief is. Bovendien is gevonden dat de ionengewisselde zeoliet Y katalysatoren stabiel waren dan de alumina gedragen katalysatoren. Een hoge O_2/NH_3 verhouding gaf een toename van activiteit maar een afname van selectiviteit te zien voor bijna alle katalysatoren. Uit deze resultaten kan worden dat CuY en Ag/ Al_2O_3 veelbelovende katalysatoren zijn voor het lage temperatuur SCO proces.

In hoofdstuk 3 is de bereiding van verschillende zeoliet Y en alumina gedragen koper oxide katalysatoren besproken. Deze katalysatoren werden bestudeerd door TPD, TPR, UV-vis spectroscopie en hoge resolutie elektronenmicroscopie (HREM) om hun werking te kunnen begrijpen en te gebruiken als basis voor een verdere optimalisatie van de katalysator. Met behulp van HREM and UV-vis werd geconcludeerd dat de CuAl_2O_4 -gelijkend fase actiever is dan de CuO-fase voor de SCO reactie. NH_3 TPD profielen op Cu-Al-10 katalysator tonen aan dat zowel oppervlakte zuurstof als ook rooster zuurstof kunnen reageren met ammoniak om stikstof te geven, maar

oppervlakte zuurstof is actiever dan rooster zuurstof bij lage temperatuur. De profielen van NH_3 TPD op CuY katalysator vertoonden drie types actieve centra voor ammoniak oxidatie. Twee van deze zijn actief bij lage temperatuur (beneden $200\text{ }^\circ\text{C}$) en een van deze is actief bij hogere temperatuur (boven $300\text{ }^\circ\text{C}$). Volgens de UV-vis spectra, zijn de $[\text{Cu-O-Cu}]^{2+}$ gelijkende species of kleine koperoxide clusters de lage temperatuur actieve centra. De concentratie van de $[\text{Cu-O-Cu}]^{2+}$ species op CuY katalysator is echter te laag. De behandeling van CuY met NaOH verhoogt de concentratie van de $[\text{Cu-O-Cu}]^{2+}$ species op CuY katalysator en zo de toename van de activiteit van ammoniak oxidatie bij lage temperatuur. De beschreven resultaten laten zien dat de omgeving of het type van de koper species heel belangrijk zijn voor de lage temperatuur ammoniak oxidatie en dat deze sterk afhankelijk is van de verschillend katalysator dragers en bereidingsmethodes.

In hoofdstuk 4 is een studie naar het reactiepad van ammoniakoxidatie over hoge oppervlakte zilverpoederkatalysator beschreven. De zilverpoederkatalysator werd bestudeerd met TPD, TPR, FT-Raman en transient alsook steady-state ammoniak oxidatie. Zilver is een zeer actieve katalysator voor ammoniakoxidatie. Bij lage temperatuur (beneden $300\text{ }^\circ\text{C}$), werd voornamelijk N_2 and N_2O gevonden. NO werd gezien als een bijproduct bij hogere temperatuur (boven $300\text{ }^\circ\text{C}$). NO was een belangrijk reactie intermediair voor deze reactie. Zelfs bij kamertemperatuur kan NO worden geproduceerd en op het oppervlak van de katalysator als NO_x geadsorbeerd. Omdat NO niet bij lage temperatuur desorbeert, wordt de actieve site voor zuurstof dissociatie geblokkeerd. De snelheidsbepalende stap voor ammoniak oxidatie moet dus de zuurstofdissociatie zijn. De selectiviteit naar N_2 , N_2O en NO wordt voornamelijk bepaald door de temperatuur en de oppervlakte bedekking van zuurstofatomen. Een lage oppervlaktebedekking met zuurstofatomen bevordert de vorming van stikstof. Geadsorbeerde NO_x , N_2O_x species verhinderen feitelijk de ammoniak oxidatie, maar ze verlagen ook de oppervlaktebedekking van zuurstofatomen. Daarom wordt de selectiviteit naar stikstof verbeterd door toenemende bedekking van deze species op het zilveroppervlak.

Het reactiepad van ammoniakoxidatie over zilverpoederkatalysator is een twee-staps reactie. Ammoniak wordt eerst geoxideerd naar NO, deze stap is heel snel over zilver katalysator. Bij gematigde temperatuur (beneden $300\text{ }^\circ\text{C}$), wordt de NO verwijderd als N_2O of N_2 door oppervlak SCR reactie, de tweede stap van ammoniak oxidatie. Bij nog hogere temperatuur, kan NO direkt desorberen als een produkt. De SCR katalytische eigenschappen van de zilver gebaseerde katalysatoren houden dus verband met de SCO katalytische eigenschappen. Ongelukkigerwijs zijn de zilver katalysatoren geen goede SCR katalysatoren, waardoor heel veel N_2O wordt

geproduceerd. In het algemeen is zilver, evenals Pt, geen goede SCO katalysator omdat te veel N_2O wordt geproduceerd. De belangrijkste conclusie van bovenstaande resultaten is dat de blokkering van actieve sites voor zuurstofactivering een doelmatige wijze is om de selectiviteit naar stikstof te verbeteren, maar met enig verlies van activiteit.

In hoofdstuk 5 is de gas-fase ammoniakoxidatie naar stikstof over Ag, Ag/ Al_2O_3 en Ag/ SiO_2 katalysatoren bestudeerd om het effect van de drager te onderscheiden. TPD, TPR, TEM, XRD en FT-Raman werden gebruikt om de zilver gebaseerde katalysatoren te onderzoeken. Er is gevonden dat alumina gedragen zilver de beste katalysator is, waarschijnlijk vanwege de interactie tussen zilver en alumina. Een groot effect van de katalysatorvoorbehandeling op de katalytische eigenschappen werd gevonden. Reduktie van de katalysator in H_2 bij een temperatuur van 200 °C zonder voorafgaande calcinatie heeft de beste activiteit getoond. Echter, de reductie in H_2 bij hogere temperatuur vertoont een vergelijkbaar effect als de oxidatie in O_2 bij hogere temperatuur. Vier verschillende zuurstof species, zoals geadsorbeerde moleculaire zuurstof, geadsorbeerde zuurstofatomen, onderoppervlak zuurstof en bulk zuurstof, werden geproduceerd over zilver als de zilver katalysator geoxideerd wordt bij hoge temperatuur. De activiteit van de zilverkatalysator voor ammoniak oxidatie is gerelateerd aan het katalysator vermogen voor zuurstof adsorptie. Bovendien is gevonden dat er een goede correlatie bestaat tussen de N_2 selectiviteit van de SCO reactie en de SCR activiteit van NO met NH_3 over zilver gebaseerde katalysatoren.

Omdat SCO uit verschillende reaktiestappen bestaat is het erg moeilijk om een enkele actieve fase te vinden die alle processen simultaan katalyseert. Multi-functionele katalysatoren proberen het probleem op te lossen door meerdere actieve katalytische fasen te combineren. Een voorbeeld van zo'n aanpak wordt beschreven in hoofdstuk 6 met de Cu-Ag/ Al_2O_3 katalysatoren. Op zilver gebaseerde katalysatoren zijn bekend om hun grote activiteit voor de SCO reactie, echter, een minpunt is hun grote selectiviteit voor de vorming van N_2O . Een Cu-Ag/ Al_2O_3 katalysator bleek niet alleen actief maar ook selectief. Karakterisatie van deze katalysatoren door XRD, XPS, LEIS, TEM en EDX hebben aangetoond dat het Ag aanwezig is als fijn verdeeld Ag deeltjes met 2.5-5.5 nm in diameter, terwijl Cu aanwezig is als koperoxide plaatjes met ongeveer 1 monolaag dikte. Ook werd geen indicatie gevonden voor de vorming van een nieuwe Cu-Ag fase of Cu-Ag legering. Bovendien is door EDX gevonden dat waar dan ook op het alumina oppervlak koper en zilver samen schijnen te bestaan. Dit suggereert dat er een intiem contact tussen zilver en koper op de Cu-Ag/ Al_2O_3 katalysatoren is opgetreden. Het mechanisme van bi-functionele katalysator kan dus het promotor effect van kopertoevoeging verklaren. Zoals al eerder gezegd zijn

Ag/Al₂O₃ katalysatoren erg actief voor de vorming van NO, de eerste stap van ammoniak oxidatie. De Cu/Al₂O₃ katalysatoren, echter, zijn erg actief voor de SCR reactie van NO met NH₃, de tweede stap van ammoniak oxidatie.

Publications

Bi-functional alumina-supported Cu-Ag catalysts for ammonia oxidation to nitrogen at low temperature

Lu Gang, B.G. Anderson, J. van Grondelle, R.A. van Santen, W.J.H. van Gennip, J.W. Niemantsverdriet, P.J. Kooyman, A. Knoester and H.H. Brongersma, J. Catal., accepted.

Intermediate species and reaction pathways of ammonia oxidation on silver powder catalyst

Lu Gang, B.G. Anderson, J. van Grondelle, R.A. van Santen, J. Catal., 199 (2001) 107.

Selective low temperature NH_3 oxidation to N_2 on copper-based catalysts

Lu Gang, B.G. Anderson, J. van Grondelle, R.A. van Santen, J. Catal., 186, 100(1999)

NH_3 oxidation to nitrogen and water at low temperatures using supported transition metal catalysts

Lu Gang, B.G. Anderson, J. van Grondelle, R.A. van Santen, Catalysis Today, 61, 179(2000)

Low temperature selective oxidation of ammonia to nitrogen on silver-based catalysts

Lu Gang, B.G. Anderson, J. van Grondelle, R.A. van Santen, Appl. Catal. B, submitted.

Break-down of liquid membrane emulsion under high electric field

Lu Gang, Q.H. Luo and P.S. Li, J. Membr. Sci., 1-6, 3349(1997)

Synthesis of Mixed Alcohols from CO_2 Contained Syngas over Supported Molybdenum Sulfide Catalyst

Lu Gang, Z.B. Zhu and C.F. Zhang, Appl. Catal. A, 150, 243(1997)

Removal of CO_2 by Electrochemical Cell with Molten Carbonates as Electrolyte

Lu Gang, Q.H. Luo and P.S. Li, J. East China University of Sci. & Tech., 22(5), 75(1996)

Molybdenum distribution on active carbon extrudes-supported molybdenum catalysts prepared by impregnation

Lu Gang, H.F. Qin, Z.B. Zhu and C.F. Zhang, J. Catal.(Chinese), 13(2), 1994

Synthesis of mixed alcohols on molybdenum sulfide based catalysts

J.L. Pi, Lu Gang, W. Gao, Z.B. Zhu and C.F. Zhang, J. Fuel Chem. & Tech.(Chinese), 21(1), 1993.

Distribution of mixed alcohols in products synthesized over molybdenum sulfide catalysts

W. Gao, Lu Gang, J.L. Pi, Z.B. Zhu and C.F. Zhang, *J. Fuel Chem. & Tech. (Chinese)*, 21(1), 1993.

Reaction-diffusion model for zinc ion permeation in liquid membrane emulsion

Lu Gang, Q.H. Luo and P.S. Li, *J. East China Institute of Chem. Tech.*, 19(4), 1993.

Rate model for phase separation of W/O emulsion in liquid surfactant membrane process at high A.C. voltage

Lu Gang, Q.H. Luo and P.S. Li, *Chinese J. of Chem. Eng.*, 1(4), 1993

Study on electric break-down of liquid membrane emulsion

Lu Gang, Q.H. Luo and P.S. Li, *Membr. Sci. Tech. (Chinese)*, 13(2), 1993

Study on stabilities of emulsion liquid membrane

Lu Gang, Q.H. Luo and P.S. Li, *Membr. Sci. Tech. (Chinese)*, 13(1), 1993

Zinc extraction by emulsion liquid membrane technique

Lu Gang, Q.H. Luo and P.S. Li, *Water Treatment (Chinese)*, 8(4), 1993

Acknowledgement

This dissertation would never have been completed successfully without the whole-hearted support of my thesis supervisors. I am very grateful to my first promoter, Professor R. A. van Santen, who offered me the opportunity to pursue my PhD program described in this thesis and provided valuable technical and personal guidance. My special thanks also go to Professor van Veen, my copromoter, for his vital support and generous guidance for the writing of this thesis.

I would thank all other reading committee members, Prof. L. Kapteijn, Prof. L. Lefferts and Dr. J. Hoebink, who reviewed the manuscript and made many valuable suggestions as well as offering many technical comments.

In the group of Laboratory of Inorganic Chemistry and Catalysis, many people have provided their invaluable help. Many thanks are due to Dr. B.G. Anderson who spent many hours on my experimental details, paper corrections and made contributions to the project. It was so nice to work with you in BESSY of Berlin. Distinctive thanks are due to Joop van Grondelle and Jos van Wolput, who are so kind to offer me continuously a great deal of help, both technically and personally. The other colleagues I should mention here are Arian, Pieter, Noud, Darek, Zhu, Ionel and Nicolae. Sonia, thanks for the enthusiasm you put in the work during your stay in Eindhoven. This was of great value for me.

I am indebted to those who also involved in the research work, especially to the group of Prof. Brongersma for the LEIS measurement, W. Gennip for the XPS and Auger measurement, P.J. Kooyman (National Centre for High Resolution Electron Microscopy) for the TEM measurement, A. Knop-Gericke (Berlin, BESSY II) for NEXAFS analysis.

Furthermore, I consciously understand that I owe my parents my gratitude greatly, since only with their love, concern and understanding was it possible for me to accomplish this research. Finally I am most happy to give my cordial thanks to my wife, Yu Li, and our daughter Lu Yang. They left all their relatives, friends and life familiar to them to join me here. Without their love, encouragement and sacrifice, I could not complete this thesis.